Spring 1-1-2010

An Investigation of Design Parameters that Affect Commercial High-Rise Office Building Energy Consumption and Demand

Margarete Rois Langner
University of Colorado at Boulder, margarete.langner@colorado.edu

An investigation of design parameters that affect commercial high-rise office building energy consumption and demand

by

M. Rois Langner

B.A., Colorado College, 2003

A thesis submitted to the

Faculty of the Graduate School of the

University of Colorado in partial fulfillment

of the requirements for the degree of

Masters of Science

Department of Civil, Environmental and Architectural Engineering

2010

This thesis entitled:
An investigation of design parameters that affect commercial high-rise office building energy consumption and demand
written by M. Rois Langner
has been approved for the Department of Civil, Environmental and Architectural Engineering

Prof. Gregor Henze, PhD, P.E.

Prof. Michael Brandemuehl, PhD, P.E.

Prof. Moncef Krarti, PhD, P.E.

Date

The final copy of this thesis has been examined by the signatories, and we find that both the content and the form meet acceptable presentation standards of scholarly work in the above mentioned discipline.

Langner, M. Rois (M.S.)

An investigation of design parameters that affect commercial high-rise office building energy consumption and demand

Thesis directed by Prof. Prof. Gregor Henze, PhD, P.E.

There are many factors that drive energy consumption and demand in high-rise commercial office buildings. Understanding the effects of individual building parameters and two-factor interactions can be very useful for directing building audits, developing energy simulation models, and for building science research in general. In an effort to expedite building audit processes and energy model development, the work presented in this thesis offers strategies and best practices for efficiently conducting audits and developing building energy models. In conjunction, a fractional factorial analysis (FFA) was conducted to evaluate a large number of building parameters in an effort to quantify their effect on energy consumption and demand associated with the chiller, HVAC system, and the facility as a whole. The FFA utilized building data collected from twenty-two building audits of high-rise commercial office buildings located in the downtown Chicago Loop area. Data from these buildings were used to determine base and test values for each factor that was evaluated. Simulation results show the effects of each factor and two-factor interactions on energy consumption and demand over a set of climate zones. They also show that there is a particular sub-set of driving factors that are of primary importance. These factors include chiller COP, supply fan pressure rise, the window solar heat gain coefficient and U-value, and lighting and equipment power density. Similarly, the two-factor interaction study identified factors that have a significant effect on building energy when paired with another factor. The two-factor interactions with high significance included the thermal mass associated with both structural components and interior furnishings paired with one of the driving factors listed above. From these results, a better understanding of the effects and interactions of building parameters on energy consumption and demand was obtained, and recommendations were made to help accelerate building audit and energy model development processes.

Acknowledgements

The author would like to thank: Gregor Henze for his guidance throughout the completion of this masters thesis; Vince Cushing and the entire Clean Urban Energy team for inspiring and supporting the efforts of this thesis - including the support and generous hospitality for the many trips made to Chicago to audit buildings; Sandro Plamp for his guidance in using EnergyPlus software and knowledge of HVAC systems; Chad Corbin for his multitude of help and guidance regarding building simulation and technical support; Professors Mike Brandemuehl and Moncef Krarti for additional support in shaping the direction of this masters thesis; and lastly, many thanks to my fellow classmates and the entire BERG team for their help and encouragement along the way.

Contents

Tables

Table

Figures

Figure

Chapter 1

Introduction

1.1 Motivation

The United States commercial building sector is responsible for 18% of the nation's energy use. With a projected growth of 1.5% per year, as predicted by the Energy Information Agency's 2008 Annual Energy Outlook, the demand for energy continues to grow, while the current energy system struggles to keep up [10]. In order to slow the energy demand growth and reduce the amount of energy use associated with buildings, it is first important to understand how energy is distributed throughout a building, and how each building parameter contributes to energy consumption and demand.

The motivation for this research came from a software development plan to optimize chiller use during summer peak demand times for large commercial office buildings in Chicago, Illinois. Connected to a building automation system (BAS), the optimization program suggests pre-cooling strategies to shift cooling loads to off-peak demand times, in response to typical building energy use and real-time electric pricing.

The sponsor of this research, Clean Urban Energy (CUE) in Chicago, Illinois, worked with the Building Owners and Managers Association (BOMA) of Chicago to solicit large office buildings to participate in the 2009 CUE summer software demonstration. Approximately fifty buildings were chosen for the project and a series of walk-through audits were conducted to collect data for building energy models using the EnergyPlus simulation program. EnergyPlus software was chosen because of its ability to model complex HVAC systems with more precision than competing software. The detail that EnergyPlus provides allowed the research team to more accurately meet project goals to optimize chiller performance during peak demand times and

to suggest pre-cooling strategies.

Time efficiency is essential to all CUE related projects. The goal was to model as many of the fifty buildings as possible and to have online optimizations running by the end of the 2009 summer, drove the decision to develop a modeling process to accurately model buildings with maximum time efficiency. With this goal in mind, a process was developed that included an analysis of existing modeling tools and the development of new tools to help manage and simplify the modeling process. In conjunction, a fractional factorial analysis was conducted to evaluate a large number of building parameters in an effort to quantify their effect on heating and cooling energy consumption and demand. Data from a 2009 summer demonstration building audits were used to determine base and test values for each factor evaluated in the analysis. Simulation results show the effects of each factor and two-factor interactions on energy consumption and demand for a set of climate zones representative of the different climates found throughout the United States. The results also show that there is a particular sub-set of driving factors that are of primary importance.

The work presented in this thesis was intended to aid in CUE related projects providing guidelines for conducting audits and developing building energy models. The work also presents a detailed analysis of high-rise commercial office building system components, that evaluates the effects of individual component factors and two-factor interactions on building energy consumption and demand. For the building science community, the results of this study are intended to be used to better understand model parameter assumptions on building energy consumption and demand, and to help direct research efforts in future high-rise commercial office building studies.

1.2 Questions to be Answered

(1) How can we expedite the modeling process for high-rise office buildings using EnergyPlus? An investigation into existing modeling tools and discussion on simple modeling tools that can be developed to aid in the modeling process.

(2) What are the best procedural steps to accurately calibrate high-rise office building models in EnergyPlus? An investigation into model calibration tools, techniques and strategies, and error analysis.

(3) What design factors greatly influence the energy consumption and demands associated with heating and cooling loads of high-rise commercial office buildings? Through a set of fractional factorial analyses, main effects and two-factor interactions were analyzed to determine the effects of a large number of model parameters for three HVAC system configurations in four United States climate zones.

1.3 Thesis Organization

The following thesis first presents building audit and energy simulation model development strategies, as well as techniques for rapidly developing building energy models. It also investigates a large fractional factorial analysis that evaluates the effects of a number of factors and two-factor interactions on energy consumption and demand associated with the chiller, HVAC system, and facility as a whole.

First, a review of relevant literature pertaining to building energy model development and fractional factorial analysis techniques is presented. Literature pertaining to energy model development includes strategies to classify building types and climate zones, as well as techniques for model calibration that include processes to evaluate error and model mismatch. The fractional factorial analysis section describes methods and techniques to conduct a fractional factorial analysis as well as related research that has used fractional factorial analysis to evaluate a set of relevant factors.

Next, a description of the overall project and goals of this masters thesis is presented. This includes an overview of the intent of the project as seen by the sponsor of the research, Clean Urban Energy. The buildings used in this study, building audit and data collection, and data organizational strategies are also discussed.

Chapter 4 provides an in-depth discussion on building energy model development and methodology, as well as model calibration techniques. These discussions focus on model development using the EnergyPlus simulation software, however, many of the techniques and strategies can be adopted for other energy simulation software or tools.

Chapter 5 discusses strategies used to conduct the fractional factorial analysis. It also describes the selection process used to determine the specific factors and the range of values for each factor needed for the

fractional factorial analysis.

Results and discussion of the main effects and two-factor interactions from the fractional factorial analysis are presented in Chapter 6. These discussions provide an overview of the energy and heat balance of a building, and how each factor and two-factor interaction contributes to energy consumption and demand associated with heating and cooling.

Lastly, conclusions about the audit and model development process, the effects found through the fractional factorial analysis, use of the results, and application of this study are presented. Options for potential future work in this field of study are also presented.

Chapter 2

Literature Review

The following literature review was conducted to support the efforts of this masters thesis research. The review was directed towards two major topics: 1) strategies used to rapidly develop building energy models for a large number of high-rise commercial office buildings, and 2) methods to conduct a fractional factorial analysis in effort to learn about the effects of major building components on building energy consumption and demand.

2.1 Building Energy Model Development

2.1.1 Building Classification

Cooling and heating loads are partially driven by weather patterns specific to a particular climate region. A number of organizations have developed methods to classify climate regions in the United States, categorizing them by the number of heating and cooling degree days or temperature and precipitation, state boundaries, etc. Henze et al. [15] conducted a simple analysis using typical meteorological year data (TMY), that computed the number of hours that temperatures occurred in 5°F bins and humidity ratios in 0.002 lbw/lbda bins. Based on data from this study, they proposed to use weather data from four cities to represent the major climate zones of the U.S.: Phoenix (hot and dry), Atlanta (warm and humid), Los Angeles (warm and dry), and New York (cool and humid). This study supported the decision to use the above listed climate zones for the fractional factorial analysis presented in this thesis, with one minor change. The author chose to substitute a Chicago weather file for New York, since both climate zones are similar and because the work in this thesis was based in Chicago.

Huang and Franconi [18] reviewed a multitude of prototypical commercial building types from engineering studies dating back to 1983. Based on this review, a set of 12 prototypical building models were developed and used for parametric studies that focused on the effects of building components on commercial heating and cooling loads, as simulated in DOE-2. The suite of investigated buildings were classified by building floor area, building type, vintage, and by their representative climate zone. Building descriptions were also classified into three major areas: the physical building characteristics, HVAC system characteristics, and internal conditions and operating patterns of the building. These classification techniques were adopted into this thesis research in an effort to manage the large number of buildings that were audited in the CUE 2009 summer demonstration.

2.1.2 Model Calibration Techniques

Reddy and Maor [32] explored a variety of tools, techniques, approaches and procedures commonly used to calibrate simulated building energy models to measured data, in an effort to develop a more systematic approach to model calibration. The proposed calibration methodology includes four steps. The first step is to heuristically define a set of prominent input parameters and schedules, along with a range of values for each parameter based on building type. Next is to perform a coarse grid search (involving thousands of simulations), subjecting the set of input parameters to a Monte Carlo simulation in order to identify a sub-set of the most sensitive parameters. Narrow bounds of variability associated the sub-set of parameters should then be defined, identifying a small set of feasible parameter vector solutions. Next is to perform a guided grid search to further refine the feasible parameter vector solutions. Lastly, the modeler uses this solution set to make predictions and determine the prediction uncertainty of the entire calibration process. Three case study buildings were used in this study (one actual building and two synthetic) to test the methodology, while using the DOE-2 building simulation software. Overall concepts of this approach were used in this masters thesis research. The fractional factorial analysis discussed in the upcoming chapters has a similar goal to the Monte Carlo approach: to identify a sub-set of sensitive parameters to direct audit, modeling and calibration efforts. However, the fractional factorial analysis requires fewer model simulations.

Liu and Henze [24], developed a methodology to improve calibration accuracy of building energy

models in an effort to improve predictive optimal control of active and passive building thermal storage. Through past research, it has been proven that the accuracy of a building model can greatly affect the performance of predictive optimal control strategies. Integrating a global optimization algorithm with a building simulation program, Liu et al. developed an optimization environment to calibrate whole-building energy models, avoiding the repetition of manually adjusting individual model parameters. From here, the calibration process is divided into two steps. The first step is to define the parameters that affect the building cooling load. Secondly, capacities, efficiencies, and part-load performance of HVAC systems should be tuned to match predicted or measured energy consumption of the building. The optimization algorithm then calibrates each parameter to minimize the root-mean-square error (RMSE). A similar auto-calibration tool was built by another member of the research team associated with this masters thesis, and was used for calibration purposes. Alongside the auto-calibration tool, the calibration process and error minimization techniques seen in the work of Liu and Henze have been adopted into this thesis.

Yoon and Lee [41], developed a systematic process to calibrate building energy models of high-rise commercial buildings using monthly utility data. The building used in this study was a 26-story commercial building located in Seoul, Korea, and was modeled in DOE-2.1E with electric cooling and gas heating. A step-by-step approached was established to calibrate the model. This process consisted of (1) base case modeling, (2) base load analysis, (3) mid-season calibration, (4) site interview and confirmation, (5) heating and cooling season calibration, (6) validation of calibrated base model, and lastly (7) the investigation of promising energy conservation measures. Steps one through six were applied to this masters thesis. Step seven did not apply to Clean Urban Energy's overall goal and was disregarded from this research. Error analysis was similar to Liu and Henze [24], and used the root-mean-square error (RMSE) and the coefficient of variation (CV) of the root-mean-square error approaches (dividing the RMSE by the average measured value during a period of time) to minimize uncertainty in the model.

Haberl and Bou-Saada [13] investigate techniques for improving calibration procedures for hourly building energy simulation models. These techniques include methods to graphically represent data, and statistical approaches to determine accuracy of a calibrated model. Traditional calibration procedures include analysis of compared simulated data to measured data by method of two-dimensional time series

plots and monthly percent difference calculations. While these traditional calibration methods are beneficial for determining hourly features within a data set and for demonstrating of goodness of fit, Haberl and Bou-Saada present alternative, in-depth graphical methods and statistical approaches to improve calibration results. Graphical approaches include binned box-whisker-mean plots which display maximum, minimum, mean and median values for binned data, scatter plots that show individual point locations, and three-dimensional calibration plots that show hourly differences on a daily scale, over a simulation period. Statistical calibration methods include monthly percent difference calculations, hourly mean bias error (MBE) and root-mean-square error (RMSE) calculations reported monthly, and hourly coefficient of variation of the RMSE (CV(RMSE)) calculations. The MBE determines a non-dimensional bias measure, or sum of errors, between the simulated and measured data sets. The RMSE measures variability between the data set, showing the how much spread is in the simulated data. The CV(RMSE) is the RMSE divided by the measured mean of all data, which allows the modeler to see how well the model fits to measured data. Models with lower CV(RMSE) values have higher calibration accuracy. By using the proposed graphical and statistical procedures represented in this paper, model calibration accuracy can be evaluated with a higher level of confidence.

2.2 Fractional Factorial Analysis

2.2.1 Methods and Techniques

Box et al. [2] describes the benefits and methods for conducting fractional factorial analyses. Factorial designs involve the analysis of all possible combinations of a number of factors or parameters at a fixed number of levels. Often, and for the purpose of this masters thesis, the factorial design will have two levels, a high and low quantitative boundary for each factor. Conducting a fractional factorial design statistically reduces the number of combinations of factors to be analyzed, while retaining the ability to represent the outcome of a full factorial analysis. The benefits of conducting a two-level fractional factorial design are as follows. First, they require fewer parametric runs for each factor studied. Secondly, they can provide direction for expanding the scope of experimentation by identifying a sub-set of more sensitive parameters out of a large range of

parameters. Lastly, the fractional factorial design allows the experimenter to observe factor dependencies or interactions between factors, which is lost when the study is conducted as a "one-factor-at-a-time" parametric study.

Similarly, the National Institute of Standards and Technology (NIST) published an e-handbook of statistical methods [29] that also describes the benefits and methods for conducting fractional factorial analyses. Paired with Box et al., methods for developing design of experiments, for conducting the fractional factorial analysis, and processes for analyzing results were established.

2.2.2 Related Research

A number of studies have used fractional factorial designs and optimization techniques to enhance the analysis of particular data sets. The following reviews have used these experimental designs and techniques to examine details of simulated data regarding building energy consumption and demand.

Cheng et-al. [5], identifies primary factors that impact the optimal control of passive thermal storage using an integrated optimization and building simulation tool. A fractional factorial analysis was conducted to identify primary factors related to building characteristics that impact energy cost savings. Results showed that peak demand was impacted the most by the level of thermal mass within the building, showing reductions of 32% and 42% for the base and test level cases. HVAC equipment properties such as efficiencies and part-load performance also had significant impact to peak demand. Cost savings were affected by the amount of internal loads within the building, followed by the mass level and HVAC equipment efficiencies. Relative savings associated with demand and total costs were found to be the greatest in Phoenix, followed by Atlanta, New York, and lastly, Los Angeles.

Braun [3] investigates the potential for cost savings associated with the optimization of central plant HVAC control strategies and the utilization of existing building thermal capacitance for high-rise buildings. A fractional factorial analysis was not used in this research, however, the research had a similar goal and the results are relevant to the topic of this thesis.Results showed that by optimizing the control of building thermal storage, energy costs and peak electrical use can be greatly reduced. Factors affecting the dynamic control of a building were identified to be the design and use of the building, the performance characteristics of

the cooling plant and air handling equipment, and the utility rate structure. These factors were identified by applying dynamic optimization techniques to building energy models focusing on building cooling systems. TRNSYS software was used to conduct this study. A variety of operational conditions were explored to determine the maximum amount of cost savings. Factors affecting the cost savings were identified, in order of importance, to be the utility rate structure, part-load characteristics of the cooling plant and air handling system, weather, occupancy schedules, and building thermal capacitance.

Other studies have been conducted to test the sensitivity of building parameters. Lam and Hui [22] examined approximately sixty parameters and their effect on the energy performance of an office building in Hong Kong. Using DOE-2 building simulation software, Lam and Hui found that building energy consumption and peak design loads are most sensitive to measures regarding internal loads, fenestration details, temperature setpoints, and efficiencies associated with the HVAC plant system.

2.3 Conclusions

A wide range of literature exists regarding building energy model simulation and calibration, as well as sensitivity studies of factors that influence building control and building energy consumption and demand. Literature regarding sensitivity analysis of model factors focused primarily on only a few specific applications. Those applications included determining a sub-set of sensitive factors that affect optimal control strategies for passive thermal storage, dynamic control strategies for buildings, energy cost savings, and the energy performance of buildings. The studies conducted by Lam and Hui [22] were most relevant to the research presented in this masters thesis. However, Lam and Hui's research was restricted to high-rise commercial buildings located in Hong Kong. This thesis research will expand on a similar scope that determines the sensitivity of factors that affect high-rise commercial office building energy performance throughout a sweep of climates, and for multiple seasons. This research will also examine design values for twenty-two commercial high-rise office buildings and will focus on three buildings for model calibration and fractional factorial analyses.

Calibration techniques presented in the reviewed literature have been adopted into the research of this masters thesis. In particular, methodology used to calibrate building energy models and the associated error

analysis were examined. Hourly sub-metered data was made available to Clean Urban Energy through the Chicago utility provider, ComEd, for each building that participated in the CUE 2009 summer demonstration. Hourly data made it possible to accurately determine operation and load schedules. However, for the purpose of this thesis, the final model calibration was based on the assessment of monthly and annual comparisons of simulated and metered data energy usage. Calibration techniques similar to those discussed by Yoon and Lee [41] were adopted to determine model mismatch on a monthly and annual basis.

Chapter 3

Background, Building Selection, and Audit Procedures

3.1 Background

3.1.1 Clean Urban Energy

Clean Urban Energy, Inc. (CUE) is a company based in downtown Chicago, Illinois. CUE technology works in tandem with building automation systems to optimize HVAC operation on an hourly basis. The optimization software returns hourly temperature setpoints, suggesting pre-cooling strategies and optimal HVAC settings that are bounded by thermal comfort boundaries throughout the day. To determine the optimal hourly temperature setpoints, the optimization algorithm considers the building thermal capacitance and thermal history, real-time electricity pricing, and weather conditions.

The CUE automated web-based technology is also intended to "integrate large commercial building HVAC operations with electric grid operations and markets." [9] With a portfolio of high-rise commercial buildings using CUE technology, source and site peak-demand loads can be shifted to off-peak hours, driving goals to:

(1) Reduce HVAC energy use and expense for each building

(2) Improve electric generation efficiency and environmental performance

(3) Introduce demand elasticity into grid markets

Preparing each building for optimization requires a number of time intensive steps. Beginning with a building walk through audit, building information is collected from drawings and site visits. This information

is then used to develop a building energy model that is calibrated to hourly utility data. Lastly, the calibrated model is fed to the optimization program which determines optimized hourly temperature setpoints based on the thermal history of the building, real-time electricity costs and current weather data. The optimized temperature setpoints are passed on to the building automation system, controlling zone temperatures while taking advantage of the thermal capacitance of the building. A schematic of this process is represented in Figure 3.1 below.

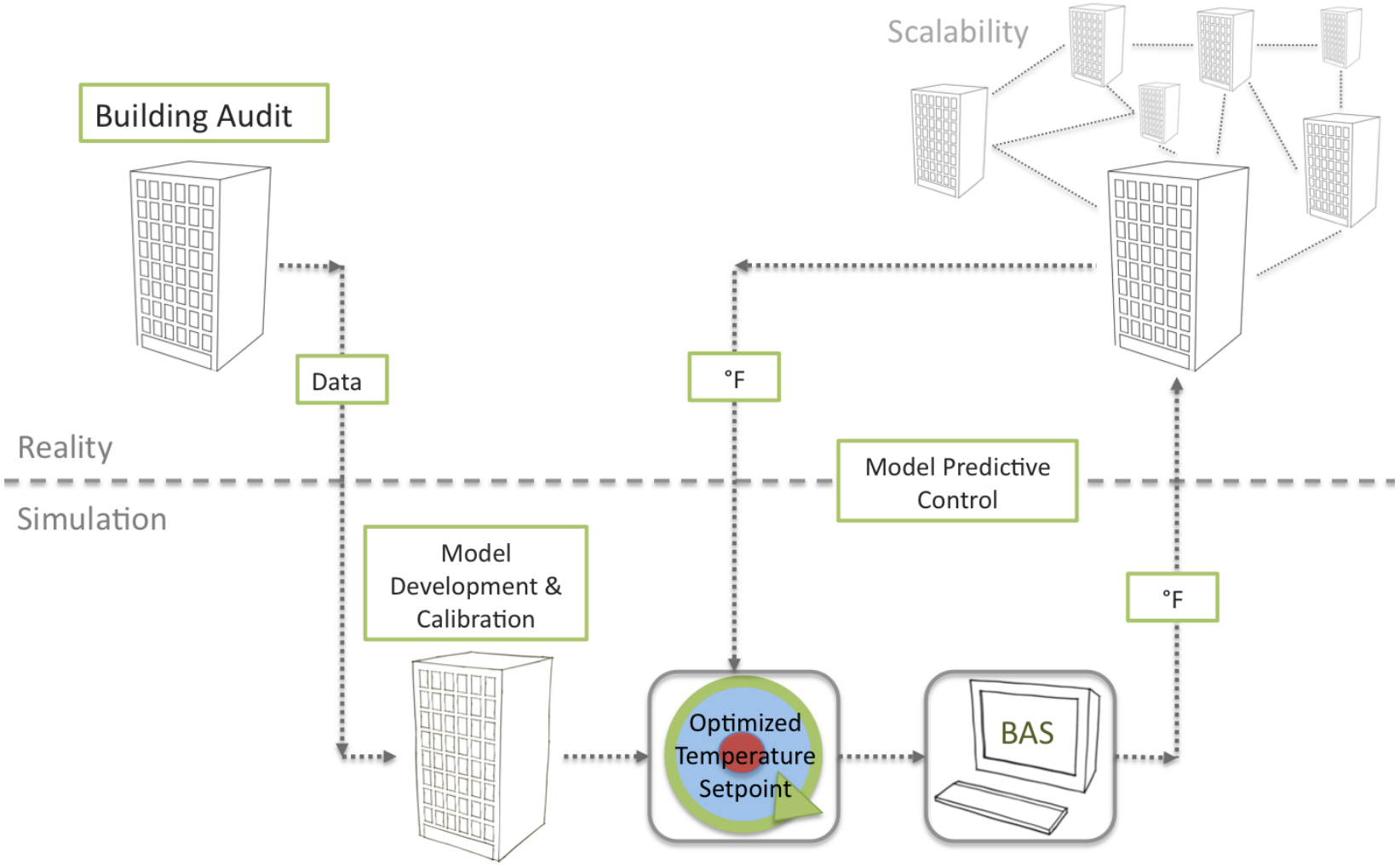

Figure 3.1: Schematic of the CUE optimization process.

3.1.2 BOMA Chicago

In anticipation of going to market in 2010, CUE partnered with the Building Owners and Managers Association (BOMA) of Chicago to solicit buildings to participate in CUE's 2009 summer demonstration. Fifty high-rise commercial office buildings in the downtown Chicago Loop participated, of which twenty-five were audited and eight have been modeled, calibrated and subjected to the optimization program, as of the end of 2009.

Data collected from the 2009 demonstration buildings were analyzed in effort to develop procedures to streamline the audit process and to expedite the development of building energy models using EnergyPlus software. A fractional factorial analysis (FFA) was also conducted using this data, to determine the effects of a large number of parameters within an energy model on electric consumption and demand associated with the chiller plant, HVAC system and the whole-building facility. The parameters used in the fractional factorial analysis were carefully chosen to represent the internal gains and systems within the building. These parameters are listed in Table 3.1 below.

Table 3.1: Factors considered in Fractional Factorial Analysis

Factor	**Units**
Envelope	
Wall Insulation Thickness	m
Window U-Value	m^2K/W
Window Solar Heat Gain Coefficient (SHGC)	%
Thermal Mass	
Mass Area of Structural Components	m^2
Mass Area of Interior Furnishings	m^2
Internal Loads	
Lighting Power Density	W/m^2
Continued ...	

Table 3.1: (continued)

Factor	**Units**
Equipment Power Density	W/m^2
Air System	
Supply Air Temperature	℃
Supply Fan Static Pressure Rise	Pa
Chilled Water Loop	
Chilled Water Loop Temperature Differential	℃
Chiller	
Chilled Water Loop Temperature Differential	℃
Chiller Efficiency	COP
Condenser Water Return Temperature	℃
Chilled Water Condenser Loop	
Condenser Water Loop Temperature Differential	℃
Cooling Tower Wet Bulb Design Air Temperature	℃

By identifying model parameters that greatly affect building energy consumption, we can direct building audits and model development processes to focus on those specific components, thus reducing time needed to audit a building and to build an accurate model. Going further, if results show that the same small sub-set of parameters have similar effects on multiple high-rise office buildings, then a prescribed audit and modeling processes can be applied to all high-rise office buildings with a high level of confidence.

3.1.3 Chicago Utility Structure

ComEd, the largest utility provider in Illinois, provides service to approximately 70 percent of the state's population [7]. Unlike most metering structures seen throughout the country, Chicago is unique in that ComEd sub-meters individual tenants as well as base building utility loads for each commercial building. ComEd also offers a free program that allows building owners and operators to monitor and track

their electricity consumption though an online program called Energy Insights Online. With access to such a detailed breakdown of electricity distribution within a building, model calibration can be achieved with greater accuracy and without the hassle of measuring electric loads by individually placing metering devices on each panel board feeder.

Although detailed meter data is beneficial, it is not always clear what end uses are associated with a particular meter and often, this information is unknown to the building owners and operators. It is also common to find a range of end uses associated with one particular meter, further complicating things. To discern these end uses, tools such as Energy Insights Online were used to analyze each meter's electricity load profile. A graphic of the online profiler can be seen in Figure 3.2 below. Here, load profiles were examined and engineering judgement was used to determine each meter's end use.

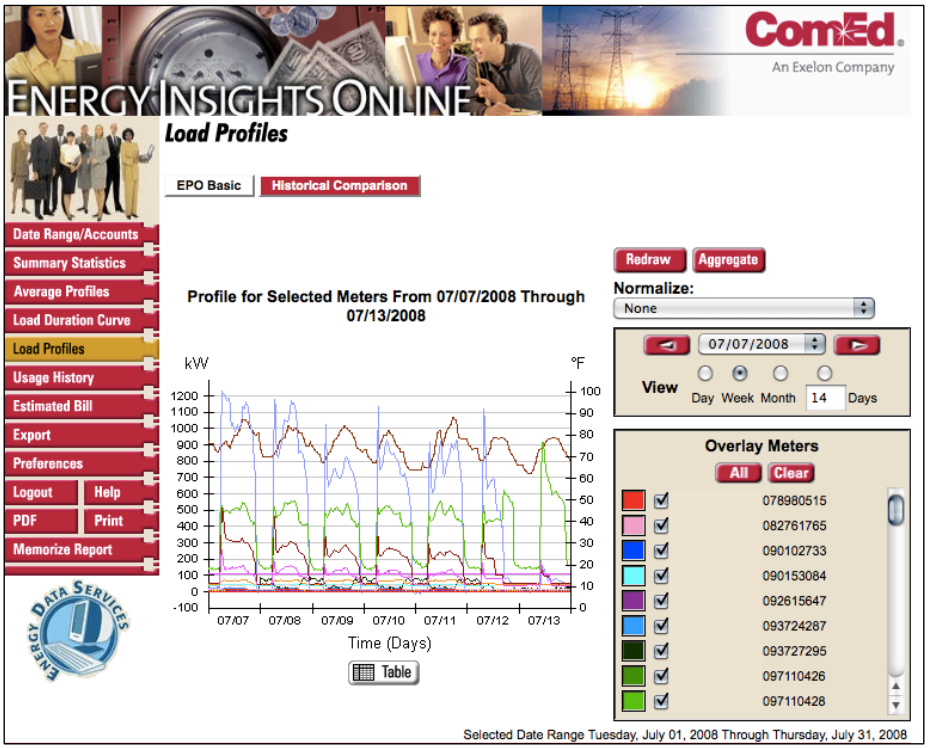

Figure 3.2: Example of ComEd's Energy Insights Online online electricity monitoring program. The graphs show load profiles for various meters associated with the building.

Chicago is also unique in that it uses electricity to heat most of it's buildings. Starting in 1892, Samuel Insull began to change public utilities in Chicago. Over 10 years, Insull established a monopoly of "central station electric service," and founded the Commonwealth Edison Company, which is now known as *ComEd* [27]. Using low rates and marketing schemes, Insull gained key power contracts that pushed Commonwealth Edison Company utilities to expand from the city of Chicago to surrounding suburban areas. Post World-War II, the Commonwealth Edison Company also became the first to own and operate a nuclear power plant. Dresden Station opened in 1960, and with it's opening, the Commonwealth Edison Company launched a building program that would make the Chicago area the most dependent metropolitan area on electric energy [27].

Following the history of ComEd, most of the buildings audited for this research used electric resistance heating. Only a handful of the buildings used hot water heating systems, which is somewhat atypical for the rest of the country. Since the research presented in this thesis is meant to represent typical commercial high-rise office buildings, the reader should take note of the HVAC system types used for the fractional factorial analysis. As noted in the following chapters, one building was considered in this research that does utilize hot-water reheat.

3.2 Building Selection and Classification

3.2.1 2009 CUE Summer Demonstration

Data from the twenty-two audited buildings were collected and used for statistical analysis in this research. As a prerequisite for CUE technologies, the buildings that participated in the summer demonstration were required to be high-rise commercial office buildings with central plant VAV systems. Ranging in vintage and size, the twenty-two buildings provided a well rounded representation of high-rise office building characteristics typically found in cities across the United States. A summary of minimum, maximum, and average values associated with each buildings's vintage and size can be found in Table 3.2 below. A complete summary of values for each building collected for this research can be found in Appendix A.

Table 3.2: Building geometry characteristics

Field	**Min**	**Max**	**Average**
Year Built	1927	2005	1980
Number of Floors	10	51	32
Footprint Area	980 m^2	3,400 m^2	2,400 m^2
Floor-to-Floor Height	3.12 m	4.35 m	3.70 m
Window-to-Wall Ratio	20%	70%	45%
Number of People	900	5,000	2,300

3.2.2 Building Classification

Buildings can be classified by three main categories: their physical characteristics, HVAC system type and configuration, and by the building's typical operational patterns [18]. As noted above, each building that participated in CUE's summer 2009 demonstration was required to be a high-rise commercial office building, with a central plant VAV system. The operational patterns and internal loads of each building were typical of a high-rise office building, and slight variance in schedules and loads could be seen in the calibration process when comparing the energy model to hourly sub-metered utility data. HVAC systems were also similar. Differences were typically seen in the reheat options and terminal system configurations. Unique to Chicago, most buildings use an electric reheat option, either as perimeter baseboard heaters or in the terminal box. Only a handful of buildings used hot water reheat.

Three terminal system configurations were found to be most common out of the 25 buildings that were audited. These system configurations included VAV terminal boxes, which had either electric baseboard reheat, electric resistance reheat in the terminal boxes, or hot water reheat in the terminal boxes. The second most common configuration were series power induction units (PIU) with electric resistance reheat, and the least common configuration were parallel PIUs with electric resistance reheat. More detail on each building's terminal system configuration can be found in Appendix A.

To classify these buildings further, building size and vintage were noted. Most buildings had simple

rectangular prism geometry, which was used for each building model to simplify the modeling process. Differences in volume due to geometrical design features were captured by altering the building footprint, while retaining the appropriate number of stories and floor-to-floor height. To further simplify the building model, each building was modeled with only three-floors and fifteen zones. Five zones were assigned to each floor, to capture the difference in heat transfer along on each facade's perimeter zone, as well as the heat transfer seen in the core of the building. Perimeter zones have a depth of twelve feet and, to account for the building's realistic number of floors and volume, a floor multiplier was applied to the middle floor. A graphical representation of a building model that was generated by the EnergyPlus OpenStudio plugin for Google SketchUp can be seen in Figure 3.3.

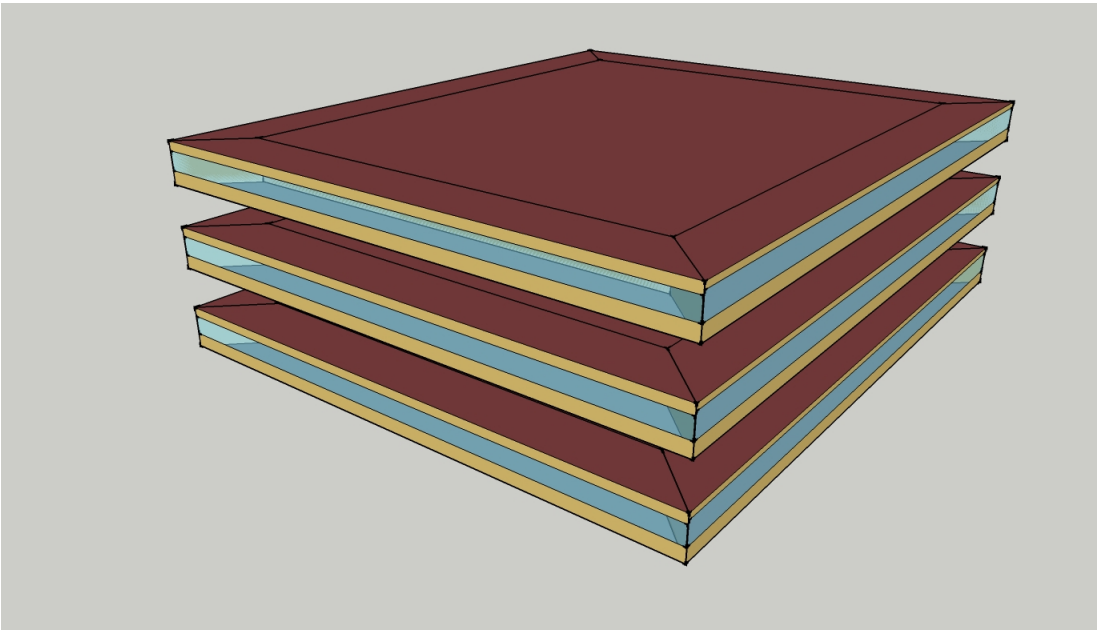

Figure 3.3: A graphical representation of a 15-zone EnergyPlus model, as depicted in Google SketchUp. A floor multiplier was applied to the middle floor to account for the building's total number of floors.

As seen in Table 3.2 above, building vintage for the 22 buildings spanned a wide range. In past research, it has been typical to classify buildings as pre- or post-1980's [18]. However, with the growing number of financial incentives to retrofit existing buildings, we found that most of the buildings had retrofitted lighting, electrical equipment and HVAC equipment within the past 10 years of this study. Thus, it was assumed that buildings of older vintage had been updated to the point where they were comparable to newer buildings.

3.3 Audit Procedure and Data Collection

3.3.1 Processes for Conducting a Walk Through Building Audit

Managing the large number of building audits for the 2009 CUE summer demonstration required a significant amount of coordination, planning and direction. To begin, a goal was identified to help direct the audit process. With CUE's intention to optimize the HVAC operation of a portfolio of high-rise office buildings, the focus of each building walk-through audit was to gather enough information to accurately represent the building HVAC system components and loads in a building energy model using the EnergyPlus software. The EnergyPlus modeling software was chosen for its ability to model HVAC systems in great detail.

Based on input parameters needed for an EnergyPlus input data file (IDF), a set of standard questions were formed to ensure that an appropriate amount of information was collected during each building audit. Before conducting the audit, a pre-audit worksheet was sent to the building operators that was to be completed prior to the audit. This worksheet requested the information listed below and was used to gain an overview of the physical and operational parameters of the building before the audit was conducted.

(1) **Building Type** — For the purpose of the CUE project and for this masters thesis research, each building was required to be a high-rise commercial office building.

(2) **Building Geometry and Construction** — Information was requested regarding the overall building geometry and construction types, including: building vintage, number of stories, footprint area, floor-to-floor height, floor-to-ceiling height, window-to wall ratio, and general exterior wall and roof construction types.

(3) **Schedules** — General occupancy and HVAC operation schedules were requested, as well as heating and cooling temperature setpoints during occupied and unoccupied operation hours.

(4) **HVAC System Type** — Information regarding main HVAC system components and equipment type were requested. This information included: equipment manufacturer, model, and size/capacity. Since each building was required to have a central plant VAV system, information about the terminal

system configuration was also requested.

(5) **Metered Data** — Metered and sub-metered data is necessary for calibrating the building energy models. As mentioned above, each building was required to register with ComEd's Energy Insights Online program, and access to metered data was requested. Any subsequent metering or data logging conducted by the building operator pertaining to zone air temperatures, outdoor temperature and humidity, power consumption of equipment, or operational settings of major HVAC equipment were also requested.

During the actual building audit, the auditors based questions on the pre-audit worksheet and confirmed HVAC system types, schedules, and monitoring systems. After a sit-down meeting with the building managers and operators, a walk through tour of at least two representative floors of the building was performed. During this time, lighting and equipment power density were evaluated, as well as a quick occupancy survey and note of interior furnishings to determine a level of internal mass within the building. Digital photographs were taken of each space to hold on record for future reference when modeling the building.

The building walk-through included a tour of the mechanical floors of each building. Touring these spaces helped to understand the HVAC system configuration, equipment, and the layout of duct work throughout the building, which is crucial for accurately developing the heating and cooling systems of the building within an energy model. Flow volume measurements, air and water temperature readings, power measurements of the chiller, lights, and plug-loads form the main circuit breaker would have helped in model development. However, due to lack of instrumentation and time, these values were determined from the design values noted in the mechanical and electrical drawings.

Most of the buildings that were audited did not have digital copies of their building drawings. The most efficient way to gather data from drawings, as determined by the auditors (which included the author of this thesis), was to take high resolution, digital photographs of the drawings needed to aid in the construction of each building energy model. To make the process of collecting this data more efficient, we requested that the following drawings to be available for the auditors upon their arrival.

(1) **Architectural** —

(a) Floor plans for typical floors representing the building

(b) Elevation plans to exhibit floor-to-floor height, number of stories, and window-to-wall ratio

(c) Detailed plans that specify wall, roof, and window construction details

(2) **Mechanical** — Mechanical schedules outlining specific HVAC equipment, manufacturers, models, and equipment characteristics

(3) **Electrical** — Lighting and power schedules as well as electrical one-line diagrams

3.3.2 Data Organization

To organize the multitude of data collected in each building audit, spreadsheets were developed by the author to manage the data. The spreadsheets also helped streamline the data collection and modeling process, by pulling particular data from the audit and drawings that is needed for the development of an EnergyPlus model and automatically converting those input parameters to the correct SI units. The data requested in the spreadsheet pertains to building loads, operation and HVAC system equipment. Table 3.3 lists the particular data collected from the building audits that was used to develop the building models.

Table 3.3: Data collected from each building audit

Factor	**Units**
Internal Loads	
Lighting Power Density	W/m^2
Equipment Power Density	W/m^2
People Density	$\#/100m^2$
Schedules	
Lighting and Equipment	Fractional
Occupancy	Fractional
HVAC	On/Off
Continued ...	

Table 3.3: (continued)

Factor	**Units**
Temperature Setpoints	Temperature ℃
Architectural Components	
Window to Wall Ratio	%
Window U-Value	m^2K/W
Window Solar Heat Gain Coefficient (SHGC)	%
Wall Insulation Thickness	m
Supply and Return Fans	
Fan Efficiency	%
Pressure Rise	Pa
Maximum Flow Rate	m^3/s
Motor Efficiency	%
Terminal System Type	
Perimeter System Type	−−
Core System Type	−−
Reheat Option	−−
Cooling Coil	
Design Water Flow Rate	m^3/s
Design Air Flow Rate	m^3/s
Design Inlet Water Temperature	℃
Design Inlet Air Temperature	℃
Design Outlet Air Temperature	℃
Heating Coil	
Maximum Water Flow Rate	m^3/s
Continued ...	

Table 3.3: (continued)

Factor	**Units**
Rated Capacity	W
Design Air Flow Rate	m^3/s
Design Inlet Water Temperature	℃
Design Inlet Air Temperature	℃
Design Outlet Water Temperature	℃
Design Outlet Air Temperature	℃
Chiller	
Reference Capacity	W
Reference COP	W/W
Reference Leaving Chilled Water Temperature	℃
Reference Entering Condenser Fluid Temperature	℃
Reference Chilled Water Flow Rate	m^3/s
Reference Condenser Water Flow Rate	m^3/s
Boiler	
Fuel Type	−−
Nominal Capacity	W
Nominal Thermal Efficiency	%
Design Water Outlet Temperature	℃
Design Water Flow Rate	m^3/s
CHW and CW Pumps	
Rated Flow Rate	m^3/s
Rated Pump Head	Pa
Rated Power Consumption	W
Continued ...	

Table 3.3: (continued)

Factor	**Units**
Motor Efficiency	%
Cooling Tower	
Design Inlet Air Wetbulb Temperature	℃
Design Water Flow Rate	m^3/s
Design Air Flow Rate	m^3/s
Design Fan Power	W

An example of the spreadsheet can be found in Figures 3.4. Note that the user inputs data from the building's mechanical schedule into the grey portion of the spreadsheet. The white box at the top of the spreadsheet, labeled "EnergyPlus Input", automatically sums or averages values from the mechanical schedule and converts them to the appropriate SI units. The "EnergyPlus Input" values are organized in the appropriate order as listed in an EnergyPlus IDF.

Fan Schedule
Sample Building

EnergyPlus Input:

Supply Fan

Fan Efficiency:	#DIV/0!
Pressure Rise (Pa):	0.00
Max Flow Rate (m3/s):	0.00
Motor Efficiency:	#DIV/0!

Return Fan

Fan Efficiency:	#DIV/0!
Pressure Rise (Pa):	0.00
Max Flow Rate (m3/s):	0.00
Motor Efficiency:	#DIV/0!

DO NOT FORMAT THIS AREA

Supply Fan

Fan	Service	Quantity	CFM	Total CFM	Total m3/s	Pressure (inWG)	Pressure (Pa)	Fan Efficiency	HP	Total HP	W	Motor Efficiency
SA1				0	0		0			0	0	
SA2				0	0		0			0	0	
SA3				0	0		0			0	0	
SA4				0	0		0			0	0	
SA5				0	0		0			0	0	
SA6				0	0		0			0	0	
SA7				0	0		0			0	0	
SA8				0	0		0			0	0	
SA9				0	0					0	0	
SA10				0	0					0	0	
SA11				0	0					0	0	
TOTAL				**0**	**0**	**0**	**0**			**0**	**0**	
AVERAGE								**#DIV/0!**		**0**	**0**	**#DIV/0!**

Return Fan

RA1				0	0		0			0	0	
RA2				0	0		0			0	0	
RA3				0	0		0			0	0	
RA4				0	0		0			0	0	
RA5				0	0		0			0	0	
RA6				0	0		0			0	0	
RA11				0	0		0			0	0	
TOTAL				**0**	**0**	**0**	**0**			**0**	**0**	
AVERAGE								**#DIV/0!**		**0**	**0**	**#DIV/0!**

Figure 3.4: An example of the organizational spreadsheet used to manage HVAC data collected from each building audit.

As each building is complex and different, the spreadsheets represent only the major components of the building and does not represent the minute details specific to any particular building. Specific operating schedules and equipment characteristics can be fine-tuned during the calibration process, when comparing simulation data to metered data.

Chapter 4

EnergyPlus Model Development and Methodology

4.1 Overview

Building energy models (BEM) have many uses that benefit the building science community. By virtually representing the transfer of energy and heat throughout a building, experiments can be conducted to better understand building thermal dynamics, energy consumption and demand trends, as well as control strategies for optimally running particular equipment within a building. A handful of energy modeling programs are available for download. The two most popular are freeware called DOE-2 and EnergyPlus. These two modeling programs are very similar in application, allowing the user to model whole-building energy components including heating, cooling, lighting and internal loads, ventilation, and other energy flows [28]. EnergyPlus was chosen for the work presented in this research and for efforts led by CUE because of its ability to model HVAC equipment in greater detail compared to DOE-2.

EnergyPlus is a "stand-alone" simulation program that lacks a user-friendly graphical interface [28]. Input and output files are in text format, which can be hard to use and manage. For better management, a number of graphical interfaces have been developed by the EnergyPlus team and by members of the private sector to create, edit and run Input Data Files (IDFs), as well as to view and compare results. A number of these graphical interfaces were used in this work to generate IDFs, size HVAC system components, check for model plausibility, and for model calibration purposes. Specific tools will be presented in the following sections of this chapter.

4.2 IDF Generation

The EnergyPlus Example File Generator (EEFG) was used to initially create the EnergyPlus IDFs for each building. The EEFG is a free online service developed by the National Renewable Energy Laboratory and the US Department of Energy that generates executable IDFs based on a select number of modeling inputs and a specified ASHRAE 90.1 design standard [21]. In detailed form, the user can specify building type, basic geometry and construction, window-to-wall ratios, simplified zoning patterns, building activity loads and power densities, simple HVAC system types and components, and amount of photovoltaics if applicable. This on-line service provided a good starting point for developing models for the efforts of this research. However, modifications to each IDF were needed in order to accurately represent the HVAC system and terminal system configurations, as seen in the buildings that were audited in Chicago.

The EEFG HVAC options are limited to ASHRAE 90.1 Appendix G system types, and System 7 and System 8 are the only two HVAC system types that are applicable to high-rise commercial office buildings. As referenced in ASHRAE Standard 90.1 Appendix G, these two system types apply to nonresidential buildings that have more than five floors or a floor area greater than 150,000ft^2. The simplified HVAC system configuration for each type are as follows.

(1) **System 7** — Variable air volume (VAV) with hot water reheat

(2) **System 8** — VAV with parallel fan powered (PFP) terminal boxes and electric resistance reheat

A number of resources were used to understand how to correctly modify the HVAC system configuration for each IDF. These resources included the EnergyPlus Input Output reference, Engineering reference, and example files that are available through the EnergyPlus download. From these references, the construction of particular system configurations relevant to this project were examined, and simple GREP (Global Regular Expression Print) codes were developed to find and replace text regarding system components and connecting nodes within the IDF. One could also develop an IDF using the reverse process, starting with an appropriate EnergyPlus example file and modifying the IDF to accurately represent the occupancy, internal loads, HVAC operation, and schedules of a real building. The disadvantage of this approach mostly pertains to the geometry and geometry modification, since the building geometry would have to be modified using

the Google SketchUp program. With the decision to use simplified geometry for this research, it was easier, and time efficient, to enter basic building geometry (length and width of the building, floor-to-floor height, and number of floors), window-to-wall ratio, and a zoning pattern into the EEFG, and modify the HVAC system types with the simple GREP codes described above.

To validate the HVAC system configuration, an SVG (scalable vector graphic) browser application was used to view the SVG file generated by EnergyPlus (in this case, the Unix-based Squiggle program was used). The SVG file contains an HVAC diagram that graphically displays color-coded system components and node connections, enabling the user to see the direction of fluid flow through each component of the HVAC system [35]. If the HVAC system was configured incorrectly, the user would be able to graphically see where errors occurred and where particular nodes were not properly connected. An example of the HVAC diagram is shown in Figure 4.1 below.

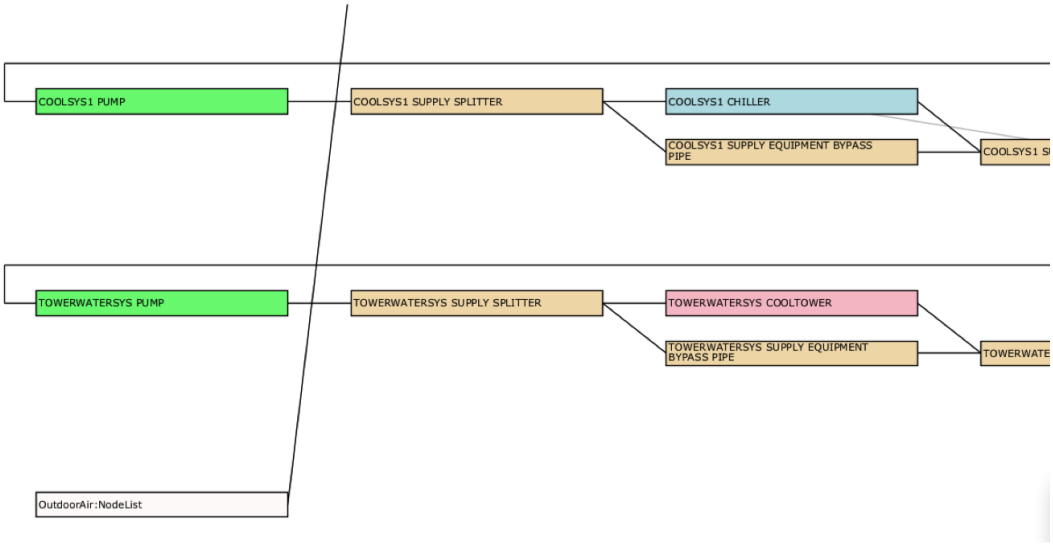

Figure 4.1: Illustration of a section of an HVAC diagram using an SVG browser.

A few assumptions were made when modeling the HVAC systems. In reality, multiple chillers were utilized to meet the cooling demands of each building. Depending on the weather conditions, the building engineers would turn on the appropriate number of chillers, combining capacities to meet the heating loads anticipated for each day. To simplify the chillers in each EnergyPlus model, only one chiller was modeled. To do this, the chiller capacities were summed and the COP values were averaged. Performance curves were

chosen to match those of the most commonly used chiller in the building. Some error is associated with this approach, for this method neglects some effects attributed to the part-load performance. By adding the chillers together, the "combined chiller" may run at a lower part-load ratio than in reality. At a lower part-load ratio, the chillers operate at a lower efficiency, thus falsely increasing the amount of power associated with the chiller in the model. However, this increase in power was assumed to be negligible compared to total power consumption of the chiller, and the approach was used for this research.

Assumptions were also made for each air-handling unit. Typically, high-rise commercial office buildings are served by multiple supply and return fans that are located on the mechanical floors of each building. To simplify the models, the fans were also combined and modeled as one. In this case, the capacities of each fan were combined and the sum was used in the model under one fan object. Typically, building engineers keep a constant pressure rise throughout the main air-handling shaft of each building. This pressure rise value was used for the "combined fan" used in the model.

4.2.1 Model Plausibility Check

With the IDF properly assembled, data collected from the building audit was merged with the IDF by using the data organization spreadsheets mentioned in Chapter 3. From here, a program called xEsoView was used to view ESO output files generated by EnergyPlus [33]. xEsoView provides a quick, graphical representation of output variable values associated with model parameters. Any output variable can be displayed using xEsoView, and typically the program is used to view output variable values associated with energy consumption and demand, temperatures, humidity on an hourly, weekly, daily, monthly or annual scale. This tool contributes to an important step in model development, which is model validation. With xEsoView, the user can confirm model energy use, power densities, and operation schedules, and begin to match those to that of the actual building. An example of the file viewer can be seen below in Figure 4.2.

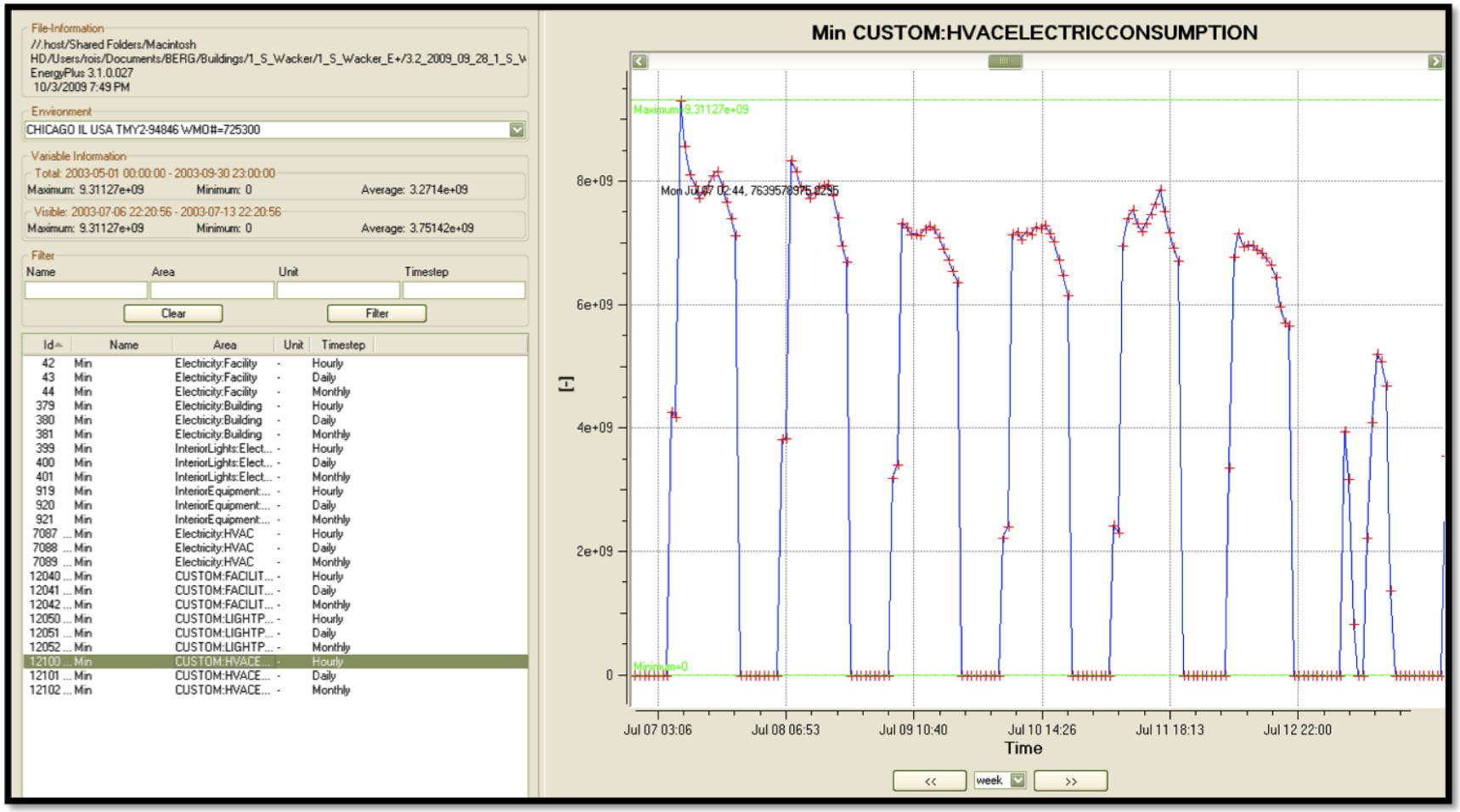

Figure 4.2: Illustration of output results for specified building energy model parameters as seen in the EnergyPlus ESO file viewer, xEsoView.

4.2.2 Utility Data Analysis and Model Calibration Techniques

Model validation continues in the calibration process. The calibration procedure is a critical process that can be long and tedious, and the accuracy of the calibration is highly dependent on the adeptness of the modeler. It can also be exceptionally difficult to calibrate models when dealing with complex buildings, such as high-rise commercial office buildings with a multitude of tenants, schedules, and plug loads. To help with this process, hourly sub-metered data was made available, with permission from the building owners, through ComEd's Energy Insights Online program. Having access to the sub-metered data made it easier to separate loads such as light and plug loads from HVAC system energy use. However, more often than not, the mapping of end-uses to sub-meters was not documented. To decipher these connections, engineering judgement was used to associate energy load profiles for each meter with particular equipment within the building, based on known typical equipment operation and energy use seen in industry.

A number of calibration methods were used in this research. These methods included trial-and-error, graphical comparisons of modeled data to sub-metered data, statistical techniques, and the use of an auto-calibration tool developed by graduate students at the University of Colorado at Boulder. The auto-calibration tool used Matlab to couple EnergyPlus to a hybrid Particle Swarm/Hooke-Jeeves optimization algorithm, to calibrate the energy of the model to sub-metered data [8]. The auto-calibration tool was most beneficial for calibrating parameters that were well represented by a particular sub-metered data set. In other cases, where multiple types of end uses were mapped to a particular sub-meter, it was more difficult to decipher whether the auto-calibration tool optimized on the correct components, or if it allowed for trade-offs between the different energy uses. An example of this would be a scenario where the auto-calibration tool attributes the best goodness of fit to HVAC energy use, when in reality, the energy use should have been associated with lighting loads. For these reasons, the auto-calibration tool could only be used in select situations and for select parameters.

To use the auto-calibration tool, model parameters within each IDF were replaced by *tokens*. The tokens act as flags, identifying those parameters that the auto-calibration tool would optimize on and find the best goodness of fit between simulated and measured data. To initiate the calibration, a range of values

were specified for each building parameter, which defined the boundaries, or decision space, for the tool to optimize within. The optimization algorithm first used the Particle Swarm (PSO) algorithm to conduct a coarse search within the decision space, because of its ability to quickly identify areas of local minima [8]. The PSO algorithm, as described by Kennedy and Eberhart, is a meta-heuristic algorithm that is based on the flocking behavior of social organisms, in that it searches the decision space according to a combination of randomized and simple rule-based decisions while sharing information about the best fit or solution found throughout the optimization [8]. Once a solution is found by the PSO, the auto-calibration tool then uses the Hooke-Jeeves algorithm to determine the local minimum in the area found by the PSO, using a general pattern search algorithm [8].

The initial values, or boundary values used in the hybrid optimization were chosen to represent a reasonable range in which a typical value for each parameter would fall. If the range was large, the algorithm more likely took a longer time to find the best "fit" for that parameter. However, with the approach that the PSO uses to search the decision space - using a combination of randomized and simple rule-based decisions - the search decisions could lead to an optimized solution in a short amount of time, even if the specified decision space is large. To ensure that the decision space wasn't too small, a simple observation was made. If the optimized result was close or equal to a limit of the decision space (boundary values), it was assumed that the optimized solution exceeded those bounds. In this case, the bounds were increased, and the auto-calibration was implemented again.

To further calibrate the model, line graphs and bar charts were used to graphically compare simulated energy use to hourly sub-metered utility data by method of two-dimensional time series plots and monthly percent difference calculations. Percent difference calculations were conducted to determine the accuracy of the model. For the purpose of this thesis, a 10% difference or less, between the energy of the model and sub-metered data, was considered acceptable for each month of data. A 5% difference or less was acceptable when comparing the data on an annual scale [20]. The percent difference was easiest to display graphically, in the form of bar charts. To make these graphical comparisons, a tool was developed by the author to view calibration results and to automate the graphing process. The program reads in EnergyPlus output data and compares it to hourly sub-metered utility data in graphical form, using both line graphs and bar charts.

The data was also segregated into four electric consumption groups: that for total facility, HVAC, light and plug, and electric heat. In Matlab, these figures are interactive, allowing the user to zoom in to a particular time period and scale. This feature is useful for determining schedule details, as well as seasonal trends in energy use. Figure 4.3 below shows a snapshot of the program's output, for a years worth of data.

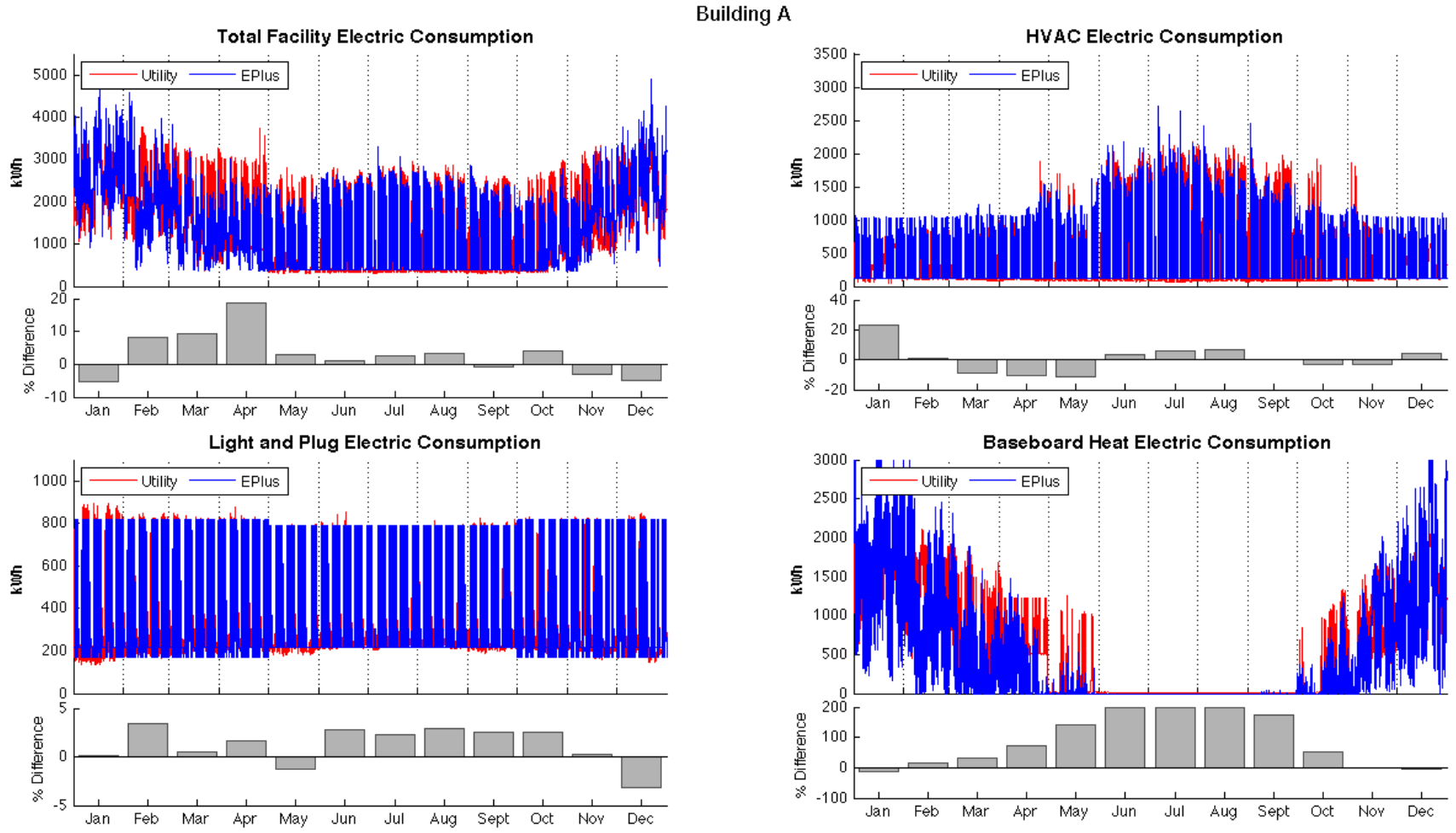

Figure 4.3: Matlab calibration tool developed by the author. The Matlab tool compares simulated energy use to sub-metered utility data in graphical form.

The graphical calibration method reveals the minute details of daily building operation schedules, portraying energy use trends for a given time scale and demonstrating model goodness of fit [13]. Since the Matlab tool is interactive, the user can zoom into specific weeks throughout the year to help fine-tune hourly schedules for occupancy, lighting, and HVAC operation. For this research, trends in the utility data were examined and a "typical week" of data was used to determine hourly schedules for week and weekend days for each season. Figure 4.4 shows an example of how the model hourly schedules for lighting, HVAC and whole building operation of Building A were matched to utility data. A "reheat coil availability schedule" set to "always on" was used for the baseboard electric heating coils. In this scenario, the heating coils are available when needed, or when outside weather conditions cause the perimeter zones of the model to dip below temperature setpoints. Therefore, with this scheduling approach, it was not possible to match hourly operation, and calibration accuracy was determined by monthly percent difference calculations.

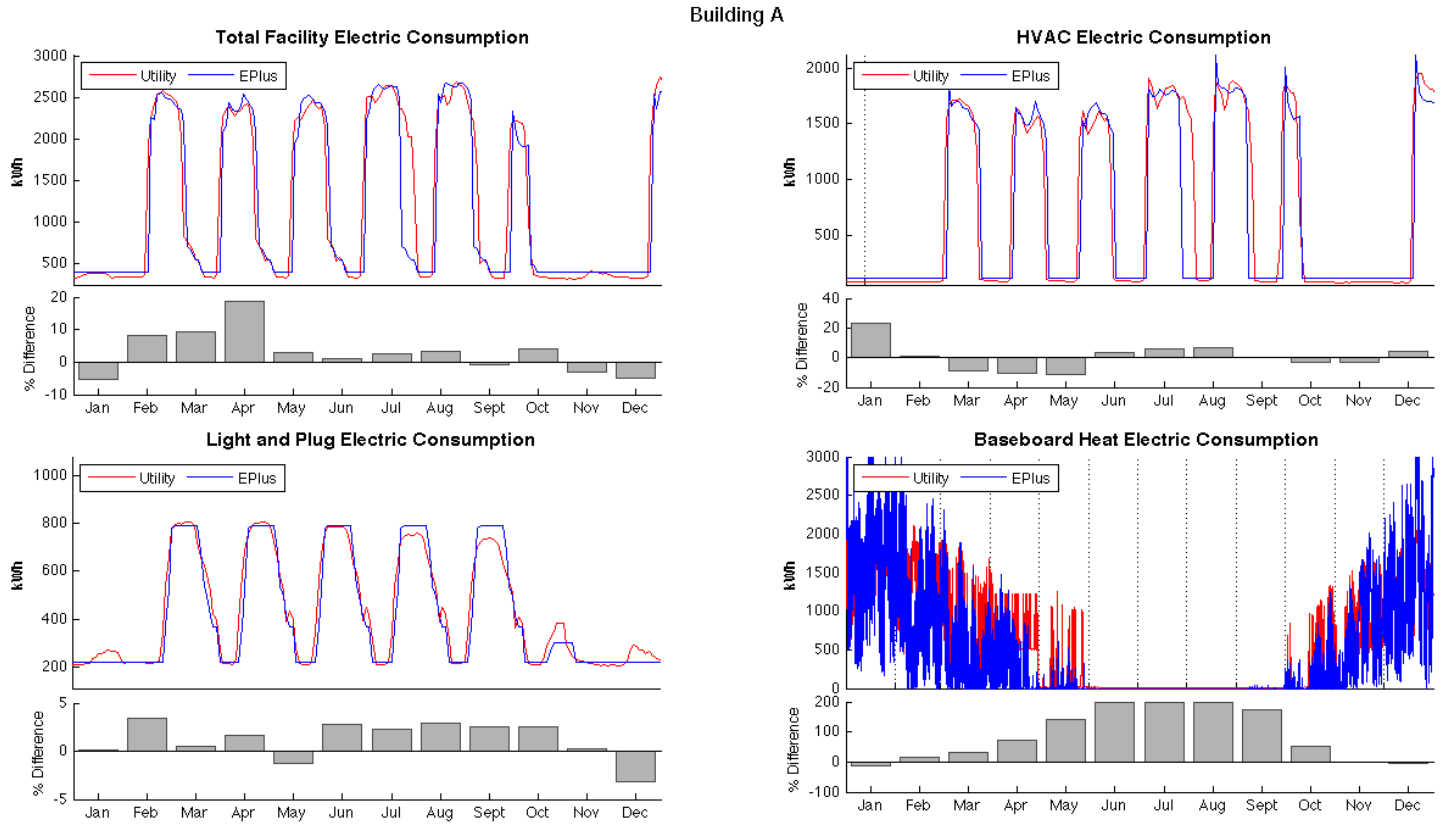

Figure 4.4: An example of how the Matlab calibration tool was used to determine hourly schedules for lighting, plug loads, and HVAC operation, based off of hourly utility data.

Some model mismatch is to be expected, for it is difficult to create hourly schedules that match utility data perfectly, especially for a 40-story building that has individual tenants on each floor. Law offices will have different operation schedules and plug and lighting load needs than those for a non-profit office. These differences are difficult to capture when modeling the building in a simplified manner, using only fifteen zones to represent the building as a whole. For the purpose of this research, schedules were created to best describe *typical* operation schedules, representing the whole building and depicting heating and cooling seasonal differences. Due to time restraints associated with the business goals of CUE, it was not possible to create more refined hourly schedules to better represent each day of the year. That said, the schedules used in each model were still sufficient to meet the goals of a 10% difference between the utility and simulated data for each month, as well as a 5% difference on an annual scale.

Seasonal schedule changes were most evident in the lighting data, for there was often a clear distinction of an increase in lighting use and operation during winter months in the utility signal. This can be seen in Figure 4.5 below, between the months of April and May, and were accounted for in the model schedules.

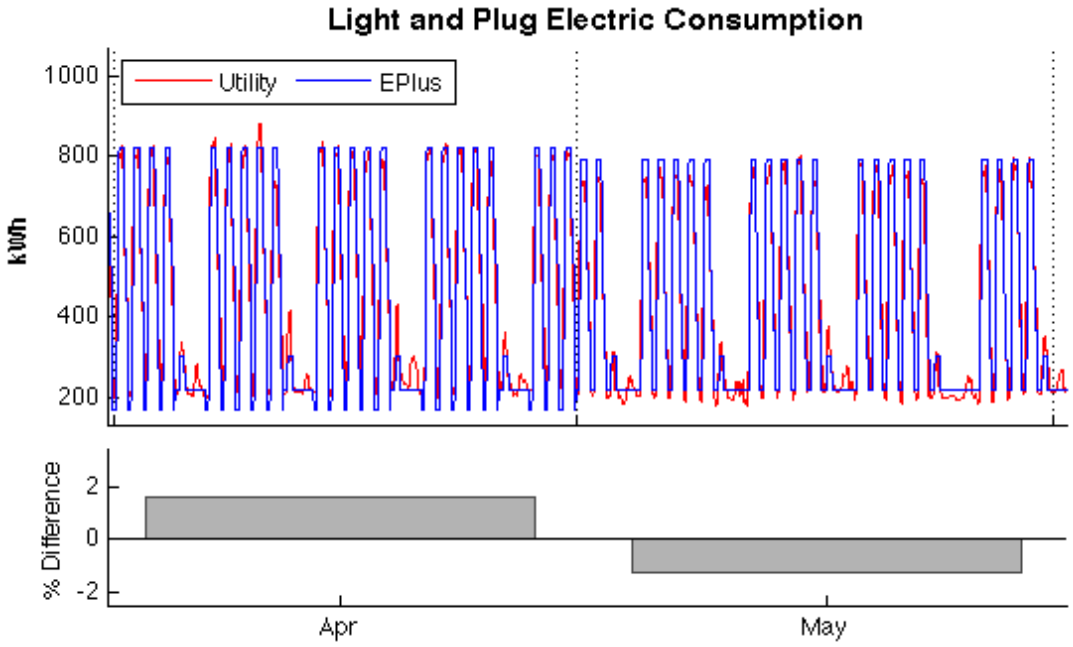

Figure 4.5: Illustration of the seasonal changes seen within the lighting and plug load utility signal for Building A.

A second tool was developed by the author (Figure 4.6), which is similar to the previously mentioned tool, but includes scatter plots of the data. Scatter plots allow the modeler to evaluate point-by-point goodness of fit, graphically and quantitatively [32]. They also help identify the variability and spread of the simulated data set. For example, in the HVAC scatter plot seen in Figure 4.6, one can see lines of data points that follow both the x and y axes. These "lines" of data show where schedules in the model hold values constant, when in reality, the those values are fluctuating and vice versa. The plots also show the spread of the simulated data, allowing the modeler to see where specific data points are being over or underestimated in the model. These plots are also beneficial for fine tuning model schedules to account for variability seen in utility data (due to weather, changes in internal gains, etc.) throughout the year.

In addition, statistical indicators were used to evaluate the calibration. The root mean square error (RSME) was calculated to quantify the variability or spread of the simulated data set compared to measured data [13]. The RMSE was calculated using the general equation below:

$$RMSE = \sqrt{\frac{1}{n}\sum_{1}^{n}(X_{n,measured} - X_{n,simulated})^2} \tag{4.1}$$

where n is the number of data points, and $X_{n,measured}$ is the sub-metered utility data and $X_{n,simulated}$ is the simulated data at each timestep. The coefficient of variation of the RMSE (CV(RMSE)) can be calculated to normalize the RMSE. The CV(RMSE) (%) is the RMSE divided by the mean of the measured data ($\overline{X_{n,measured}}$), which allows the modeler to have a better perspective on how well the model fits to measured data. A more accurately calibrated model will have a lower CV(RMSE). Hourly mean bias error (MBE) calculations determine a non-dimensional bias measure, measuring the sum of errors between the simulated data and metered data. This calculation provides a more accurate approach to evaluating monthly discrepancies between simulated and measured data, for in monthly percent difference calculations, the modeler is never sure if the calculation is presenting an accurate evaluation of model errors, or if positive and negative errors are canceling each other out [13]. The equations used for CV(RMSE) and MBE are noted below and a full set of calibration results can be found in Appendix A.

$$CV(RMSE) = \frac{\sqrt{\frac{1}{n}\sum_{1}^{n}(X_{n,measured} - X_{n,simulated})^2}}{\overline{X_{n,measured}}} * 100 \tag{4.2}$$

$$MBE = \frac{\frac{1}{n}\sum_{1}^{n}(X_{n,measured} - X_{n,simulated})}{\overline{X_{n,measured}}} * 100 \tag{4.3}$$

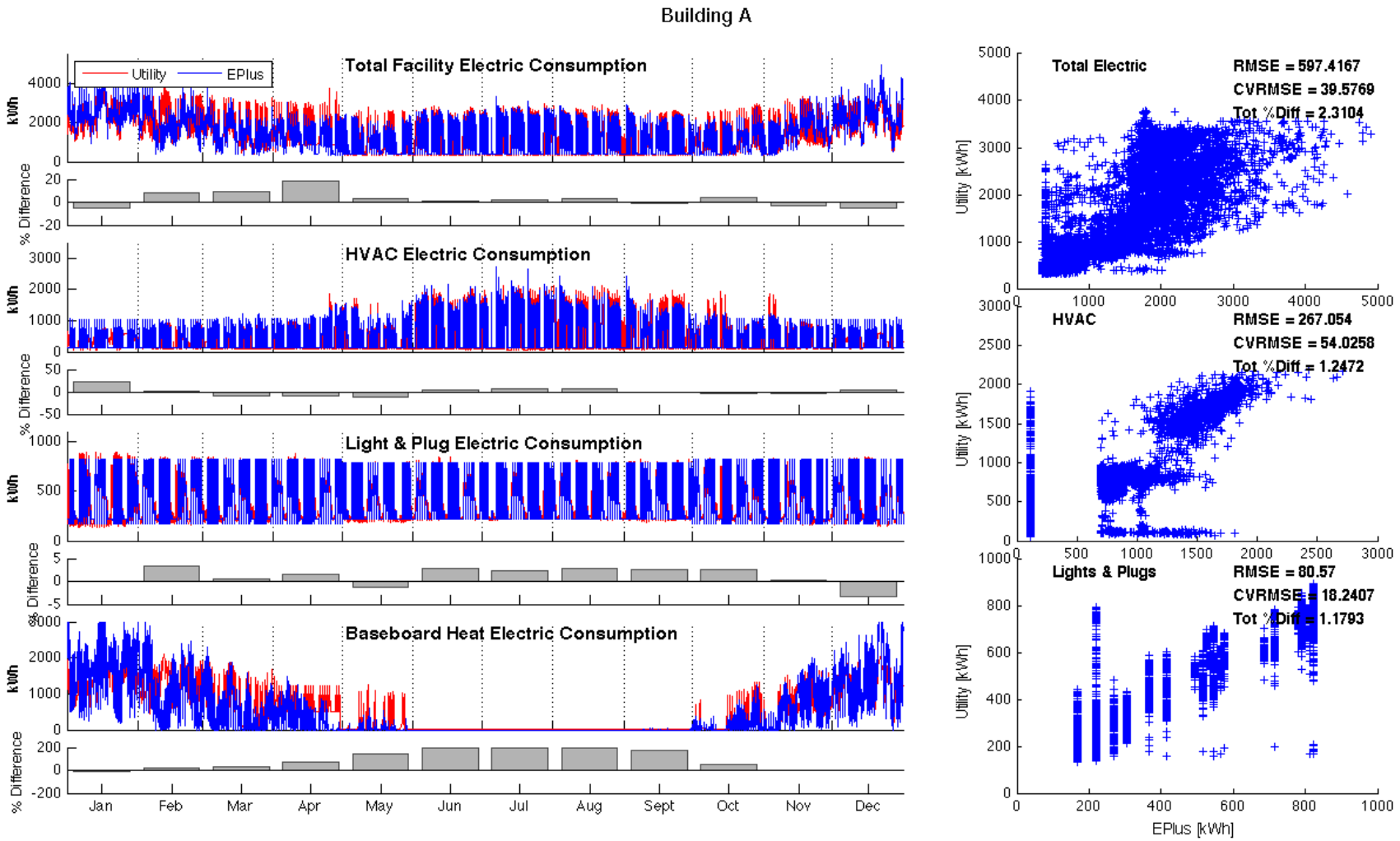

Figure 4.6: A second Matlab tool developed by the author. This tool includes scatter plots of the data to evaluate a point-by-point goodness of fit, and also displays the root mean square error.

To summarize the strategies and steps taken for auditing a building, developing a building model, and the calibration of a model to sub-metered data, a graphical flow chart was developed for quick reference. This flow-chart can be found in Appendix E and is intended to be used as a reference for future audit and modeling projects.

Chapter 5

Fractional Factorial Analysis

5.1 Overview

A two-level fractional factorial analysis (FFA) was conducted using a set of pre-determined factors (listed in Table 3.1) to evaluate the effects of each individual factor and two-factor interactions on the energy use associated with the heating and cooling loads of three buildings. The three buildings were chosen from the portfolio of buildings audited during the CUE 2009 summer demonstration. The buildings were chosen for two reasons. First, each of these buildings had a significant amount of data pertaining to building component details and sub-metered utility data. Secondly, they were chosen because they represented the most common HVAC system configurations that were seen out of the twenty-five audited buildings. It should also be noted that each building that participated in the CUE 2009 summer demonstration was required to have a central plant with a VAV all-air system. Differences between HVAC system type were only seen in the terminal system configuration (secondary air-loop).

The goal of conducting a FFA on each building was to better understand the effects of each factor on building energy use associated with heating and cooling. It is hoped that the information gained from this analysis can be used to guide efforts associated with building audits and building energy model development by providing the auditor and modeler with a hierarchical perspective on the effects of each major building component. With this perspective, a number of recommendations have been made that suggest best practices for collecting detailed information on the most significant building parameters. These recommendations will be explained in Chapter 6.

5.2 Factors and Building Selection

The buildings chosen for this analysis are described in Table 5.1 below. Information regarding the name and specific location of each building is confidential, henceforth the buildings have been renamed Building A, B, and C for the purpose of this thesis. As mentioned in the previous paragraph, each building exhibits a central plant with a VAV all-air system. Differences are seen in the terminal system configurations, specifically in the reheat options of the perimeter zones.

Table 5.1: FFA building characteristics

Field	**Building A**	**Building B**	**Building C**
Year Built	1980	1973	2005
Number of Floors	39	44	42
Footprint Area	2,400 m^2	2,900 m^2	2,700 m^2
Floor-to-Floor Height	3.35 m	3.66 m	3.96 m
Average Window-to-Wall Ratio	54%	57%	50%
Number of People	1,800	4,000	5,000
Terminal System Configuration			
Core	VAV, NoReheat	VAV, NoReheat	VAV, NoReheat
Perimeter	VAV w/Baseboard Electric Reheat	VAV w/Hot Water Reheat	Series PIU w/Electric Reheat

The factors evaluated in this analysis were chosen to represent major building components associated with large chiller plant systems. These factors are listed in Chapter 3, and are organized by building component and load. Heating and cooling loads are represented by building envelope characteristics, the thermal mass of the building, lighting power density, and equipment power density. The thermal mass, as represented in EnergyPlus, is described by the mass surface area exposed to the zone that can participate in radiation and convective heat exchanges [36]. Affecting the zonal response to temperature changes, the

thermal mass is also described by material properties and construction, and is included in the heat balance calculation for each zone. On the supply side, the HVAC system was represented by factors related to the air system, chilled water loop, chiller, and the condenser water loop (cooling tower). For better interpretation of these factors and how they are represented within the building, a graphical representation of the parameters and their associated system components can be found in Figure 5.1.

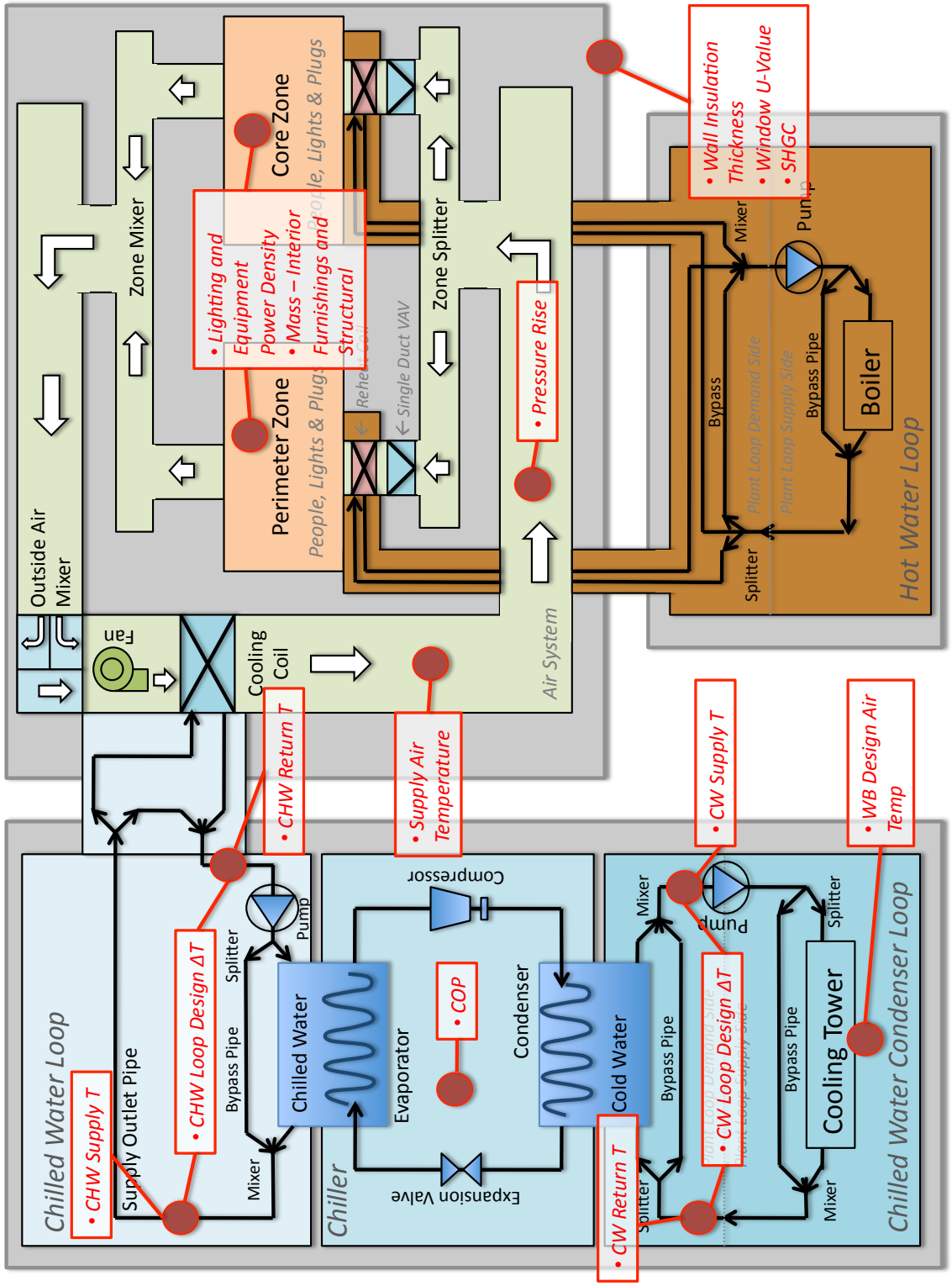

Figure 5.1: Graphical representation of parameters used in the fractional factorial analysis.

Out of the parameters listed in Table 3.1, sixteen were adjusted in the energy models for buildings A, B, and C for the fractional factorial analysis. A list of these parameters is enumerated below, along with the associated EnergyPlus object name. The EnergyPlus object describes where each parameter can be found in an IDF. Note that parameters can be associated with multiple EnergyPlus objects.

(1) **Wall Insulation Thickness** — Material, Wall Insulation

(2) **Window U-Value** — WindowMaterial:SimpleGlazingSystem

(3) **Window Solar Heat Gain Coefficient** — WindowMaterial:SimpleGlazingSystem

(4) **Mass Area of Structural Components, Core** — InternalMass

(5) **Mass Area of Structural Components, Perimeter** — InternalMass

(6) **Mass Area of Interior Furnishings, Core** — InternalMass

(7) **Mass Area of Interior Furnishings, Perimeter** — InternalMass

(8) **Lighting Power Density** — Lights, Watts per Zone Floor Area

(9) **Equipment Power Density** — ElectricEquipment, Watts per Zone Floor Area

(10) **Supply Air Temperature** — Sizing:Zone; Sizing:System; Coil:Cooling:Water

(11) **Supply Fan Pressure Rise** — Fan:VariableVolume

(12) **Chilled Water Loop Temperature Differential** — Sizing:Plant, CoolSys1

(13) **Chilled Water Supply Temperature** — Sizing:Plant, CoolSys1; Coil:Cooling:Water

(14) **Chiller COP** — Chiller:Electric:EIR

(15) **Condenser Water Return Temperature** — Chiller:Electric:EIR

(16) **Condenser Water Loop Temperature Differential** — Sizing:Plant, TowerWaterSys

The Simple Glazing System in EnergyPlus (released in v4.0) is a window object that describes an entire glazing system rather than individual layers as seen in other *WindowMaterial* glazing objects. Since the fractional factorial analysis focuses on only a few glazing parameters that were collected during the building audits, the Simple Glazing System was used because it provided an efficient way to manipulate performance indices such as the overall U-value and SHGC of the window [38].

It should also be noted that there are many factors that could have been considered in this analysis. The sixteen factors used in this study were chosen because they represent the major systems that are typically found in high-rise commercial office buildings, and because the design values for these factors are generally easy to collect during a walk-through building audit. Some factors, such as the outdoor air fraction, window-to-wall ratio, and chiller part-load performance were not considered for this analysis, but are recognized as factors that have a large impact on building energy consumption and demand. In future studies, these factors should be taken into consideration. Reasons why these factors were not included in this research are discussed below, along with methods that were used to account for these factors, and methods for collecting or calculating values for these factors for future studies.

The outdoor air fraction was determined by discussions with the building engineers, or assumed to follow the ASHRAE 62.1-2004 design standard. A fixed minimum outdoor-air flow rate was used in each the model, which was typically 20% of the overall supply air flow rate. If present in the building, economizers were also modeled to take advantage of free-cooling when possible. However, to determine a more detailed minimum outdoor-air fraction (min OA) schedule, hourly data would need to be collected from the Building Automation System to provide typical daily schedules for each season. Due to time constraints and access to data, detailed min OA schedules were not collected, but should be considered for future studies since the outdoor-air fraction can greatly influence the amount of energy needed to heat and cool the building.

The window-to-wall ratio is an easy parameter to ascertain, but is difficult to modify within an energy model. Modifying this value would require the modeler to change the vertices of each corner of every window within the IDF. This approach was too complex for the fractional factorial analysis, and thus it was decided to modify the window U-value and solar heat gain coefficient instead, which also captures effects of solar gains from windows.

Chiller part-load ratios were taken from manufacturer data provided by the EnergyPlus Chiller data set. To acquire a true part-load ratio for each chiller, testing of the system operation would be required. The part-load ratio is defined as the chiller coefficient of performance (COP) for cyclic operation divided by the steady-state COP [31]. The steady-state COP can be calculated by taking the ratio of the chiller capacity to the power of the chiller. The COP for cyclic operation takes into account the total cooling capacity for a cycle of the chiller operation. The *cyclic* capacity be calculated by the following equation:

$$\dot{Q}_{cyc} = \dot{m} c_p \int_{t_1}^{t_2} (T_{CHW,R} - T_{CHW,S})\, dt \tag{5.1}$$

where $\dot{m}$ is the mass flow rate of the chilled water, Cp is the specific heat of water, t_1 and t_2 are the times that the chilled water pump was turned on and off, and $T_{CHW,R}$ and $T_{CHW,S}$ are the return and supply temperatures of the chilled water.

The COP for cyclic operation can then be calculated by dividing Q_{cyc} by the power input over the time interval t_1 to t_2 [31]. Lastly, the part-load factor can be calculated by dividing the COP for cyclic operation by the steady-state COP.

Most of the audited buildings had multiple chillers to cool the building. Typically, the buildings had three, which were sequenced appropriately to meet the cooling load. With three chillers, the building engineers could alternate which chiller was used, and also turn on a combination of chillers to meet the cooling demand of the building. On a very hot day, all three chillers could be used. On a cooler day, perhaps just one is used. The purpose of sequencing the chillers is to both minimize the number of chillers used at any point in time, as well as to spread out the load so that any one chiller is not running at full capacity. It also minimizes occurrences where chillers run at close to zero capacity - when they are the least efficient [39].

Sequencing strategies allow multiple chillers to more effectively work together. At a low cooling load, the main chiller (the *lead* chiller) will run until it reaches its rated capacity. Once at the rated capacity, a second chiller (a *lag* chiller) is turned on. Assuming a building has three identical chillers, two chillers working in tandem will be able to meet the load at 16.5% of their rated capacities - sharing a third of the overall rated plant capacity. If the load increases and both chillers reach their rated capacity, a third *lag*

chiller can be turned on - sharing two-thirds of the overall rated plant capacity. In this scenario, each chiller meets the load at 22% of their rated capacities [39]. A diagram of this sequencing pattern is presented below.

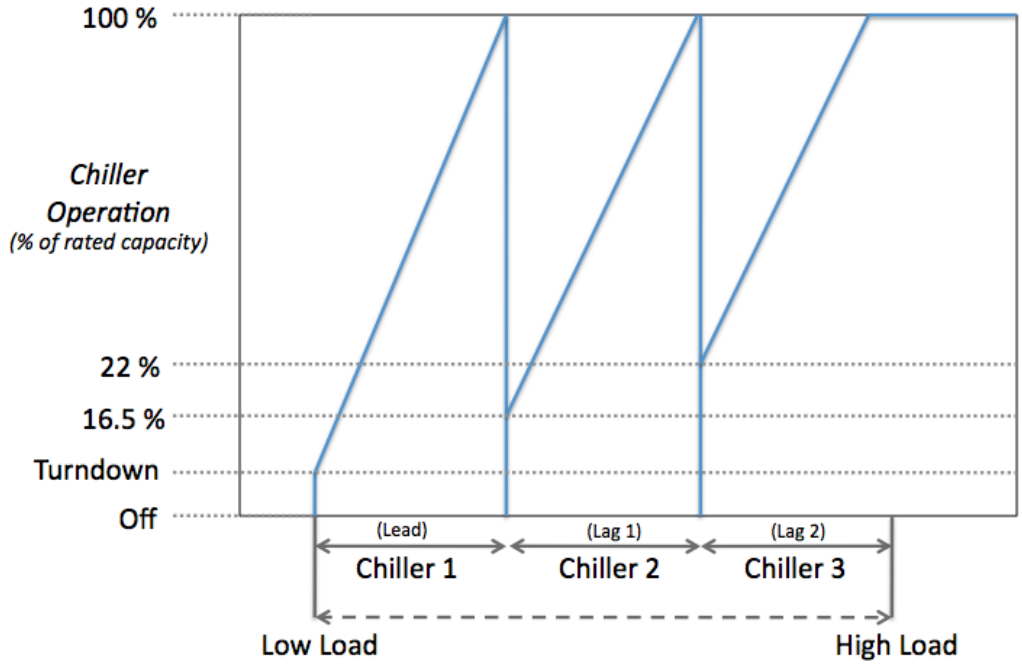

Figure 5.2: Graphical representation of the sequencing of multiple chillers.

To simplify the modeling process, multiple chillers were modeled as one in EnergyPlus. To do so, the capacity of each chiller was added together, and an average value for the reference COP, leaving chilled water temperature, entering condenser temperature, chilled water flow rate, and condenser flow rate was used. As mentioned above, a "best-matching" chiller performance curve was chosen out of the EnergyPlus Chiller data set, based on the capacity of the largest chiller and the average COP. To determine a more robust performance curve, the fraction of full load power (FFLP) as a function of the part-load ratio (PLR) for each chiller would need to be analyzed and compared to the sequencing strategy. A curve could then be fit to accommodate both, to ensure that the chiller is not oversized and running at a part-load ratio that is too low. Another strategy would be to model each chiller separately, and set the priority for each chiller to match the sequencing strategy.

The supply and return fans were treated in a similar manner, where the flow rate for each air handler

was added together, the maximum pressure rise was used (if there was variation), as well as the average value for the fan and motor efficiencies. There were two reasons behind this modeling approach. The first was to reduce the amount of time spent modeling each building by combining the fan characteristics into one large AHU. It was assumed that the energy associated with one large AHU would be similar to that of multiple smaller ones - if the fan characteristics were similar. The second reason was that most of the air handling units within each building delivered the same amount of air to the different zones of the building and had the same or similar pressure drops. For example, Building C has four identical supply and return fans that serve four quadrants of the building. When looking at the equation for fan power (below), this makes sense. Whether you calculate the fan power for four identical small AHUs or for one large one, the power is the same.

$$P_{fan} = \frac{\dot{V}_{air}\Delta P}{\eta} \tag{5.2}$$

where P_{fan} is the fan power $[W]$, $\dot{V}_{air}$ is the supply air volume flow rate $[m^3/s]$, ΔP is the supply fan static pressure rise $[Pa]$, and η is the fan efficiency.

5.3 Fractional Factorial Design

Fractional factorial analyses are conducted to reduce the number of experiments associated with a full factorial design, while retaining the ability to identify the effects of individual factors and major interactions [15]. A full factorial design at two levels investigates all combinations of a set of factors (k) at both a base and test level, requiring 2^{k} runs. Results from this type of analysis provide the experimenter with information regarding the effects of each factor and two-factor interactions on the output of an experiment. In the context of this research, the factors are parameters within a building energy model, and the experiments are model simulations. The effects of each parameter on building energy consumption and demand are quantified by examining output data from each simulation.

A quick example of a full factorial experimental design with three factors at two levels can be seen in Table 5.2 below. This example evaluates three parameters at both a base and test level, which are indicated by a $'-'$ for the base level and $'+'$ for the test level. The yield (Y), is the calculated energy consumption

output by the energy model for each case, when run with that particular combination of high and low values for each factor.

Table 5.2: Example of a 2^3 full factorial design

	parameter			
Case	**1**	**2**	**3**	*Yield*
1	–	–	–	Y_1
2	+	–	–	Y_2
3	–	+	–	Y_3
4	+	+	–	Y_4
5	–	–	+	Y_5
6	+	–	+	Y_6
7	–	+	+	Y_7
8	+	+	+	Y_8

The main effect for each factor can then be calculated by subtracting the average yields for all cases where the factor is at the base level ($\overline{Y_-}$), from the average yields for all cases where the factor is at the test level ($\overline{Y_+}$) [2]. This is seen below in Equation 5.3:

$$M_n = \overline{Y_+} - \overline{Y_-} \tag{5.3}$$

where M_n is the main effect of each factor n.

The *relative impact* (R_n) of each factor is similar to the main effect, but is normalized to the average of all yields ($\overline{Y}$). By normalizing the effects, the experimenter is able to better compare the effects of multiple factors. For this research, the relative impact was calculated to quantify the effects of each factor on energy consumption, and to rank the factors by level of significance. The relative impact can be calculated using Equation 5.4 below.

$$R_n = \frac{\overline{Y_+} - \overline{Y_-}}{\overline{Y}} \tag{5.4}$$

The effects of two-factor interactions can also be calculated. Two-factor interactions show how the interdependency of any two factors affects energy consumption. For example, an interdependent relationship can be described using passive solar heating. In a hypothetical scenario, two parameters are investigated: (1) the solar heat gain coefficient (SHGC) of a window, and (2) the thermal mass in a building zone. If we look at each parameter independently, the calculated relative impact may tell us that the window SHGC has a greater affect on heating and cooling loads than the building thermal mass. However, when looking at two-factor interactions, it may be the case that the thermal mass and SHGC *combined* have a more significant effect on building heating and cooling loads. These interdependencies are often lost when only one-off parametric studies are examined. Using the 16 parameters listed above, the two-factor interactions were determined by simulating 120 different cases. Organized by magnitude of effect on the model energy consumption and demand, the ten most effective interactions were documented in the results section of this thesis for each building. The equation used to calculate the relative impact of any two factors n and m (R_{nm}) is described below:

$$R_{nm} = \frac{(\overline{Y_{nm}} + \overline{Y_{NM}}) - (\overline{Y_{Nm}} + \overline{Y_{nM}})}{\overline{Y}} \tag{5.5}$$

where $\overline{Y_{nm}}$ is the average yield of the experiment where the factors n and m are at the base level, $\overline{Y_{NM}}$ is the average yield of the experiment where the factors N and M are at the test level, and $\overline{Y_{nM}}$ and $\overline{Y_{Nm}}$ is the average yield of the experiment where the factors n and m are at either the base or the test level.

As previously mentioned, a full factorial analysis accommodates all possible combinations of k parameters at two levels, requiring 2^{k} runs [2]. With 16 parameters specified in this research, over 65,000 EnergyPlus simulations would have to be run to complete a full factorial analysis. At approximately five minutes per simulation, this would take over 225 days for completion. To reduce the time associated with a full factorial analysis, a fractional factorial analysis was implemented. The fractional factorial analysis systematically reduces the number of simulations needed to calculate the effects of each factor. However,

this comes at a cost. To reduce the number of simulations, the impact of some combinations or interactions are confounded with those of other parameters or parameter combinations, thus reducing the precision of the analysis [15]. Nevertheless, we can assume that higher order interactions between three or more parameters are insignificant to the experiment, and in a properly designed fractional factorial experiment, the main effects are confounded only with higher level interactions. Therefore, the ability to identify the effects of individual factors and major interactions is preserved [15].

The level of confounding is characterized by the *resolution* of the fractional factorial design. Lower resolution designs require fewer simulations or runs but have a higher level of confounding. Reversely, higher resolution designs require more simulations and less confounding. The most commonly used designs are described below [29]:

Resolution III Designs — Main effects are confounded with two-factor interactions

Resolution IV Designs — No main effects are confounded with two-factor interactions, but two-factor interactions are aliased with each other

Resolution V Designs — No main effect or two-factor interaction is confounded with any other main effect or two-factor interaction, but two-factor interactions are confounded with three-factor interactions

For the purpose of this research, a resolution III design was used to determine the relative impact of each factor and a resolution V design was used to determine the impacts of two-factor interactions. Resolution III designs are commonly used as *screening* designs, since they allow the experimenter to determine the effect of many factors with an efficient number of runs [29]. The resolution V design was used to determine the effects of two-factor interactions because the design only confounds main effects and two-factor interactions with higher order interactions, which are assumed to be insignificant to the experiment. In this resolution, more simulations are required, but uncertainty in confounding effects is reduced. In this case, a more precise analysis of the impacts of two-factor interactions can be presented [29].

The *FracFact* generator tool in Matlab was used to generate the design of experiments. The *FracFact* generator provides factor settings for a two-level fractional factorial design as described by Box, Hunter and Hunter [2]. This tool uses the Franklin-Bailey algorithm to find generators for the smallest two-level fractional factorial design for estimating linear model terms, and returns a cell array that shows the confounding pattern

among the main effects and two-factor interactions [25]. The Matlab code used in this research allowed the author to specify factors, base and test level values for each factor, and the resolution of the experimental design. For the resolution III screening, Matlab returned a design that consisted of 32 runs, while the resolution V design consisted of 120 runs.

5.4 Determining Range of Values for Two-Level Designs

In order to determine a base and test level value for each factor, a statistical analysis was conducted on building equipment and load design values collected from the twenty-two buildings audited during the 2009 CUE summer demonstration. The goal of this analysis was to determine an appropriate range of base and test level values for each factor, while avoiding unintentional preference to any particular factor in the experiment. To reduce the potential for one factor dominating the effects, the standard deviation (σ) for each factor was calculated at a 70% confidence level. By evaluating all factors at the same level of confidence, each factor will have an equivalent level of uncertainty. Thus, each factor is evaluated equally. The 70% confidence level was chosen somewhat arbitrarily, but with the assumption that approximately 70% of high-rise commercial office buildings would have a value for each factor within the range of the base and test level values used in this thesis.

As described by the central limit theorem, the sample can only be approximated by a normal distribution if the sample size is greater than 30 [40]. Since building audit data was collected for only twenty-two buildings, the *Student's t* statistic was applied to the data set to account for uncertainty in the standard deviation. The Student's t distribution (t) can be determined by using the *degrees of freedom* (which is equal to the sample size minus 1), and the level of confidence. This function is built into a number of statistical analysis programs (including Microsoft Excel) and can be acquired through existing tables. The equation for calculating the standard deviation for a smaller sample size is shown in Equation 5.6 below:

$$S = \sqrt{\sum_{i=1}^{N} \frac{(x_i - \overline{x})^2}{n-1}} \tag{5.6}$$

where x_i is the value of each factor within the smaller sample population, $\overline{x}$ is the average value of the factors, and n is the sample size. The base and test level values (μ) were then be calculated by the following

equation:

$$\mu = \overline{x} \pm t_{\alpha/2} \frac{S}{\sqrt{n}} \tag{5.7}$$

where $\overline{x}$ is the average of the sample population, $t_{\alpha/2}$ is the Student's t distribution, α is the confidence level, S is the smaller sample size standard deviation, and n is the sample size.

The full set of data for each building used in this statistical analysis is listed in Appendix A. From this data set, the final base and test level values for each factor were determined based on the calibrated value of each factor plus and minus the normalized deviation for a 70% confidence level. Table 5.3 below lists these values. It should be noted that three of the factors have a very small range of values. These factors are the supply air temperature, the chilled water loop temperature differential, and the condenser water return temperature. The range is small because little variation was found between these factors during the audit of each building used in this study. However, the base and test level values for these three factors were calculated using the same methodology as for the other factors, and to ensure that each factor was evaluated with an equivalent level of uncertainty, the values were left unchanged.

Factor	Calibrated Value			Population Average	Standard Deviation	Base/Test Level Value					
						A		B		C	
	A	B	C			Base	Test	Base	Test	Base	Test
Envelope											
Wall Insulation Thicknes [m]	0.05	0.076	0.05	0.056	0.005	0.045	0.055	0.071	0.081	0.045	0.055
Window U-Value [m^2K/W]	1.33	5.596	1.28	3.111	0.461	0.873	1.795	5.135	6.057	0.819	1.741
Window Solar Heat Gain Coefficient [%]	0.49	0.934	0.36	0.505	0.053	0.441	0.547	0.881	0.987	0.307	0.413
Thermal Mass											
Mass Area of Structual Components, Core [m^2]	233	--	--	3.396	4.311	102.535	362.865	102.535	362.865	102.535	362.865
Mass Area of Structual Components, Perimeter [m^2]	86	--	--	4.751	5.693	38.995	132.465	38.995	132.465	38.995	132.465
Mass Area of Interior Furnishings, Core [m^2]	3,163	3,868	1,820	1.587	0.193	2,819.683	3,506.684	3,447.605	4,287.595	1,622.262	2,017.518
Mass Area of Interior Furnishings, Perimeter [m^2]	407	234	222	2.382	0.996	287.028	526.972	165.108	303.132	156.857	287.983
Internal Gains											
Lighting Power Density [W/m^2]	10.50	9.00	13.00	12.417	1.100	9.400	11.600	7.900	10.100	11.900	14.100
Equipment Power Density [W/m^2]	7.50	4.00	7.50	8.785	1.496	6.004	8.996	2.504	5.496	6.004	8.996
Plant System											
Supply Air Temperature [C]	11.11	10.00	8.61	11.009	0.400	10.710	11.510	9.600	10.400	8.210	9.010
Supply Fan Static Pressure Rise [Pa]	1,961	620	1,241	1562.213	150.277	1,810.763	2,111.317	470.073	770.627	1,090.413	1,390.967
Chilled Water Loop Temperature Differential [C]	8.88	6.67	9.84	7.549	0.358	8.527	9.242	6.312	7.028	9.482	10.198
Chilled Water Supply Temperautre [C]	5.56	6.11	3.33	6.669	1.294	4.261	6.850	4.816	7.404	2.036	4.624
Chiller Efficiency [COP]	3.62	4.51	5.05	4.982	0.230	3.388	3.848	4.280	4.740	4.820	5.280
Condenser Water Return Temperature [C]	29.44	29.44	29.44	29.442	0.006	29.439	29.450	29.434	29.446	29.434	29.446
Condenser Water Loop Temperature Differential [C]	8.34	5.6	7.12	6.777	0.489	7.846	8.825	5.111	6.089	6.631	7.609
Area											
Area of Perimeter/4 [m^2]	203.50	158.27	216.62								
Area of Core [m^2]	1,581.59	1,933.80	1,819.89								

Figure 5.3: Base and test level values used for each factor in each building. Values are calculated based on the calibrated value of each factor plus and minus the normalized deviation for a 70% confidence level.

5.5 Climate Study

The effects of each factor and two-factor interactions were analyzed for each building in four different climate zones. These climate zones were chosen based on research conducted by Henze et al. [15], which suggests using weather data for four major cities to represent the major climate zones seen across the United States. Typical meteorological year data (TMY) was used for Phoenix (hot and dry), Atlanta (warm and humid), Los Angeles (warm and dry), and Chicago (cool and humid).

Modifications to each EnergyPlus IDF were made to account for differences typically seen in HVAC plant system sizing, due to the different heating and cooling requirements for each climate. To modify each file, the EnergyPlus *autosize* function was used to resize system components, while using the appropriate TMY weather file for each city presented above. In each autosize run, EnergyPlus outputs autosized values used in the simulation into an EIO output file. Taking these values, the system components were hard-sized in the model before each fractional factorial analysis was run. With the system components accurately sized, results from the fractional factorial analysis were properly represented for each climate zone.

Chapter 6

Results and Discussion

The fractional factorial analysis was run for three buildings (buildings A, B, and C) in four difference climate zones using TMY data for Phoenix (hot and dry), Atlanta (warm and humid), Los Angeles (warm and dry), and Chicago (cool and humid). These cities are representative of the major climate zones in the U.S., and also of urban areas where high-rise commercial office buildings are common. The results discussed in this chapter reflect the impact of individual factors and two-factor interactions for an annual simulation, except for Building C. The analysis for Building C was conducted for only the summer months (cooling season), due to insufficient data regarding heating components and building loads for the winter and swing months.

6.1 Screening Results

The screening results provide insight to the driving factors that greatly affect energy consumption and demand associated with heating and cooling loads. As anticipated, a sub-set of factors emerged from this analysis as being of primary importance for each building used in this study. These factors differ slightly depending on climate zone, but when looking at the overall results, the same six to seven factors can be regarded as driving factors that affect the energy consumption and demand of high-rise commercial office buildings. A summary of averaged results showing the relative effect on energy consumption and demand over building type and climate zone can be seen in Figure 6.1 and Figure 6.2, where the y-axis describes the magnitude of each effect. Averaged results for the relative effect on chiller, HVAC and facility electric consumption and demand over all climate zones for each building can be seen in Figures 6.3 to 6.5. Based

on these results, the level of impact (or significance) of the 16 factors can be evaluated. Table 6.1 describes the level of significance for each factor on electric consumption and demand.

It should be noted that the chilled water loop temperature differential and the condenser water return temperature factors show low significance to energy consumption and demand. This may be caused, in part, by the small range in base and test level values that was used for each of these factors. However, as noted in Chapter 5, the base and test level values for these three factors were calculated using the same methodology and confidence level as the other factors and were left unchanged to ensure that each factor was evaluated with an equivalent level of uncertainty.

Table 6.1: Factors that have significant effect on energy consumption and demand associated with heating and cooling loads of high-rise commercial office buildings

Factor	**Description**	**Units**	**Significance, Consumption**	**Significance, Demand**
1	Mass Area of Structural Components, Core	m^2	Low	Low
2	Mass Area of Structural Components, Perimeter	m^2	Low	Low
3	Mass Area of Interior Furnishings, Core	m^2	Low	Low
4	Mass Area of Interior Furnishings, Perimeter	m^2	Low (Med in LAX and PHX)	Low
5	Wall Insulation Thickness	m^2	Low	Low
6	Window U-Value	m^2K/W	Low (Med in CHI)	Low (Med in CHI)
Continued ...				

Table 6.1: (continued)

Factor	**Description**	**Units**	**Significance, Consumption**	**Significance, Demand**
7	Window Solar Heat Gain Coefficient	%	Med	Med
8	Lighting Power Density	W/m^2	High	Med
9	Equipment Power Density	W/m^2	High	Med
10	Supply Fan Pressure Rise	Pa	Med	Med
11	Supply Air Temperature	℃	Low	Med
12	Chilled Water Supply Temperature	℃	Low	Low
13	Chilled Water Loop Temperature Differential	℃	Low	Low
14	Chiller Efficiency	COP	High	High
15	Condenser Water Return Temperature	℃	Low	Low
16	Condenser Water Loop Temperature Differential	℃	Low	Low

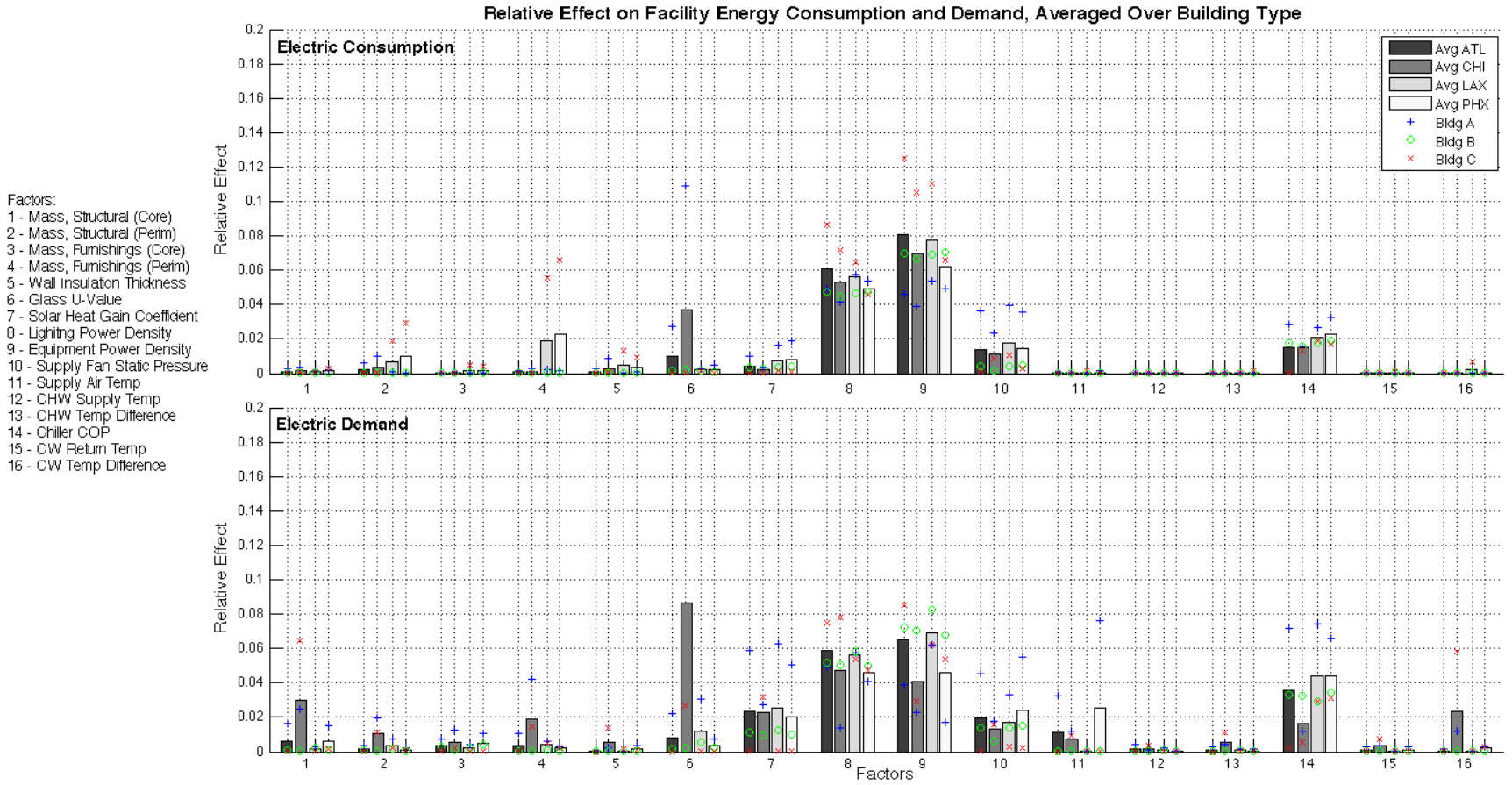

Figure 6.1: The relative effect on facility electric consumption and demand of all buildings averaged over four climate zones. Overlaying the bar charts are points marking the relative effect, also on facility electric consumption and demand, for each building in each climate zone.

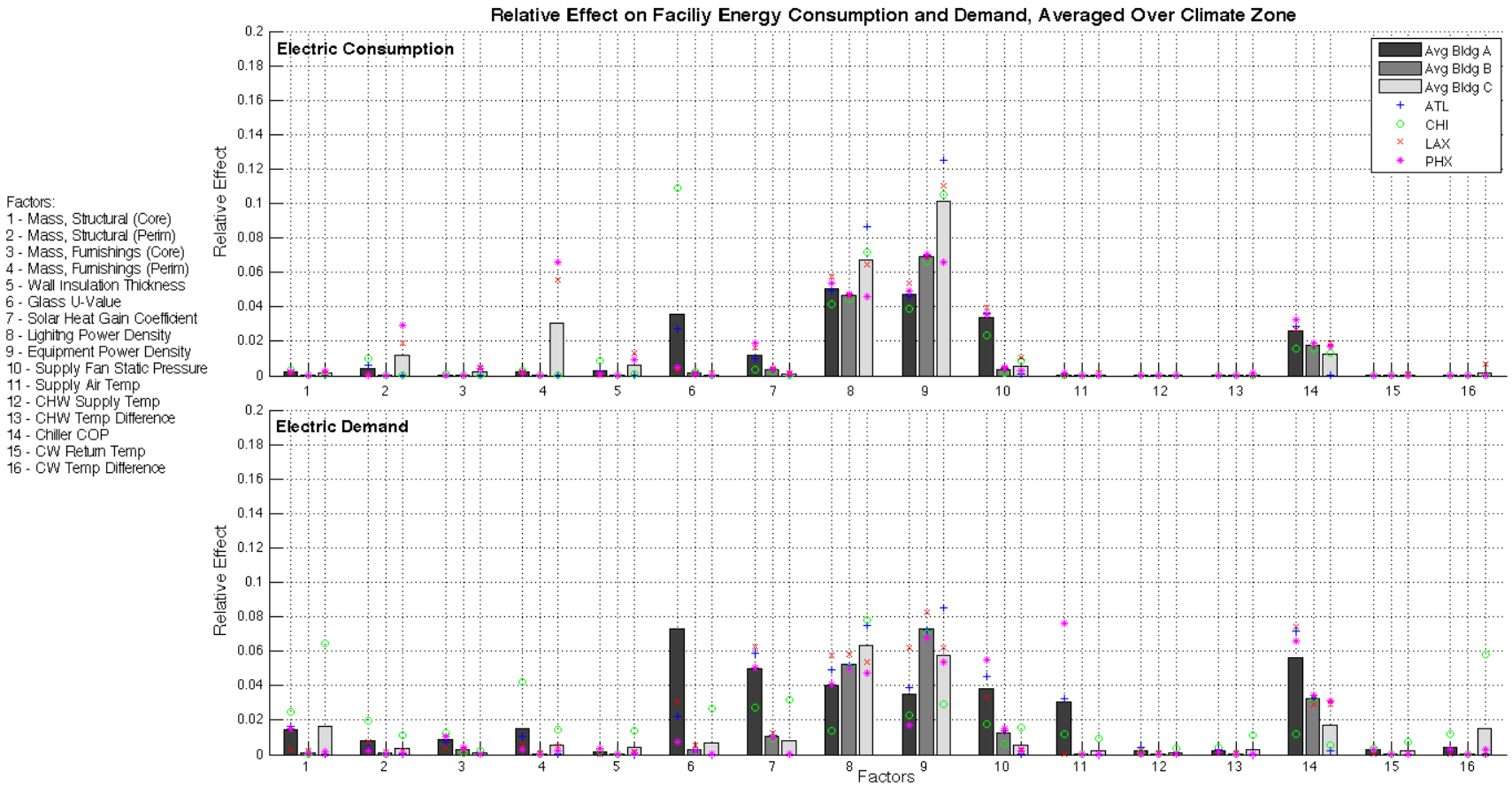

Figure 6.2: The relative effect on facility electric consumption and demand of all climate zones averaged over each building type. Overlaying the bar charts are points marking the relative effect, also on facility electric consumption and demand, for each climate zone and building type.

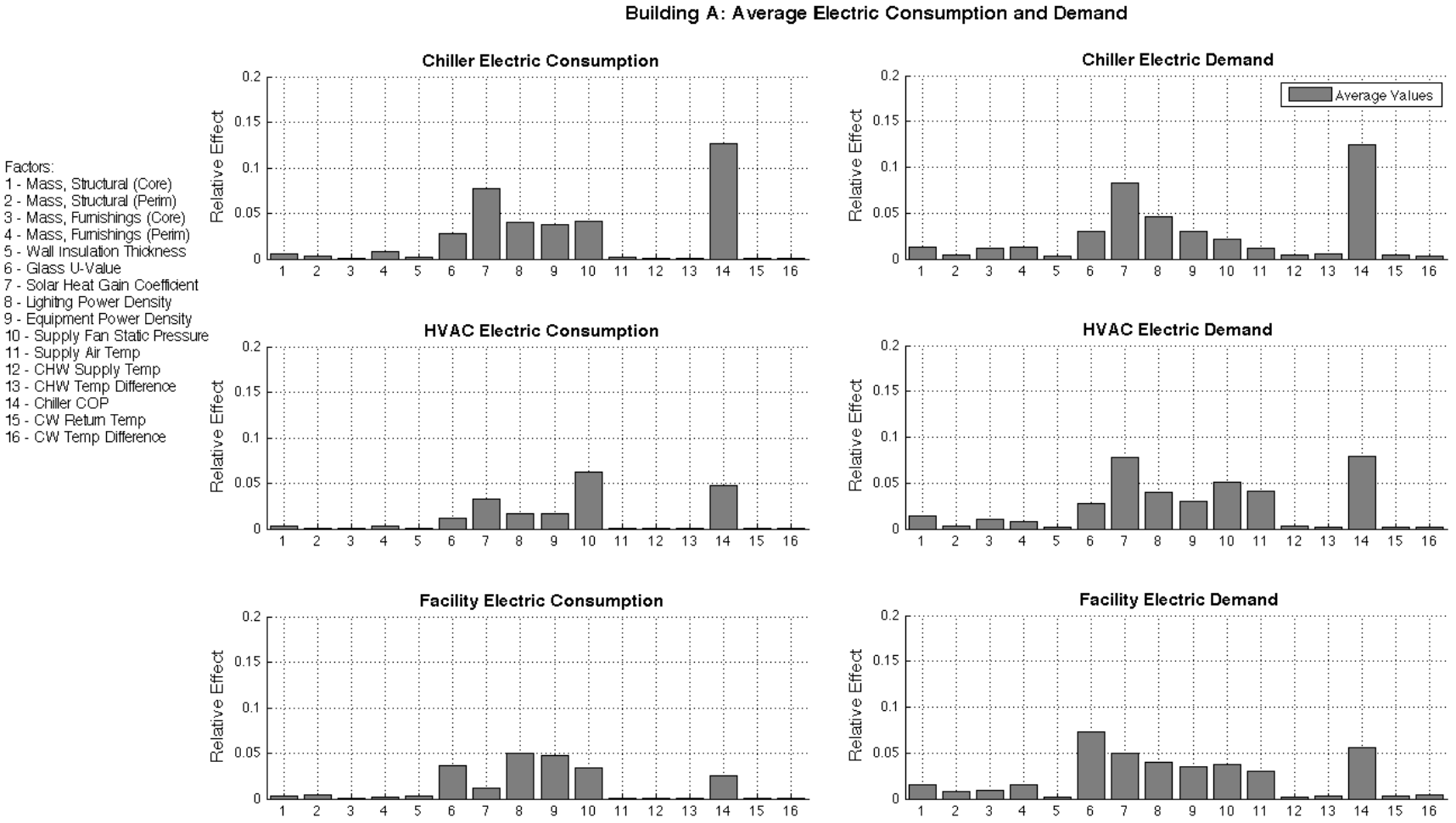

Figure 6.3: Average relative impact over four climate zones, Building A

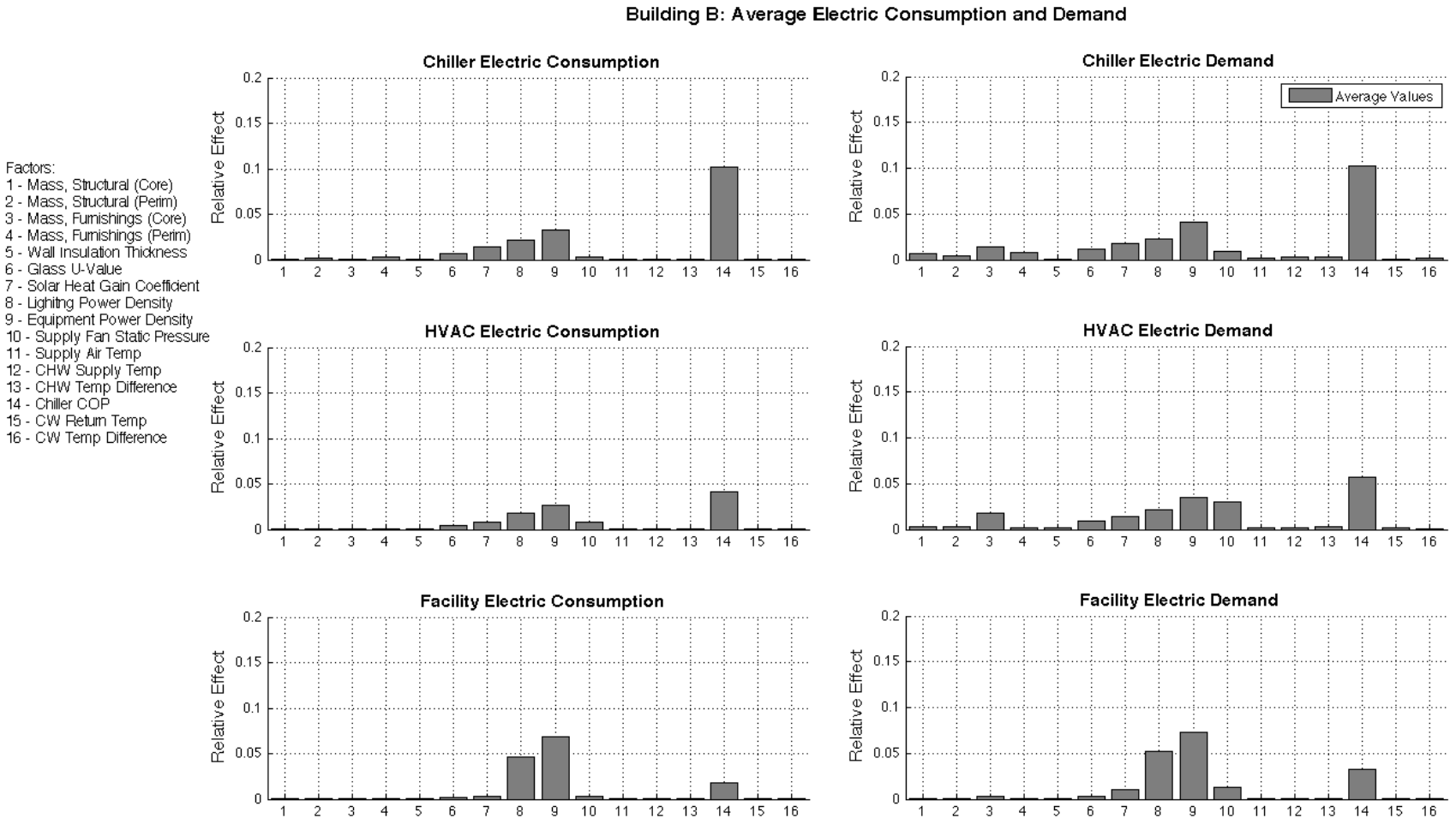

Figure 6.4: Average relative impact over four climate zones, Building B

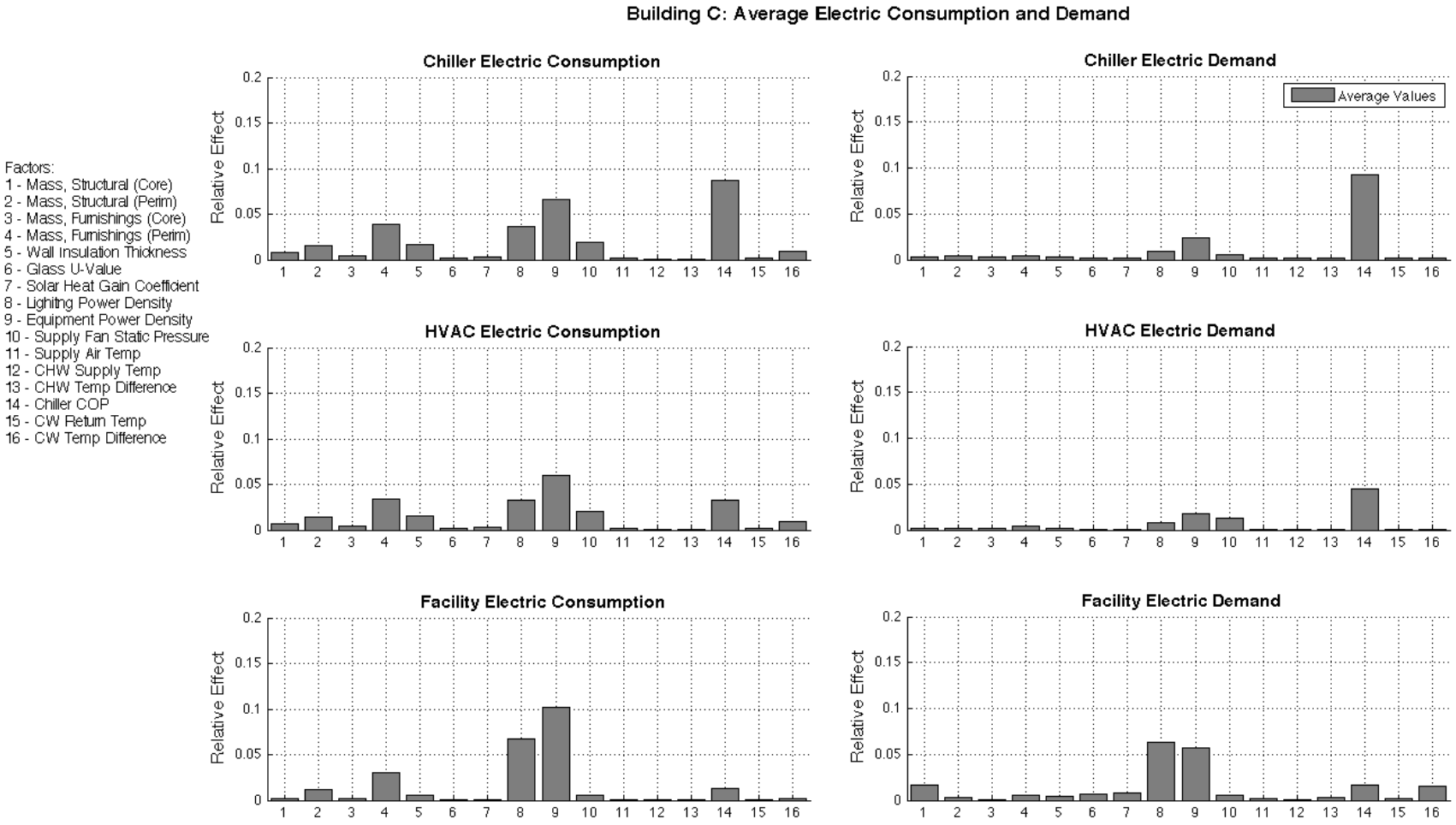

Figure 6.5: Average relative impact over four climate zones, Building C

A full set of screening results for each building can be found in Appendix C. The results are organized by average impact over all climate zones, relative impact for each climate zone, and by relative impact for each factor organized by magnitude in descending order. Lastly, scatter plots of the data are presented to show the distribution of the effect of each factor over all climate zones.

The impact of the parameters on energy associated with heating and cooling loads can be justified by inspecting heat and power balance equations associated with building zones and HVAC equipment. For instance, the chiller COP has an inverse relationship with chiller power. As the chiller efficiency increases, the required power needed for the chiller decreases, and vice versa. As described in the EnergyPlus engineering reference, the chiller power is calculated using the following equation:

$$P_{chiller} = \dot{Q}_{avail} \frac{1}{COP_{ref}} (EIR_{temp})(EIR_{PLR})(CCR) \tag{6.1}$$

where $P_{chiller}$ is the chiller power $[W]$, $\dot{Q}_{avail}$ is the available cooling capacity, COP_{ref} is the reference COP, EIR_{temp} is the energy input to cooling output factor as a function of temperature, EIR_{PLR} is the energy input to cooling output factor as a function of the part-load ratio, and CCR is the cycling ratio, where the chiller is cycled on and off dependent on the minimum part-load ratio.

Over time, the efficiency of a chiller can decline due to fouling or lack of maintenance to the system. If possible, it is recommended that a building auditor measure the chiller COP to acquire a realistic value (rather than a design value) that can be used as input to an energy model. To do so, the chiller cooling capacity and power input must be calculated. The cooling capacity can be calculated by installing a flow meter on the chilled water supply (measuring gallons per minute - GPM), and two temperature sensors to measure the chilled water supply and return temperatures. The cooling capacity ($\dot{Q}_{chiller}$) can be calculated in tons using the following equation:

$$\dot{Q}_{chiller} = \rho C_p \dot{V} (T_{CHW,R} - T_{CHW,S}) \tag{6.2}$$

where ρ is the density of water, C_p is the specific heat of water, $\dot{V}$ is the chilled water supply flow rate, $T_{CHW,R}$ and $T_{CHW,S}$ are the temperatures of the chilled water return and supply lines, respectively. The

power input can be measured by installing a power meter on the chiller, and once the power (kW) and cooling capacity (tons) of the chiller are known, the efficiency can be calculated by dividing the power by the cooling capacity. The chiller COP can then be calculated by the following equation:

$$COP = 12/(kW/ton)/3.412 \tag{6.3}$$

The energy use associated with cooling loads is significant when looking at whole-building energy consumption, accounting for approximately 8-17% depending on climate zone. To represent percent energy consumption by end use for a typical high-rise commercial office building, the EnergyPlus benchmark IDF for a large office building was simulated for each climate zone. The EnergyPlus benchmark building files were developed to capture whole-building energy performance of typical commercial building stock [28]. Figure 6.6 below was generated using the results from the benchmark simulations, and was included to illustrate typical differences in energy consumption by end-use for high-rise commercial office buildings.

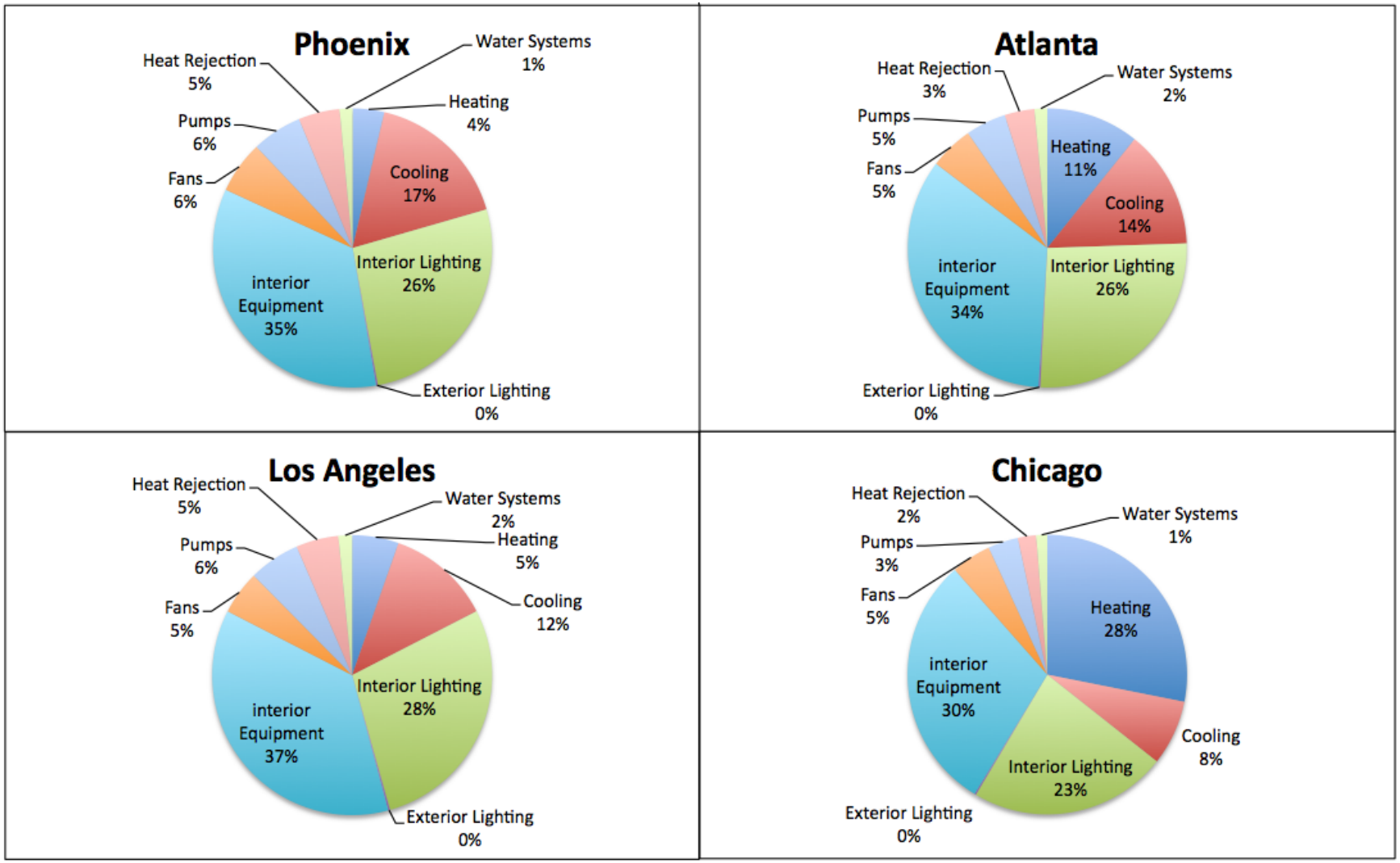

Figure 6.6: Energy consumption breakdown by end use for select climate zones found in the United States.

Figure 6.6 also reveals the significance of fan power associated with the HVAC system. Regarding the above graphs, fans consume 5-6% of the facility energy use, and over 25% of the energy use required for heating and cooling. To represent the supply fan in the fractional factorial analysis, the supply fan static pressure parameter was used because the static pressure is proportional to fan power. This is described in Equation 6.4:

$$P_{fan} = \frac{\dot{V}_{air}\Delta P}{\eta} \tag{6.4}$$

where P_{fan} is the fan power $[W]$, $\dot{V}_{air}$ is the supply air volume flow rate $[m^3/s]$, ΔP is the supply fan static pressure rise $[Pa]$, and η is the fan efficiency. If the static pressure rise increases, the fan has to work harder to overcome the pressure in the main air shaft in order to distribute air throughout the building. Naturally, if the fan works harder, the fan requires more power. Thus, the static pressure has a significant effect on the energy consumption associated with the fan. In addition, the fan adds heat to the supply airstream, which ultimately is another load that must be met by the chiller - increasing energy associated with the chiller.

It is recommended that the fan pressure rise be measured, if possible. Analyzed data from the 2009 CUE summer demonstration shows that there is no correlation linking fan pressure rise to the size of a building. This is clearly seen in Figure 6.7 below. Since this parameter has such a large effect on building energy use, it is important to determine a realistic value. This data also presents reasons why the fan pressure rise has a large effect on the model's energy use. With such a scattered set of data, the standard deviation with a 70% confidence level (which determined the base and test level values for the FFA) is large in comparison to the other parameters. This may account in-part for reasons why the analysis shows that the fan pressure rise has such a great effect on the model. However, since there is little or no correlation of the pressure rise to the size of the building, and because the fan energy accounts for a large portion of the HVAC and facility energy use, it is still reasonable to recognize this parameter as a driving factor on energy use associated with heating and cooling loads.

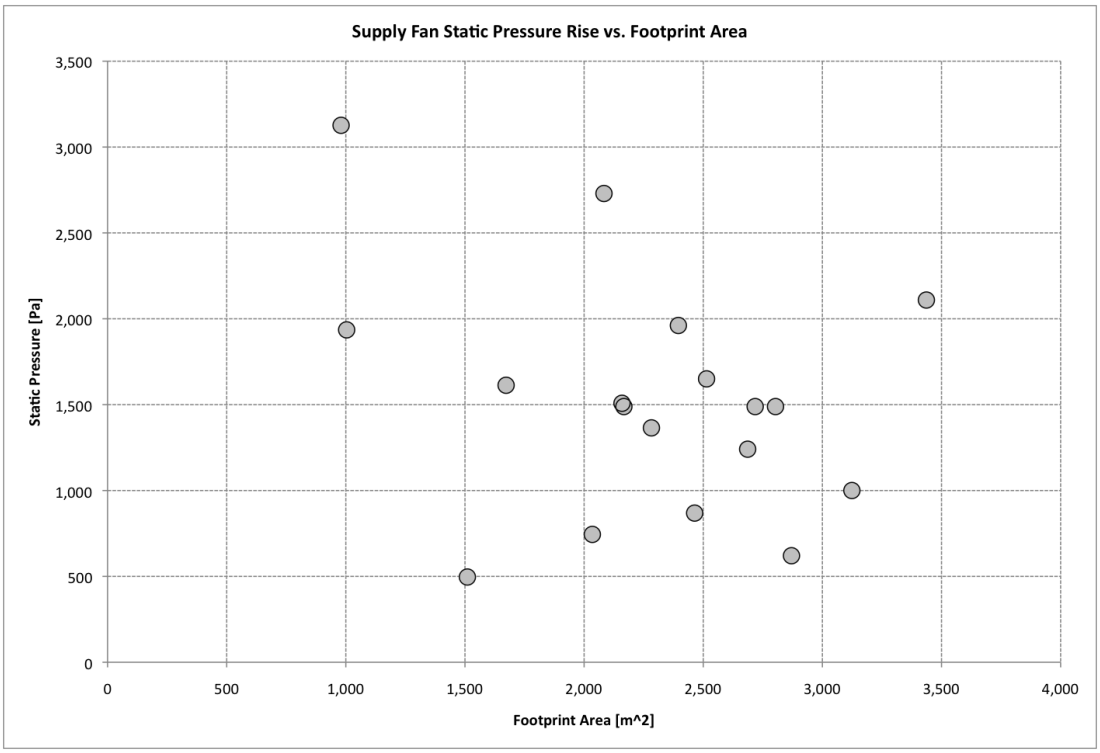

Figure 6.7: Relationship between fan static pressure and building footprint area for the buildings audited during the 2009 CUE summer demonstration.

Internal gains that affect heating and cooling loads include lighting power density, equipment power density, people, transmitted solar radiation, etc. The heat balance equation used in EnergyPlus to calculate the loads in a building zone is described in Equation 6.5 below:

$$q_{LWX} + q_{SW} + q_{LWS} + q_{ki} + q_{sol} + q_{conv} = 0 \tag{6.5}$$

where q_{LWX} is the net long wave radiant exchange flux between zone surfaces, q_{SW} is the net short wave radiant flux to surfaces from lights, q_{LWS} is the long wave radiation from equipment in the zone, q_{ki} is the conduction flux through the zone walls, q_{sol} is the transmitted solar radiation flux absorbed at a surface, and q_{conv} is the convective heat flux to the zone air.

Lights and plug-load equipment directly contribute to the electric consumption of a building, accounting for over 50% of the energy use as seen in Figure 6.6. The lights and equipment also produce heat, influencing heating and cooling loads which ultimately must be met by the chiller and HVAC system. Depending on the climate zone and season, these loads can either reduce or contribute to heating and cooling loads. With these reasons, it is obvious why lights and equipment have a great effect on building electric consumption and demand.

Solar radiation can also greatly affect the heating and cooling loads of a building. EnergyPlus calculates the absorbed direct and diffuse solar radiation heat flux on exterior and interior surfaces. Since windows are have a lower thermal resistance than walls, it makes sense that the solar heat gain coefficient and window U-value have a greater effect on building energy consumption than wall insulation thickness. However, it must be noted that these effects are also influenced by the location of the building, surface angle and tilt, surface face material properties, and climatic conditions [36]. Window shading will also have an effect on the amount of solar radiation that enters a building. During building audits, it is important to note any external or internal shading devices used on the building, what the control strategies are for using those devices, and operation schedules associated with them.

A full set of screening results for buildings A, B, and C can be found in Appendix C. The results include average effects over all climate zones, as well as individual effects associated with particular climate zones and for particular HVAC system types.

6.2 Two-Factor Interactions

Results from the two-factor interaction study also exhibit interesting effects. Using Building A as an example, trends can be seen when looking at the effects of the most significant two-factor interactions. For this study, the top ten results (those with the highest magnitude of effect on the model) of each study were analyzed, out of the 120 cases per study that were considered.

Results for Building A can be seen below in Figure 6.8, Figure 6.9, and Figure 6.10, which are fairly representative of the results seen in buildings B and C as well. A complete set of results for each building can be viewed in Appendix D. Under close examination of Building A, one should notice that a large number of the paired factors affecting the chiller, HVAC system and facility electric consumption and demand are comprised of the most significant main effects determined from the screening test, as described in Table 6.1 of the previous section. However, a few exceptions are seen in each study.

The mass associated with structural components and interior furnishings is most prominent in two-factor interactions related to the HVAC system and facility electric consumption and demand, and has an even greater effect in warm and hot - *dry* climate zones. When considering the latent and sensible heating loads in these climates, the magnitude of the effects make sense - since the internal mass acts as a thermal battery for sensible heat, shifting peak demand loads to off-peak or unoccupied hours. In these climates, the HVAC system typically removes a greater portion of sensible heat than latent heat. Thus, having a "sensible heat" thermal battery greatly reduces the demand on the HVAC system during peak demand times.

There are a few instances in particular climate zones where some of the less significant factors (as derived by the screening test) have an impact on the two-factor interaction results. For instance, wall insulation paired with window U-value has a significant effect on facility electric demand in the Chicago (cool and humid) climate zone. When considering heating and cooling loads associated with Chicago's climatic conditions, it is obvious why wall insulation paired with the window U-value would have a great affect on the model. Preventing unwanted gains or losses to pass through the building envelope can have a great affect on the overall energy consumption and demand of the building.

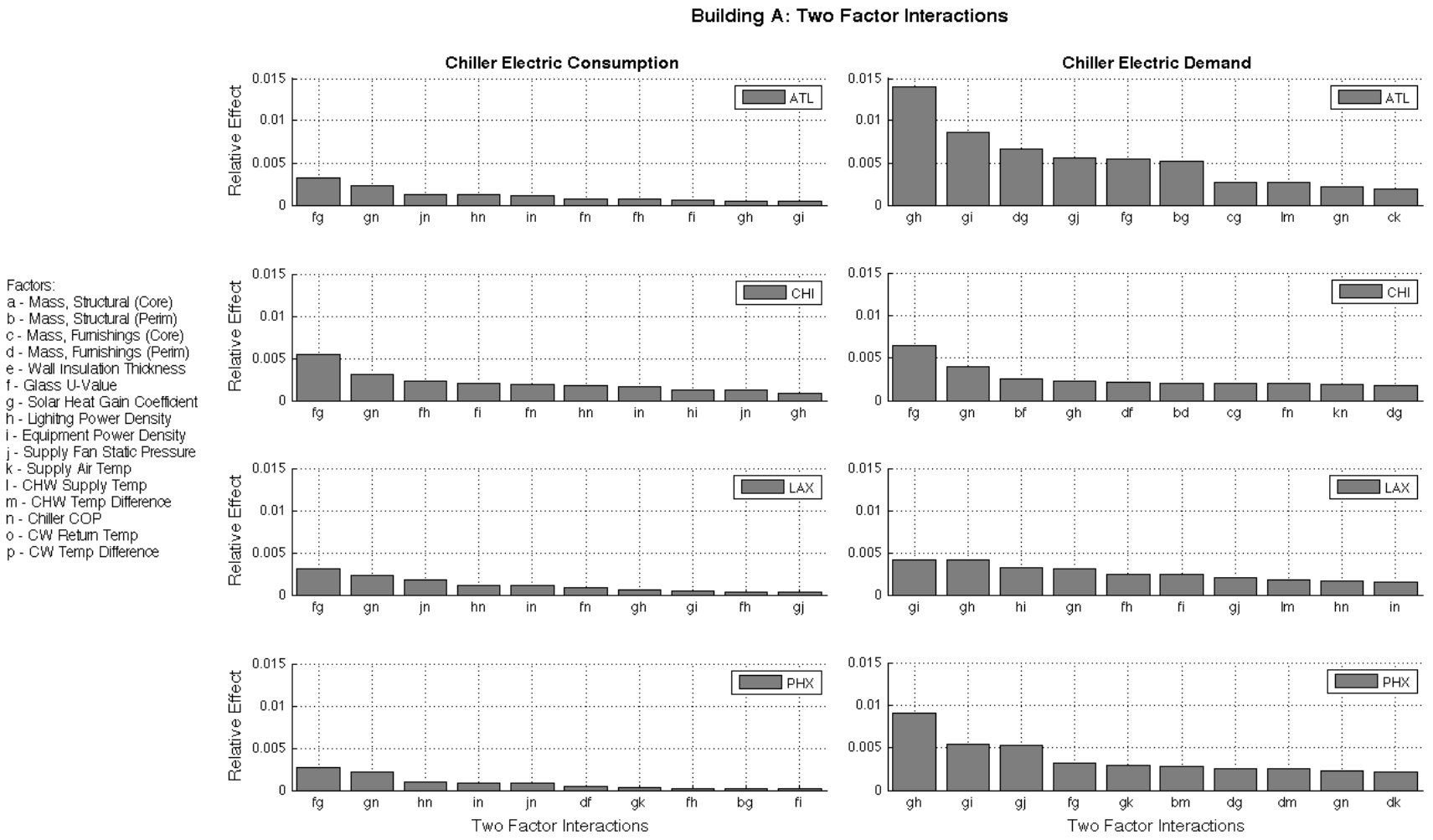

Figure 6.8: Relative impact of two-factor interactions on chiller energy, Building A

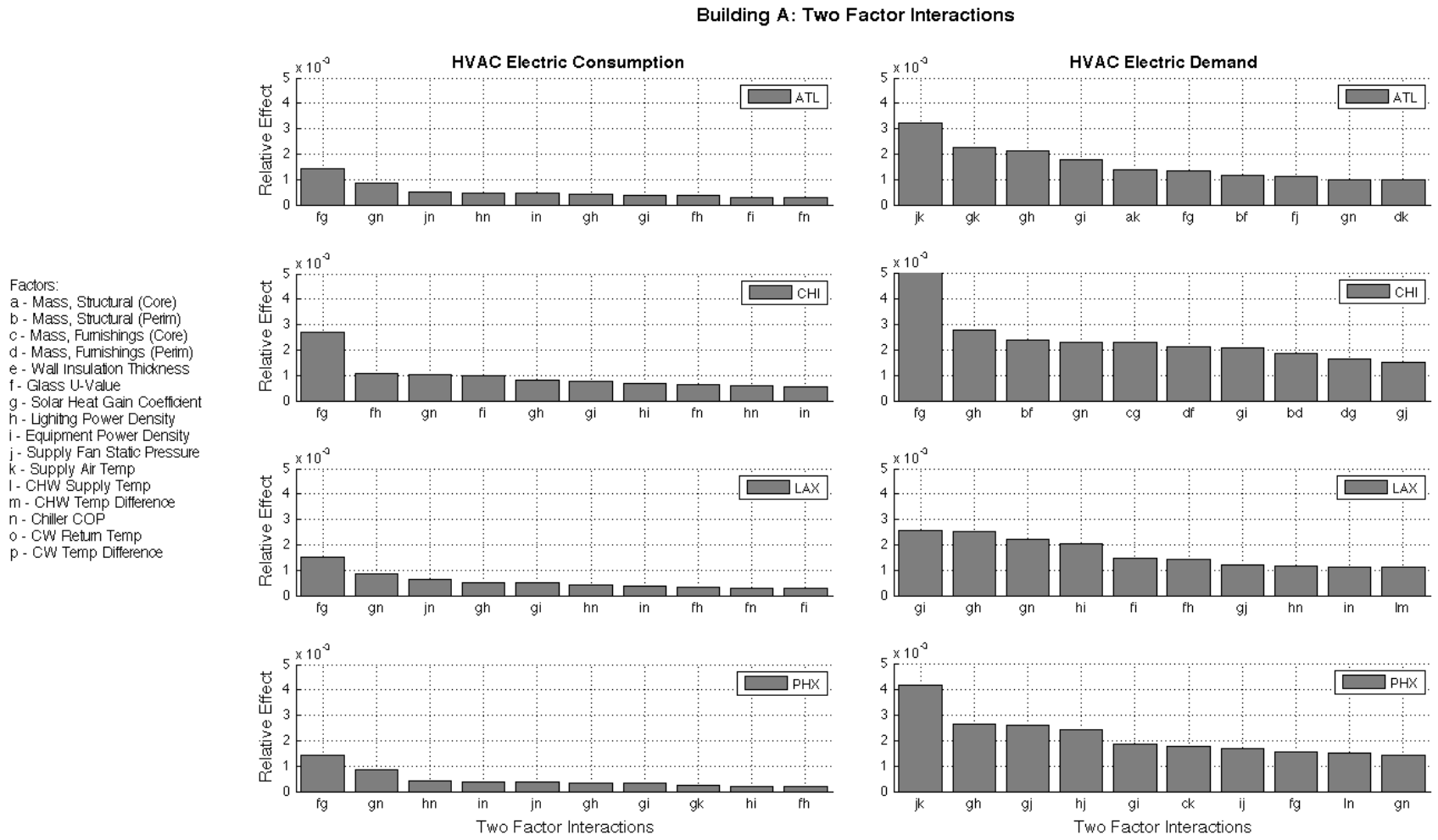

Figure 6.9: Relative impact of two-factor interactions on HVAC system energy, Building A

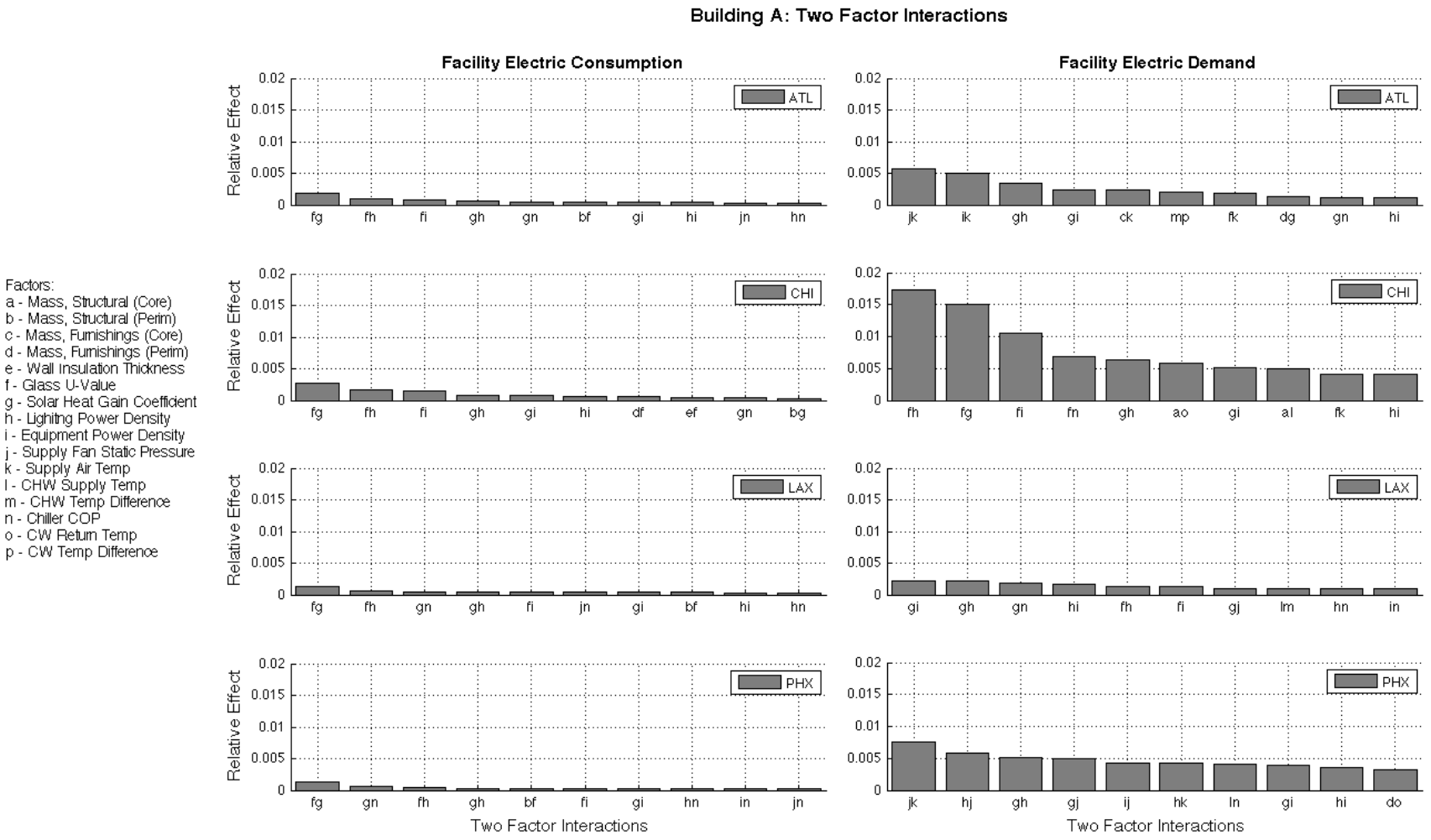

Figure 6.10: Relative impact of two-factor interactions on facility energy, Building A

Analysis of the results for each building type in each climate zone can provide auditors, building energy modelers, and researchers with a hierarchical perspective of how building components and loads affect building electric consumption and demand. A summary of the most significant factors is listed below in order of importance, along with recommendations for proper measurement of each factor. A full set of results are presented in Appendices C and D, which can be used for further evaluation of building parameters for each climate zone and HVAC system configuration.

(1) **Chiller Efficiency (COP)** — Over time, the efficiency of a chiller can decline due to fouling and lack of maintenance. When developing a building model, the design COP may not be a realistic value that describes current conditions of the chiller. To determine a more accurate value, a number of measurements can be made. First, the chiller cooling capacity should be calculated. To do so, a flow meter must be installed on the chilled water supply line and two temperature sensors must be installed to measure the chilled water supply and return temperatures. Using equation 6.2, the capacity can then be calculated. Next, the chiller power must be measured. This can be done by installing a power meter on the chiller. The efficiency can then be calculated by dividing the input power (kW) by the cooling capacity (tons).

(2) **Supply Fan Pressure Rise** — It is recommended that the supply fan pressure rise be measured if possible. Since this building parameter has such a large effect on fan energy consumption, and the fan energy consumption accounts for a large portion of the HVAC and facility energy use, it is important to determine a realistic value for this parameter.

(3) **Window Solar Heat Gain Coefficient and U-value** — The window solar heat gain coefficient (SHGC) and U-value are pieces of data that should be easy to find, and are important to collect since they can have a great impact on building energy consumption and demand. If these numbers are not readily available during the audit, it is recommended that the auditor contact the glass manufacturer. Shading devices should also be noted, as well as any control strategies and schedules for those control strategies.

(4) **Lighting and Equipment Power Density** — Lighting and equipment power density can be hard

to collect in a high-rise commercial office building with multiple tenants. If this is the case, multiple spaces must be audited, if not the entire building. Lighting and equipment plug loads make up a large portion of the energy use of a building and it is important to make sure that these numbers are accurate and not being traded for energy use associated with the HVAC system.

(5) **Thermal Mass** — The internal mass of furnishings and structural components has a medium to low significance on building energy use. However, if possible, it is beneficial to estimate the mass area, and general mass material within the building. This is important because a higher level of internal mass has the potential to dampen the energy profiles throughout the day, shifting peak demand loads to off-peak hours.

Chapter 7

Conclusions and Future Work

7.1 Conclusions

The motivation for this research came from a software development plan to optimize HVAC energy use during summer peak-demand times for large commercial office buildings. Sponsored by a Chicago-based company Clean Urban Energy (CUE), the project partnered with the Building Owners and Managers Association (BOMA) of Chicago to solicit fifty high-rise commercial office buildings in the downtown Chicago Loop to participate in a summer demonstration in 2009. The goals of the summer demonstration were to audit and model as many of the fifty buildings as possible, and subject the models to the CUE optimization software. Out of the fifty buildings, twenty-five buildings were audited, and eight buildings were modeled, calibrated (for summer months), and optimized by the the end of 2009.

From the building audits conducted in 2009 came the goals for this research. Along with the development of the optimization program for CUE, processes for conducting the building audits and for developing building energy models were needed. To help direct these processes, a fractional factorial analysis was conducted on a number of building parameters chosen to represent major building system components and loads, to analyze the effect of each parameter on electric consumption and demand. The results from this analysis provide a hierarchical perspective on how each building component affects the electric consumption and demand associated with the chiller, HVAC system, and building facility for climate zones seen across the United States.

General procedures and best practices are documented for conducting building walk-through audits

and for developing energy models using the EnergyPlus simulation software for high-rise commercial office buildings. These guidelines are explained in detail in Chapters 3 and 4, and provide suggestions for data organization, modeling strategies, and tools to aid in the audit and modeling process. A flow-chart of these processes and tools are presented in Appendix E.

The fractional factorial analysis was conducted to determine the effects of individual factors and two-factor interactions. A set of sixteen factors were chosen to represent the major system components and loads of a building. The base and test level values for each factor were determined by a statistical analysis of design values collected from twenty-two of the Chicago-based buildings that were audited in summer 2009.

Three of these buildings were chosen for the fractional factorial analysis. These buildings were chosen because they represent the most common HVAC system configurations that were seen out of the twenty-five audited buildings, and because they had a significant amount of data pertaining to building component details and sub-metered utility data. With the detailed data, each building was modeled using EnergyPlus version 4.0 and calibrated to sub-metered utility data.

Results from the fractional factorial analysis quantify the effects of each factor on building energy consumption and demand. The level of significance of each factor is described in Table 7.1 below, and graphical representations of these results can be seen in Figure 7.1 and 7.2.

Table 7.1: Factors that have significant effect on energy consumption and demand associated with heating and cooling loads of high-rise commercial office buildings

Factor	**Description**	**Units**	**Significance, Consumption**	**Significance, Demand**
1	Mass Area of Structural Components, Core	m^2	Low	Low
Continued ...				

Table 7.1: (continued)

Factor	**Description**	**Units**	**Significance, Consumption**	**Significance, Demand**
2	Mass Area of Structural Components, Perimeter	m^2	Low	Low
3	Mass Area of Interior Furnishings, Core	m^2	Low	Low
4	Mass Area of Interior Furnishings, Perimeter	m^2	Low (Med in LAX and PHX)	Low
5	Wall Insulation Thickness	m^2	Low	Low
6	Window U-Value	m^2K/W	Low (Med in CHI)	Low (Med in CHI)
7	Window Solar Heat Gain Coefficient	%	Med	Med
8	Lighting Power Density	W/m^2	High	Med
9	Equipment Power Density	W/m^2	High	Med
10	Supply Fan Pressure Rise	Pa	Med	Med
11	Supply Air Temperature	℃	Low	Med
12	Chilled Water Supply Temperature	℃	Low	Low
13	Chilled Water Loop Temperature Differential	℃	Low	Low
14	Chiller Efficiency	COP	High	High
15	Condenser Water Return Temperature	℃	Low	Low
Continued ...				

Table 7.1: (continued)

Factor	**Description**	**Units**	**Significance, Consumption**	**Significance, Demand**
16	Condenser Water Loop Temperature Differential	℃	Low	Low

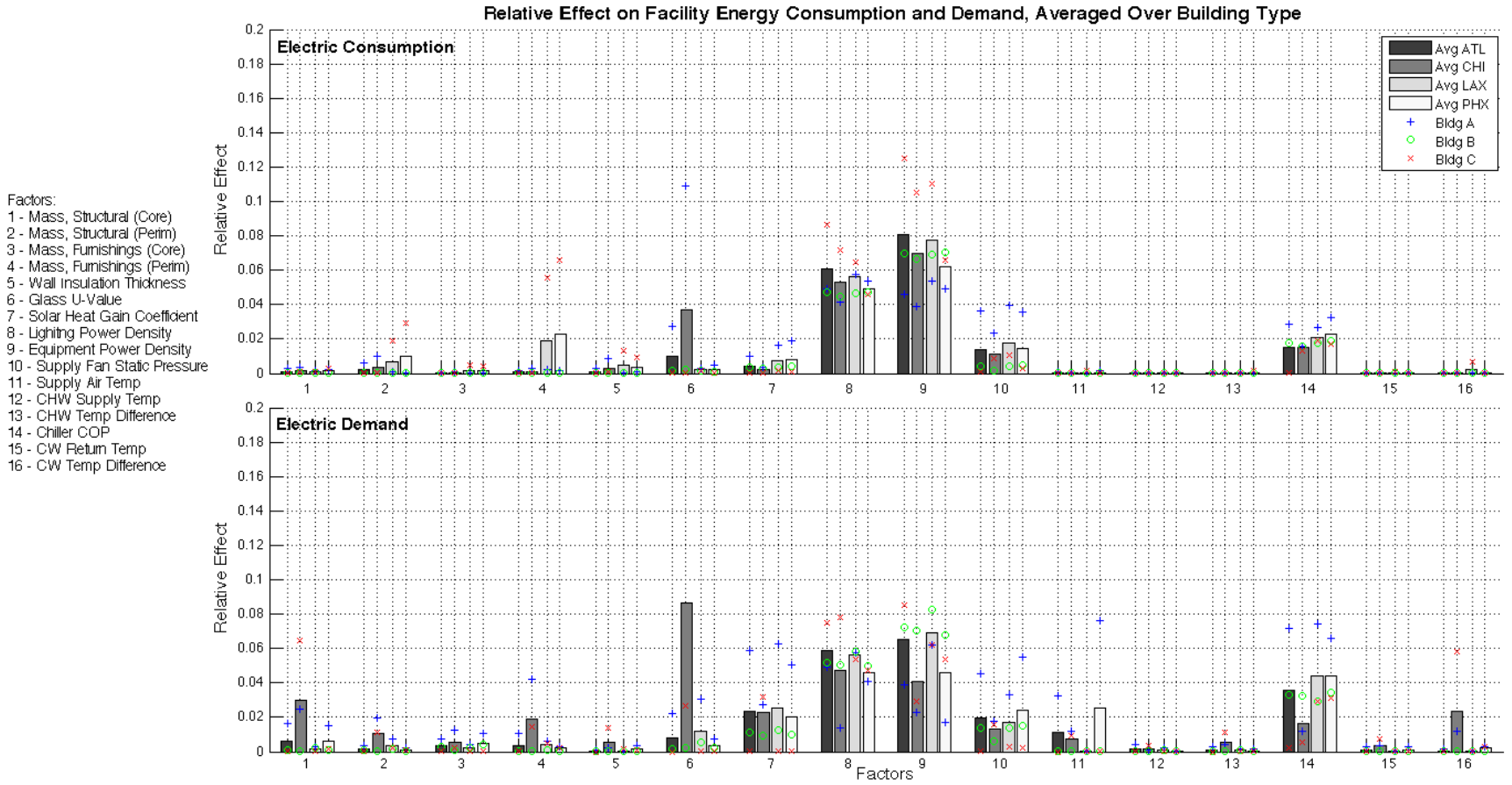

Figure 7.1: The relative effect on facility electric consumption and demand of all buildings averaged over four climate zones. Overlaying the bar charts are points marking the relative effect, also on facility electric consumption and demand, for each building in each climate zone.

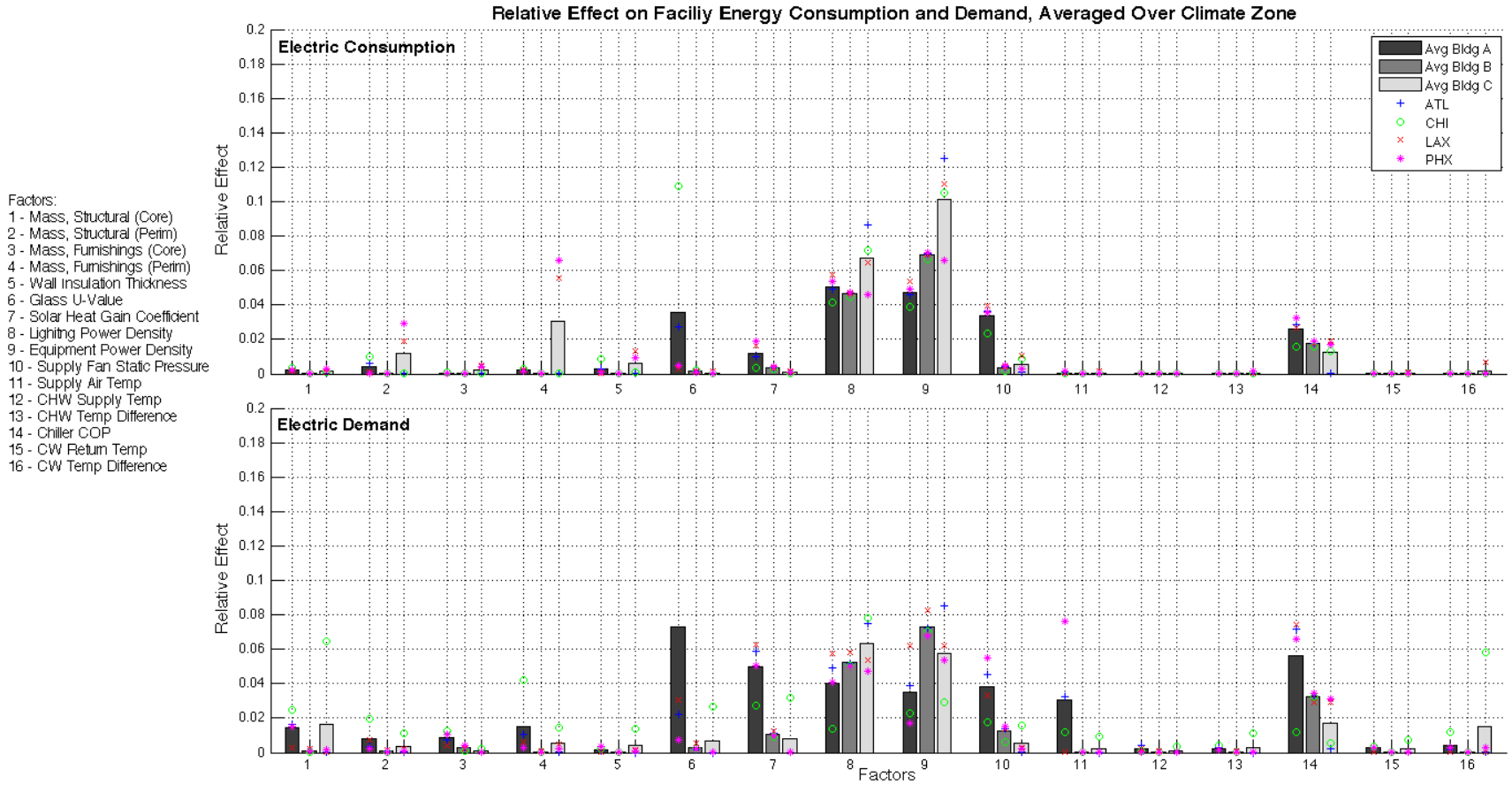

Figure 7.2: The relative effect on facility electric consumption and demand of all climate zones averaged over each building type. Overlaying the bar charts are points marking the relative effect, also on facility electric consumption and demand, for each climate zone and building type.

The two-factor interactions highlight a few of the less significant factors listed in Table 7.1. When coupled with factors of high significance, the less significant factors have a greater affect on chiller, HVAC system, and facility energy consumption and demand. The less significant factors include the thermal mass associated with structural components and interior furnishings, chilled water and condenser water temperature differentials (describing the chiller and cooling tower), and wall insulation and glass U-values that describe the envelope system.

Thermal mass is an important factor to consider since it can affect the thermal response of a building. Thermal mass has the ability to store thermal energy and shift peak demand loads to off-peak, or unoccupied hours. This effect flattens the energy consumption profile, which ultimately affects consumption levels and the magnitude of the electric demand over a specified time period.

Envelope systems, such as wall insulation thickness and window U-value, also have an effect on building energy use. Together, these factors naturally influence the amount of unwanted gains or losses that pass through a building envelope and contribute to energy consumption and demand associated with heating and cooling loads.

In summary, the most significant factors found in this research include the chiller efficiency, supply fan pressure rise, window solar heat gain coefficient and U-value, lighting and equipment power density, and the level of thermal mass seen in the building. Recommendations were made that suggest methods to collect realistic values for each of these parameters. Some of these recommendations require measurements, while others require observations of control strategies and equipment schedules. A summary of these recommendations is presented below.

(1) **Chiller Efficiency (COP)** — Over time, the efficiency of a chiller can decline due to fouling and lack of maintenance. When developing a building model, the design COP may not be a realistic value that describes current conditions of the chiller. To determine a more accurate value, a number of measurements can be made. First, the chiller cooling capacity should be calculated. To do so, a flow meter must be installed on the chilled water supply line and two temperature sensors must be installed to measure the chilled water supply and return temperatures. Using equation 6.2, the

capacity can then be calculated. Next, the chiller power must be measured. This can be done by installing a power meter on the chiller. The efficiency can then be calculated by dividing the input power (kW) by the cooling capacity (tons).

(2) **Supply Fan Pressure Rise** — It is recommended that the supply fan pressure rise be measured if possible. Since this building parameter has such a large effect on fan energy consumption, and the fan energy consumption accounts for a large portion of the HVAC and facility energy use, it is important to determine a realistic value for this parameter.

(3) **Window Solar Heat Gain Coefficient and U-value** — The window solar heat gain coefficient (SHGC) and U-value are pieces of data that should be easy to find, and are important to collect since they can have a great impact on building energy consumption and demand. If these numbers are not readily available during the audit, it is recommended that the auditor contact the glass manufacturer. Shading devices should also be noted, as well as any control strategies and schedules for those control strategies.

(4) **Lighting and Equipment Power Density** — Lighting and equipment power density can be hard to collect in a high-rise commercial office building with multiple tenants. If this is the case, multiple spaces must be audited, if not the entire building. Lighting and equipment plug loads make up a large portion of the energy use of a building and it is important to make sure that these numbers are accurate and not being traded for energy use associated with the HVAC system.

(5) **Thermal Mass** — The internal mass of furnishings and structural components has a medium to low significance on building energy use. However, if possible, it is beneficial to estimate the mass area, and general mass material within the building. This is important because a higher level of internal mass has the potential to dampen the energy profiles throughout the day, shifting peak demand loads to off-peak hours.

With a greater understanding of how these factors effect energy consumption and demand, and with the above recommendations for conducting a building audit, the time required to conduct an audit and

for model development can be accelerated. These results also provide background information for future research that examines building energy consumption and demand.

7.2 Future Work

Future work regarding the fractional factorial analysis could include a number of objectives. First, to obtain a more accurate sample of buildings of this particular type, the study could be expanded to include a larger portfolio of buildings. Data from more high-rise commercial office buildings with a central plant and VAV all-air system could be collected to increase the certainty in the range of values chosen for each parameter studied in the fractional factorial analysis.

On a similar note, the study could explore different building types. High rise commercial office buildings make up only a fraction of the building population as a whole. It would be interesting to see the effects of factors on different building types, with different HVAC system configurations, schedules, and loads. It would also be interesting to see if a similar sub-set of driving factors are prominent for those building types as well.

Building geometry could also be considered. For the current study, the model geometry was simplified to a rectangular prism for all buildings. Model zoning was also simplified to fifteen zones and three floors, with a floor multiplier on the middle floor. Future work could include more complex geometries and zoning patterns. A comparison of the simplified geometry and zoning pattern to a more complex strategy would be an interesting study as well.

With the processes developed in this work, future studies regarding additional building types, HVAC system configurations, and geometrical design features could be conducted with relative ease.

Bibliography

[1] ASHRAE. **ASHRAE Handbook of Fundamentals**. The American Society of Heating, Refrigeration and Air-Coniditioning Engineers, Inc., 2005.

[2] George E. P. Box, J. Stuart Hunter, and William G. Hunter. **Statistics for Experimenters: Design, Innovation, and Discovery , 2nd Edition**. Wiley-Interscience, 2 edition, May 2005.

[3] J.E. Braun. Reducing energy costs and peak electrical demand through optimal control of building thermal storage. **ASHRAE Transactions**, 96(2):876–887, 1990.

[4] H. Cheng. Impacts on the cost savings potential for using passive thermal storage for cooling control. Master's thesis, University of Colorado, Boulder, Colorado, 2006.

[5] H. Cheng, M.J. Brandemuehl, G.P. Henze, A.R. Florita, and C. Felsmann. Evaluation of the primary factors impacting the optimal control of passive thermal storage. **ASHRAE Transactions**, 114(2):57–64, 2008.

[6] B. Coffey. A development and testing framework for simulation-based supervisory control with application to optimal zone temperature ramping demand response using a modified genetic algorithm. Master's thesis, Concordia University, Montreal, Quebec, Canada, 2008.

[7] ComEd. Comed, February 2010.

[8] C. Corbin, E. Greensfelder, and P. May-Ostendorp. Fractional factorial analysis and automated calibration of building energy models using a hybrid particle swarm/hooke-jeeves optimization algorithm. University of Colorado course research project, May 2009.

[9] Clean Urban Energy. Clean urban energy, February 2010.

[10] B. Griffith, N. Long, P. Torcellini, R. Judkoff, D. Crawley, and J. Ryan. Methodology for modeling building energy performance across the commercial sector. Technical Report NREL/TP-550-41956, National Renewable Energy Laboratory, Golden, Colorado, March 2008.

[11] J. S. Haberl and M. Abbas. Development of graphical indices for viewing building energ data: Part i. **Journal of Solar Energy Engineering**, 120(3):156–161, August 1998.

[12] J. S. Haberl and M. Abbas. Development of graphical indices for viewing building energ data: Part ii. **Journal of Solar Energy Engineering**, 120(3):162–167, August 1998.

[13] J. S. Haberl and T. E. Bou-Saada. Procedures for calibrating hourly simulation models to measured building energy and environmental data. **Journal of Solar Energy Engineering**, 120(3):193–204, 1998.

[14] G.P. Henze. Sensitivity analysis of optimal building thermal mass control. **Journal of Solar Energy Engineering**, 129:473–485, November 2007.

[15] G.P. Henze, M.J. Brandemuehl, C. Felsmann, A.R. Florita, and H. Cheng. Evaluation of building thermal mass savings. Research Project 1313-RP, ASHRAE, September 2007.

[16] G.P. Henze, C. Felsmann, and A.R. Florita. Optimization of building thermal mass control in the presence of energy and demand charges. **ASHRAE Transactions**, 2008.

[17] T. Hong. Energyplus run time analysis. Paper LBNL-1311E, Lawrence Berkeley National Laboratory, University of California, 2009.

[18] E. Franconi J. Huang. Commercial heating and cooling loads component analysis. Technical Report LBL-37208, Lawrence Berkeley National Laboratory, Berkeley, CA, November 1999.

[19] M.J. Jimenez. Models for describing the thermal characteristics of building components. **Building and Environment**, 43:152–162, 2008.

[20] M. Krarti. **Energy Audit of Building Systems**. CRC Press, 2000.

[21] National Renewable Energy Laboratory and US Department of Energy. Energyplus example file generator.

[22] Joseph C. Lam and Sam C. M. Hui. Sensitivity analysis of energy performance of office buildings. **Building and Environment**, 31(1):27–39, 1996.

[23] S. Liu and G.P. Henze. Impact of modeling accuracy on predictive optimal control of active and passive building thermal storage inventory. **ASHRAE Transactions**, 110(1):151–163, 2004.

[24] S. Liu and G.P. Henze. Calibration of building models for supervisory control of commercial buildings. **Building Simulation**, 2005.

[25] The MathWorks. Matlab help files, 2009a.

[26] F.C. McQuiston, J.D. Parker, and J.D. Spitler. **Heating, Ventilating, and Air Conditioning**. John Wiley Sons, sixth edition edition, 2005.

[27] Encyclopedia of Chicago. Gas and electricity, June 2010.

[28] US Department of Energy. Energyplus energy simulation software.

[29] National Institute of Standards and Technology. **e-Handbook of Statistical Methods**. NIST/SEMATECH, February 2010.

[30] Federal Energy Management Program. Mv guidelines: Measurement and verification for federal energy projects. U.S. Department of Energy, 2008.

[31] R. Radermacher, S. Klein, and D. A. Didion. Investigation of the part-load performance of an absorption chiller. **ASHRAE Transactions**, 89(1), 1983.

[32] T. A. Reddy and I. Maor. Procedures for reconciling computer-calculated results with measured energy data. Research Project 1051-RP, ASHRAE, January 2006.

[33] Christian Schiefer. xesoview.

[34] B. Stein, J.S. Reynolds, W.T. Grondzik, and A.G. Kwok. **Mechanical and Electrical Equipment for Buildings**. John Wiley Sons, tenth edition edition, 2006.

[35] EnergyPlus Development Team. **Auxiliary EnergyPlus Programs**. University of Illinois and the Lawrence Berkeley National Laboratory, April 2009.

[36] EnergyPlus Development Team. **Engineering Reference**. University of Illinois and the Lawrence Berkeley National Laboratory, October 2009.

[37] EnergyPlus Development Team. **Getting Started with EnergyPlus, Basic Concepts Manual**. University of Illinois and the Lawrence Berkeley National Laboratory, April 2009.

[38] EnergyPlus Development Team. **Input Output Reference**. University of Illinois and the Lawrence Berkeley National Laboratory, October 2009.

[39] C. P. Underwood. **HVAC Control Systems**. Taylor Francis, 1999.

[40] A.J. Wheeler and A.R. Ganji. **Introduction to Engineering Experimentation**. Pearson Education, Inc., second edition edition, 2004.

[41] J.H. Yoon and E.J. Lee. Calibration procedure of energy performance simulation model for a commercial building. **Proceedings of Building Simulation**, 3:1439–1446, 1999.

Appendix A

Summary of Building Values

The following appendix provides a detailed summary of building values collected during the 2009 CUE summer demonstration audits. Building names and addresses are proprietary information to CUE and have been purposely removed from this thesis report. To mask their identity, each building has been labeled alphabetically. Data for buildings A, B, and C match the buildings discussed in the main body of this thesis.

	Field	A	B	C	D	E	F	G	H	I	J	K
Building Geometry and Vintage	Year Built	1980	1973	2005	1984	1992	1982	2004	1992	1987	1984	1966
	Number of Floors	39	44	42	36	19	39	12	49	40	40	21
	Foodprint Area [m2]	2,396	2,870	2,686	1,673	217,929	2,718	3,124	2,159	2,514	2,514	3,437
	Floor-to-Floor Height [m]	3.35	3.66	3.96	3.51	4.35	3.51	4.02	3.96	3.51	3.51	3.61
	Window-to-Wall Ratio [%]	54%	57%	50%	44%	33%	42%	54%	54%	41%	41%	57%
Building Envelope	Wall Insulation Thickness [m]	0.05	0.076	0.05	0.05	0.05	0.05	-	-	-	-	0.08
	Glass U-Value [W/m2K]	1.33	5.60	1.28	1.28	1.70	2.47	-	-	-	-	5.60
	SHGC	0.49	0.72	0.36	0.21	0.34	0.36	-	-	-	-	0.72
Internal Loads	Number of People	1,800	4,000	5,000	1,350	7,000	3,000	975	1,650	1,986	1,986	-
	Lighting Power Density [W/m2]	10.50	9.00	13.00	13.25	11.84	10.50	14.00		11.00	11.00	-
	Equipment Power Density [W/m2]	7.50	4.00	7.50	7.00	5.38	7.50	10.00	-	9.00	9.00	-
Internal Mass	Mass - Structural (Core) [m2]	233	-	-	-	-	789	-	20,850	-	-	-
	Mass - Structural (Perim) [m2]	86	-	-	-	-	189	-	3,031	-	-	-
	Mass - Interior Furnishings (Core) [m2]	3,163	1,007	1,820	1,007	18,876	3,694	2,153	3,584	-	-	-
	Mass - Interior Furnishings (Perim) [m2]	407	166	222	166	930	435	242	1,990	-	-	-
Airside Equipment	Supply Fan Pressure Rise [Pa]	1,961	620	1,241	1,613	1,613	1,489	1,000	1,508	1,650	1,650	2,109
	Supply Air Temperature [C]	11.11	10.00	8.61	12.22	9.46	10.83	12.80	8.30	11.61	11.67	11.47
Chilled Water Loop	Chilled Water Supply Temperature [C]	5.56	6.11	3.33	5.56	5.56	5.56	6.67	5.56	5.56	5.56	6.11
	Chilled Water Return Temperature [C]	14.44	-	13.17	13.33	13.33	12.22	12.77	13.36	12.22	12.22	-
	Chilled Water Loop Design Temperature Differential [C]	8.88	6.67	9.84	7.77	7.77	6.66	6.10	7.80	6.66	6.66	-
Chiller	Chilled Water Supply Temperature [C]	5.56	6.11	3.33	5.56	5.56	5.56	6.67	5.56	5.56	5.56	6.11
	Chilled Water Loop Design Temperature Differential [C]	5.56	-	3.33	7.77	7.77	6.66	6.10	7.80	6.66	6.66	-
	COP	3.62	4.51	5.05	4.86	5.01	4.97	5.40	5.05	5.24	4.88	-
	Condenser Water Return Temperature [C]	29.44	-	29.44	29.44	29.44	29.44	29.40	29.44	29.44	29.44	-
Cooling Tower	Condenser Loop Design Temperature Difference [C]	8.34	5.6	7.12	7.23	7.95	8.34	1.70	5.60	8.34	8.34	-
	Condenser Water Return Temperature [C]	29.44	29.44	29.44	29.44	29.44	29.44	29.40	29.44	29.44	29.44	-
	Condenser Water Supply Temperature [C]	37.78	37.78	36.56	36.67	37.39	37.78	31.1	35.04	37.78	37.78	-
	Design Inlet Air Wetbulb Temperature [C]	25.56	26.11	25.56	25.56	26.00	25.56	25.5	26.11	25.56	25.56	-

Figure A.1: Summary of building data from collected from buildings A-K during the CUE 2009 summer demonstration.

	Field	L	M	N	O	P	Q	R	S	T	U	V
Building Geometry and Vintage	Year Built	1956	1991	1927	1966	1986	1992	1972	1965	1989	1966	1991
	Number of Floors	19	39	23	21	34	51	22	23	31	35	10
	Foodprint Area [m2]	980	1,003	2,464	3,437	2,035	2,283	2,803	1,510	3,157	2,083	2,167
	Floor-to-Floor Height [m]	3.96	3.66	3.12	3.61	3.81	3.90	3.20	3.96	3.96	3.45	3.81
	Window-to-Wall Ratio [%]	67%	51%	15%	57%	31%	44%	71%	21%	22%	35%	41%
Building Envelope	Wall Insulation Thickness [m]	-	0.08	0.05	0.03	0.08	-	0.03	0.05	0.08	0.03	0.08
	Glass U-Value [W/m2K]	2.78	2.70	1.64	-	2.70	5.60	3.29	-	2.70	5.60	1.69
	SHGC	0.49	0.40	0.24	-	0.70	0.72	0.38	-	0.70	0.72	0.37
Internal Loads	Number of People		-	-	-	-	2,800	-	2,000		2,200	900
	Lighting Power Density [W/m2]	11.00	-	-	-	-	21.50	-	-	-	-	-
	Equipment Power Density [W/m2]	8.25	-	-	-	-	21.50	-	-	-	-	-
Internal Mass	Mass - Structural (Core) [m2]	-	-	-	-	-	-	-	-	-	-	-
	Mass - Structural (Perim) [m2]	-	-	-	-	-	-	-	-	-	-	-
	Mass - Interior Furnishings (Core) [m2]	-	-	-	-	-	-	-	-	-	-	-
	Mass - Interior Furnishings (Perim) [m2]	-	-	-	-	-	-	-	-	-	-	-
Airside Equipment	Supply Fan Pressure Rise [Pa]	3,127	1,935	868	2,109	744	1,365	1,489	496	-	2,730	1,489
	Supply Air Temperature [C]	11.11	11.11	12.78	10.83	13.28	6.67	11.67	13.33	-	12.61	9.72
Chilled Water Loop	Chilled Water Supply Temperature [C]	5.56	5.56	5.56	6.11	29.44	2.78	5.56	-	-	6.11	5.56
	Chilled Water Return Temperature [C]	-	12.22	-	-	-	11.67	13.11	-	-	11.67	14.44
	Chilled Water Loop Design Temperature Differential [C]	-	6.66	-	-	-	8.89	7.55	0.00	-	5.56	8.88
Chiller	Chilled Water Supply Temperature [C]	5.56	5.56	5.56	6.11	29.44	2.78	5.56	-	-	6.11	5.56
	Chilled Water Loop Design Temperature Differential [C]	-	6.66	-	-		8.89	7.55	-	-	5.56	8.88
	COP	-	4.70	-	-	7.56	4.55	4.43	-	-	-	4.89
	Condenser Water Return Temperature [C]	-	29.50	-	-	29.44	29.44	29.44	-	-	-	29.44
Cooling Tower	Condenser Loop Design Temperature Difference [C]	-	8.33	-	-	5.56	8.34	8.34	6.56	-	0.00	8.34
	Condenser Water Return Temperature [C]	-	29.50	-	-	29.44	29.44	29.44	29.44	-	-	29.44
	Condenser Water Supply Temperature [C]	-	37.83	-	-	35	37.78	37.78	36	-	-	37.78
	Design Inlet Air Wetbulb Temperature [C]	-	25.56	-	-	25.56	25.56	-	25.56	-	-	25.56

Figure A.2: Summary of building data from collected from buildings L-V during the CUE 2009 summer demonstration.

Appendix B

Calibration Results

The following appendix shows two sets of calibration results for buildings A, B, and C. The first set shows hourly comparisons between the simulated data and measured data in line graph format, as well as monthly percent differences displayed in bar chart format. The second set of results show the same data as in the first set, but also includes scatter plots of the data, percent difference over the entire simulation, and the root mean square error.

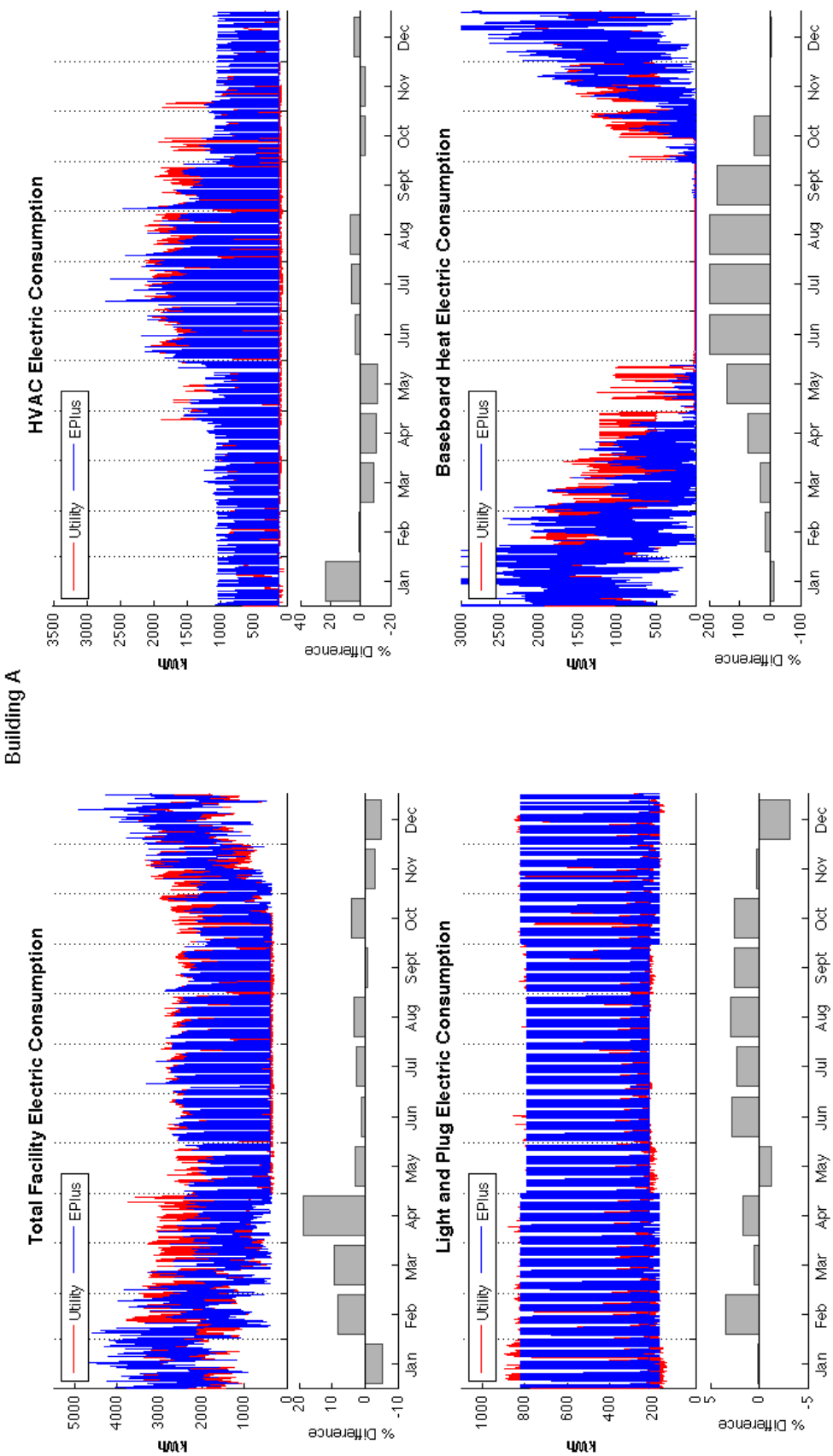

Figure B.1: Calibration results for Building A.

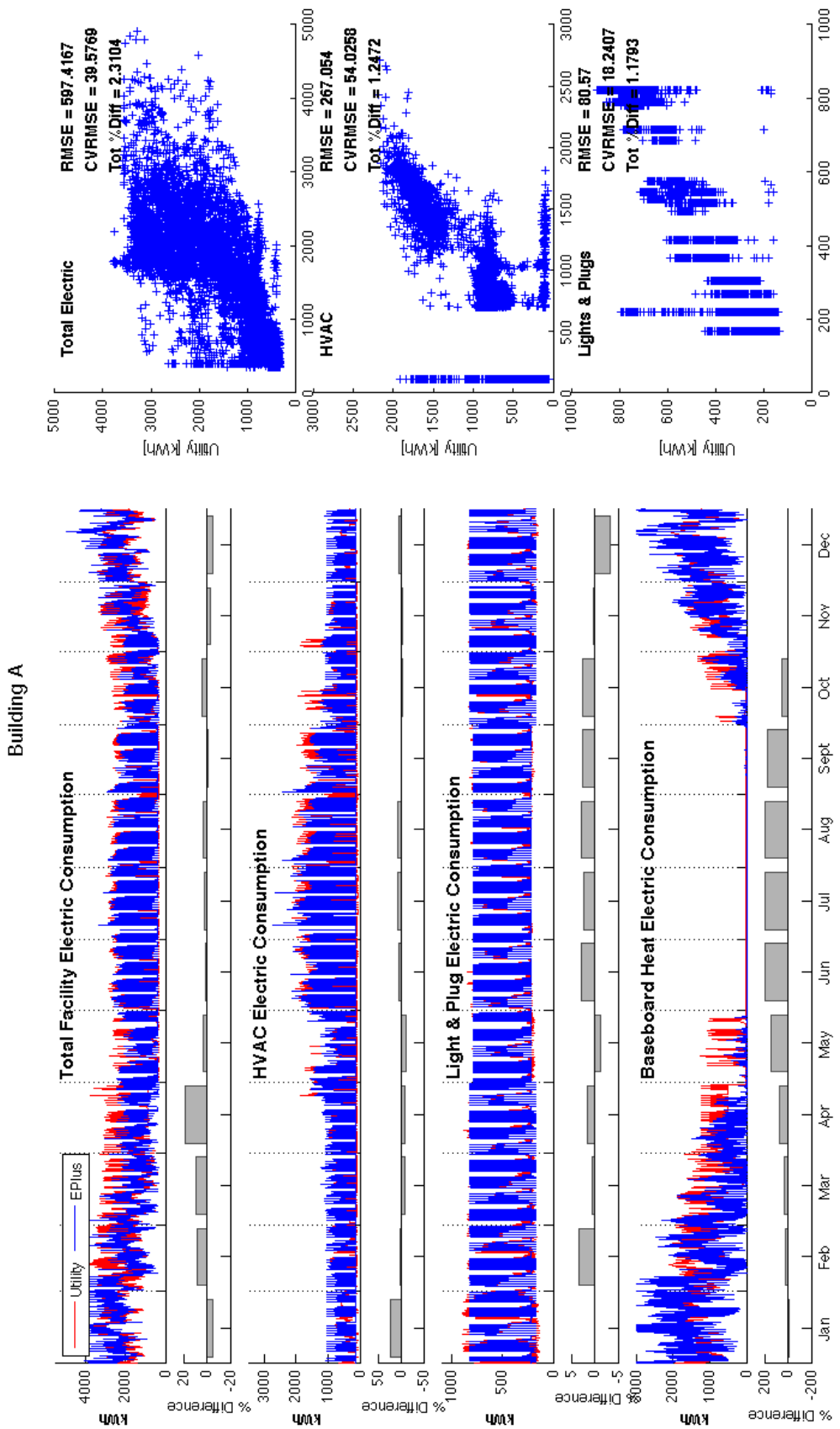

Figure B.2: Calibration results for Building A.

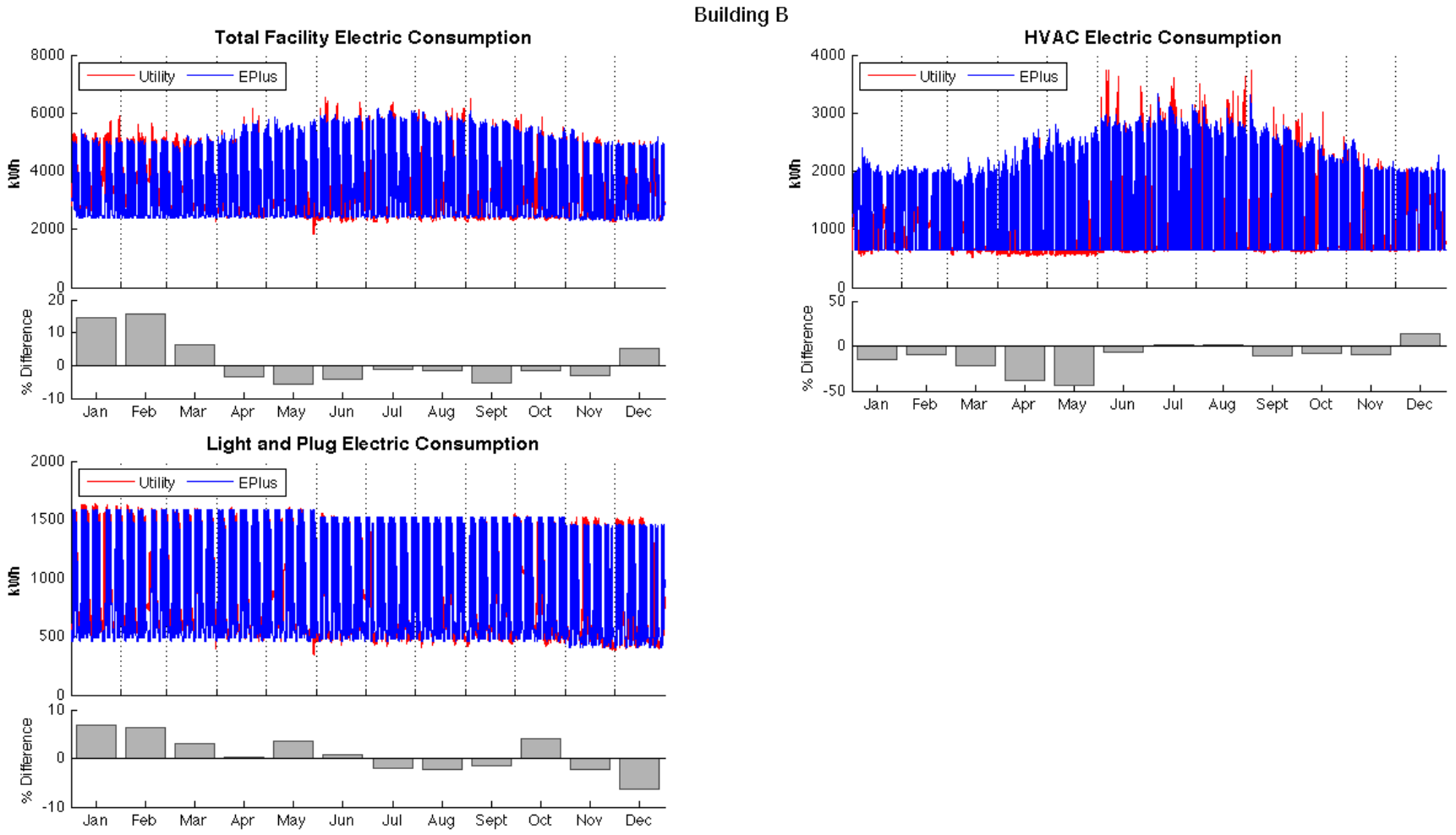

Figure B.3: Calibration results for Building B.

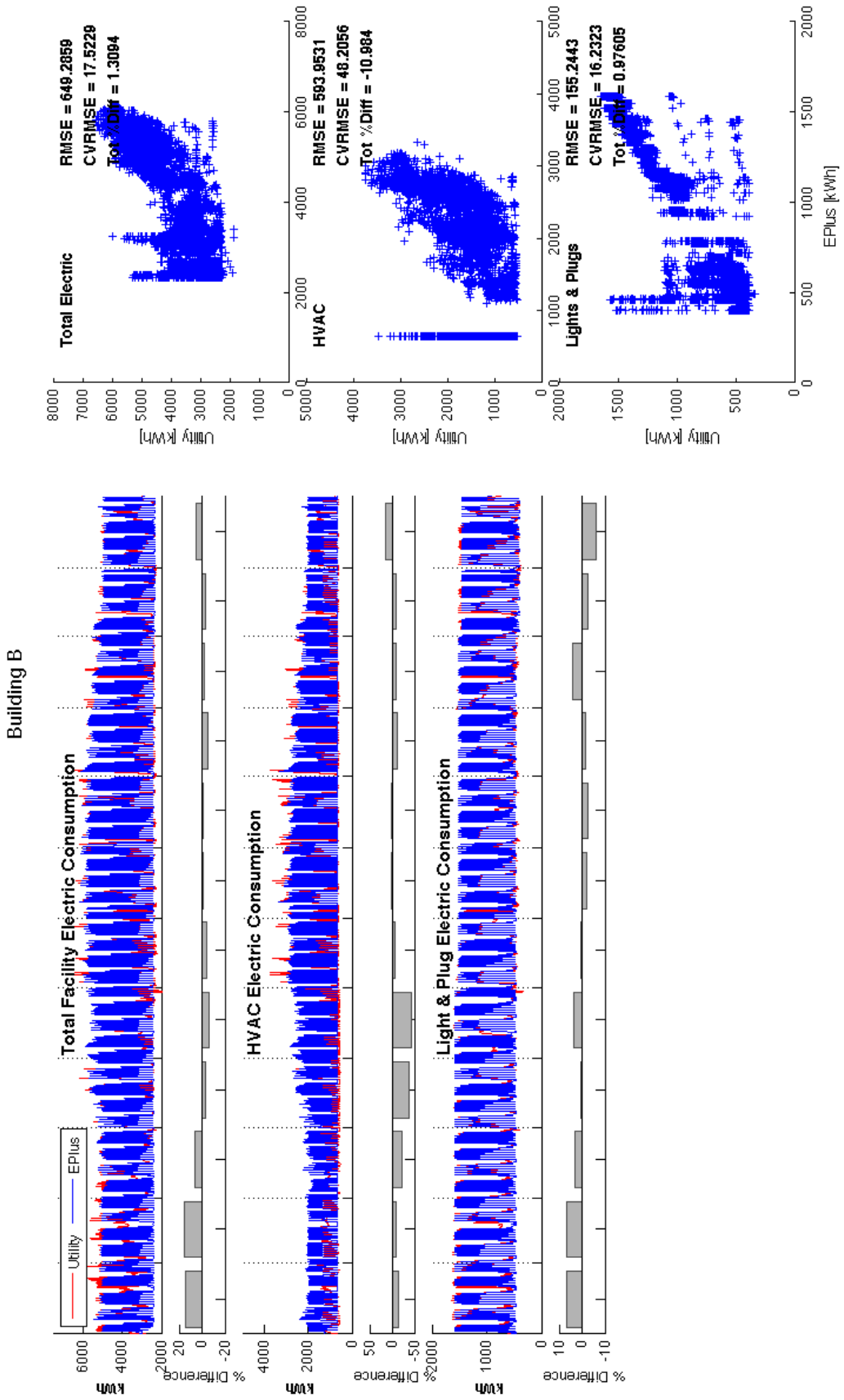

Figure B.4: Calibration results for Building B.

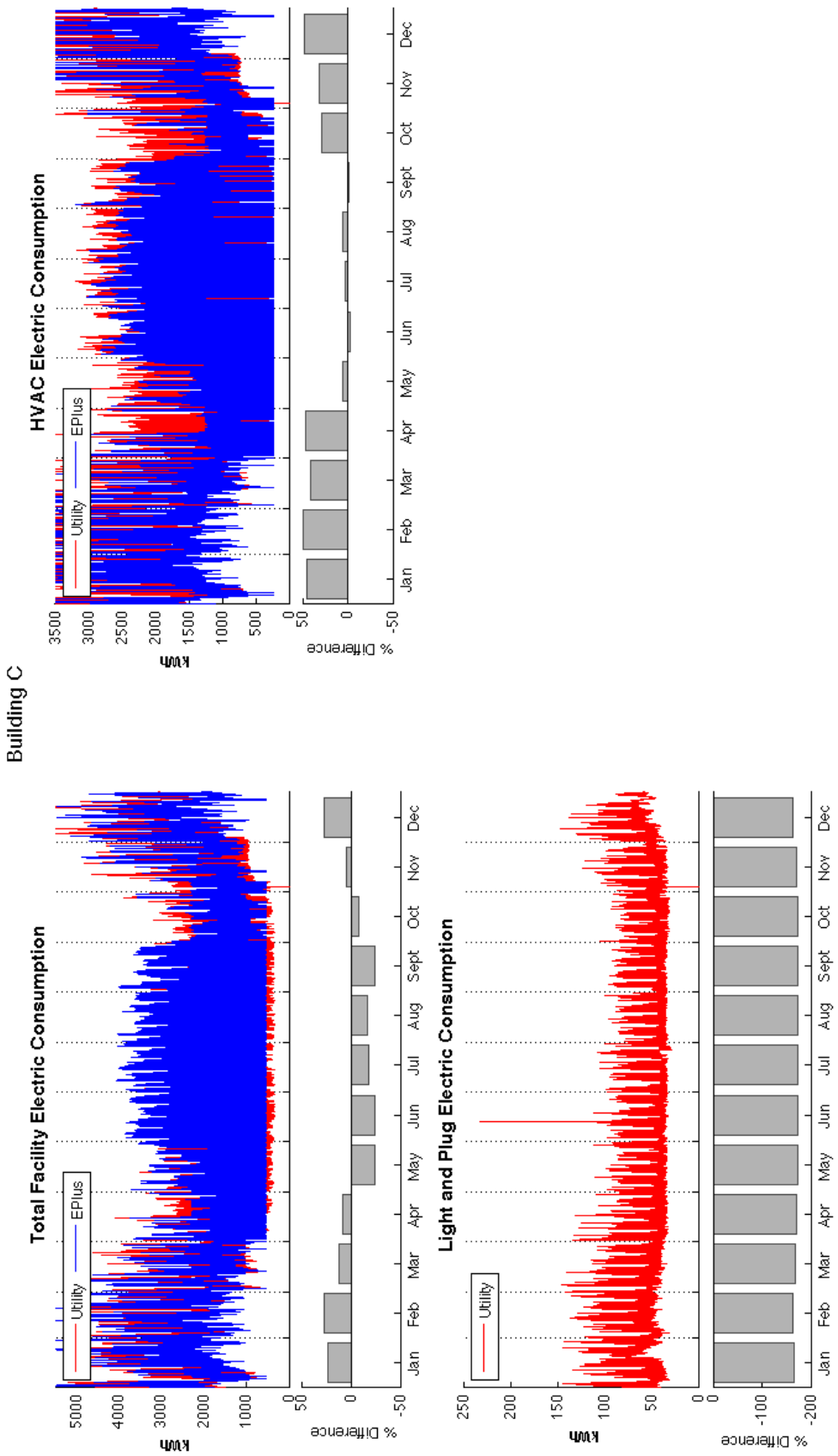

Figure B.5: Calibration results for Building C.

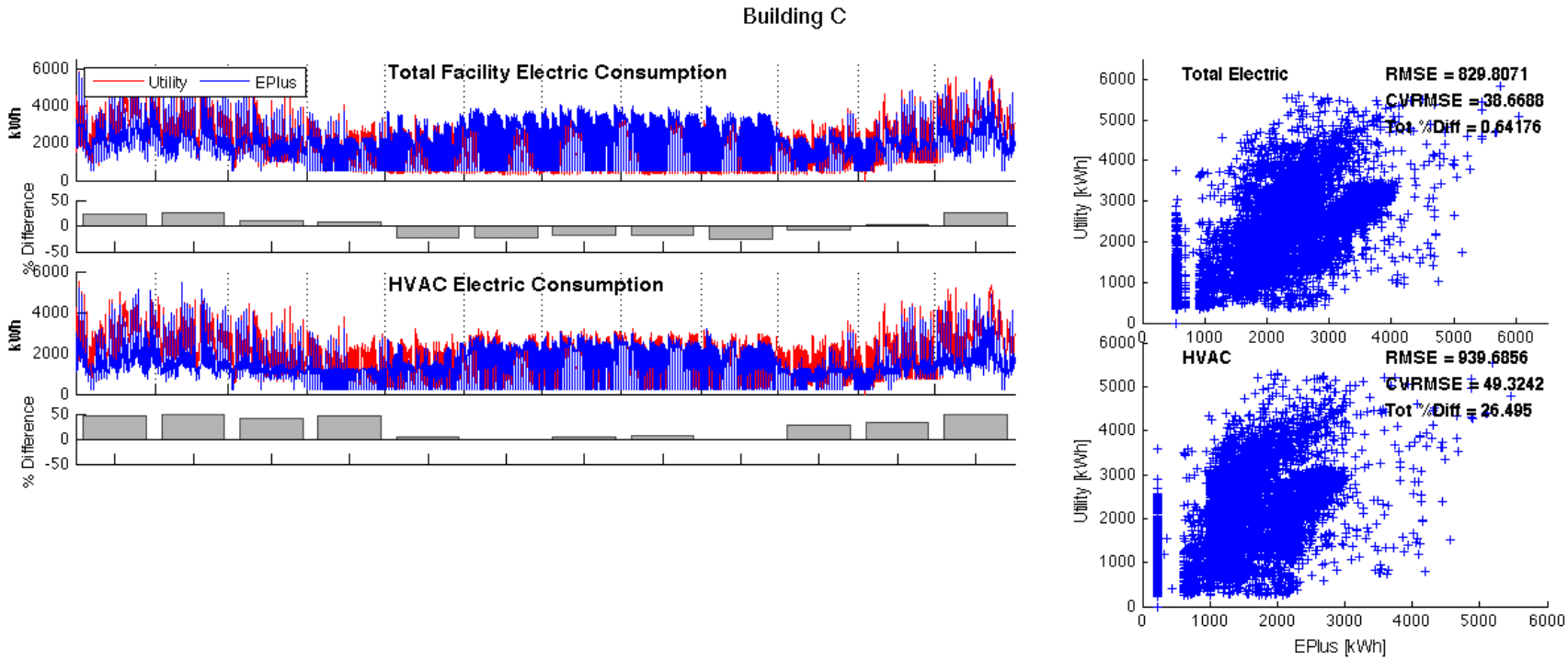

Figure B.6: Calibration results for Building C.

Appendix C

Main Effects

The following appendix of charts reports fractional factorial analysis screening results for annual simulations. The results are organized in the following manner. First, the averaged main effects over each climate zone are shown for energy consumption and demand associated with the chiller, HVAC system, and whole-building facility for each building. Secondly, main effects on energy consumption and demand associated with the chiller, HVAC system, and whole-building facility are shown for each building and for each climate zone. The scale on each graph is the same to illustrate the difference in magnitude of the effects for each case. The analysis for Building C was conducted for only the summer months, due to insufficient data regarding building heating components and building loads for the winter and swing months.

For reference, a quick summary of the building component values can be seen in Table C.1 below.

Table C.1: FFA building characteristics

Field	**Building A**	**Building B**	**Building C**
Year Built	1980	1973	2005
Number of Floors	39	44	42
Footprint Area	2,400 m^2	2,900 m^2	2,700 m^2
Floor-to-Floor Height	3.35 m	3.66 m	3.96 m
Average Window-to-Wall Ratio	54%	57%	50%
Number of People	1,800	4,000	5,000
Continued ...			

Table C.1: (continued)

Field	**Building A**	**Building B**	**Building C**
Terminal System Configuration			
Core	VAV, NoReheat	VAV, NoReheat	VAV, NoReheat
Perimeter	VAV w/Baseboard Electric Reheat	VAV w/Hot Water Reheat	Series PIU w/Electric Reheat

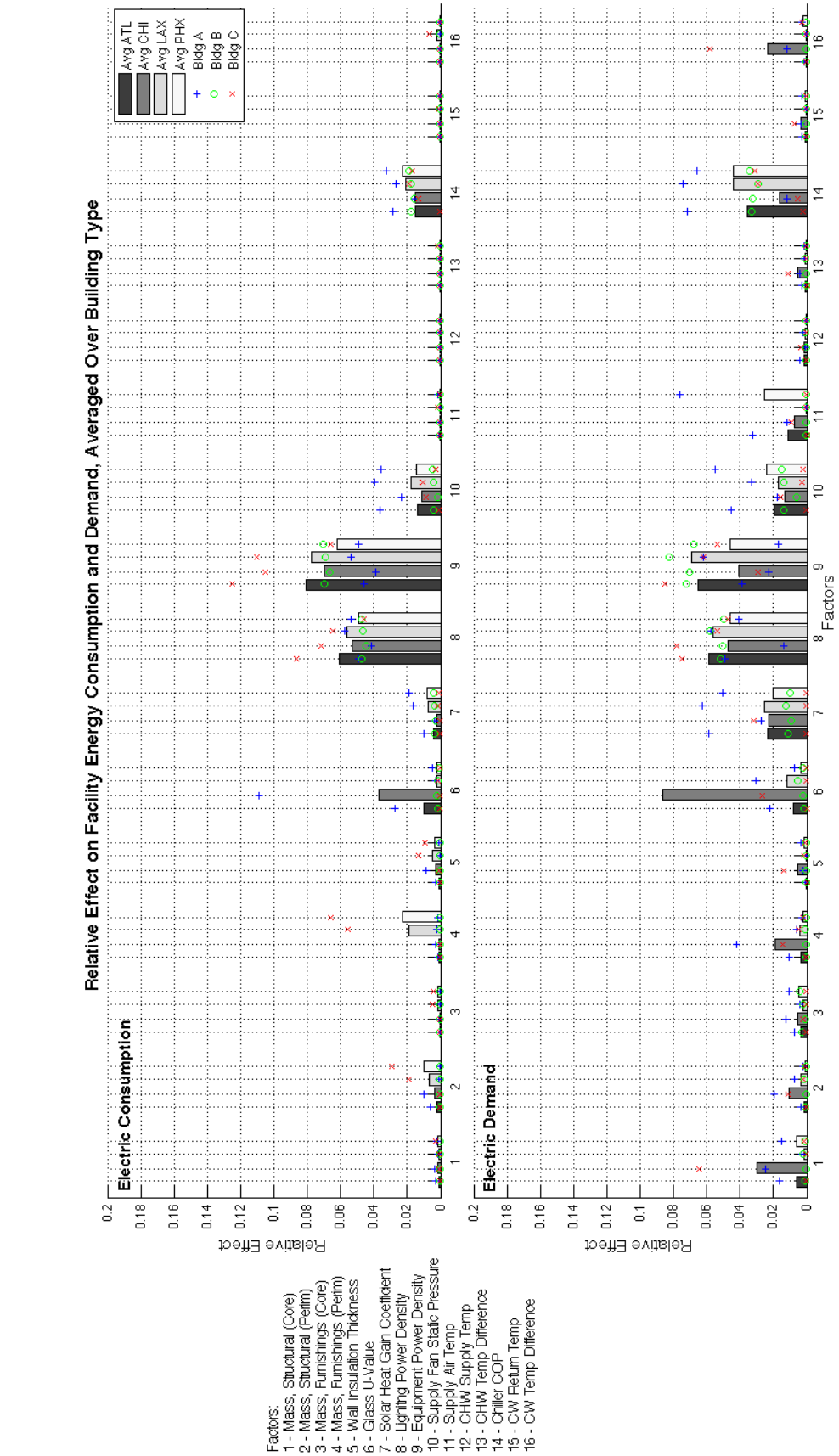

Figure C.1: The relative effect on facility electric consumption and demand of all buildings averaged over four climate zones. Overlaying the bar charts are points marking the relative effect, also on facility electric consumption and demand, for each building in each climate zone.

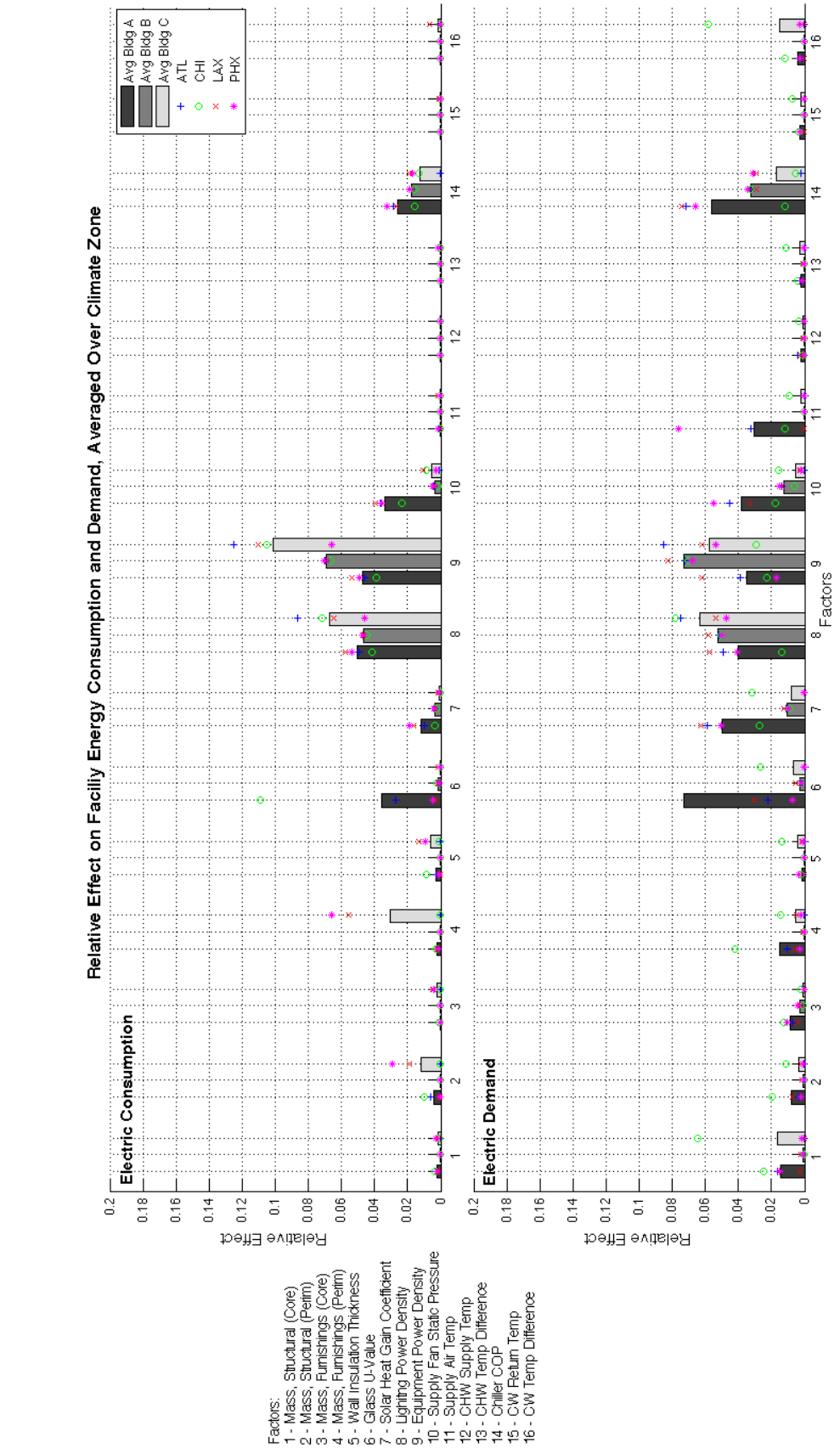

Figure C.2: The relative effect on facility electric consumption and demand of all climate zones averaged over each building type. Overlaying the bar charts are points marking the relative effect, also on facility electric consumption and demand, for each climate zone and building type.

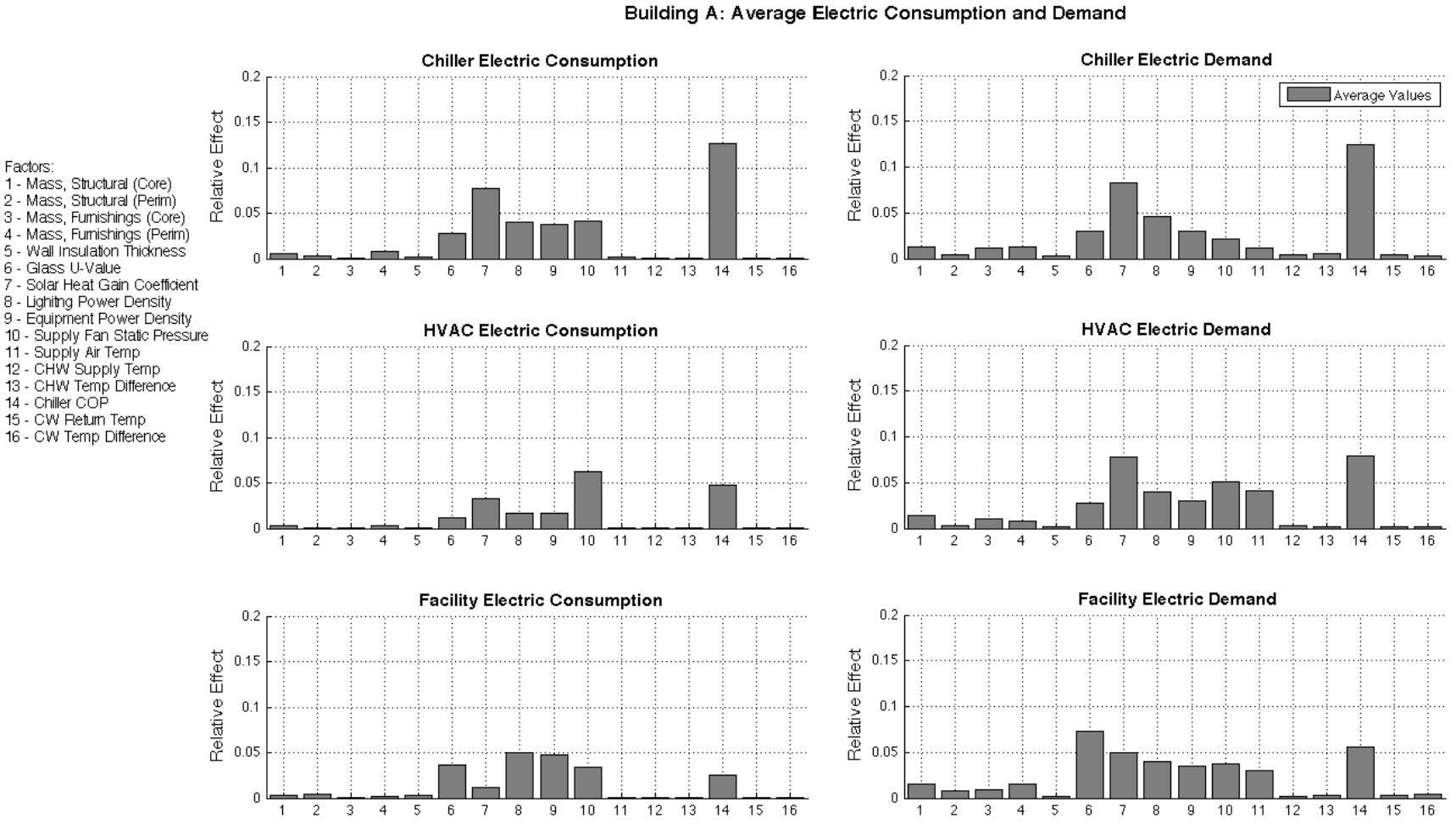

Figure C.3: Average relative impact over four climate zones on chiller, HVAC system, and facility electric consumption and demand for Building A

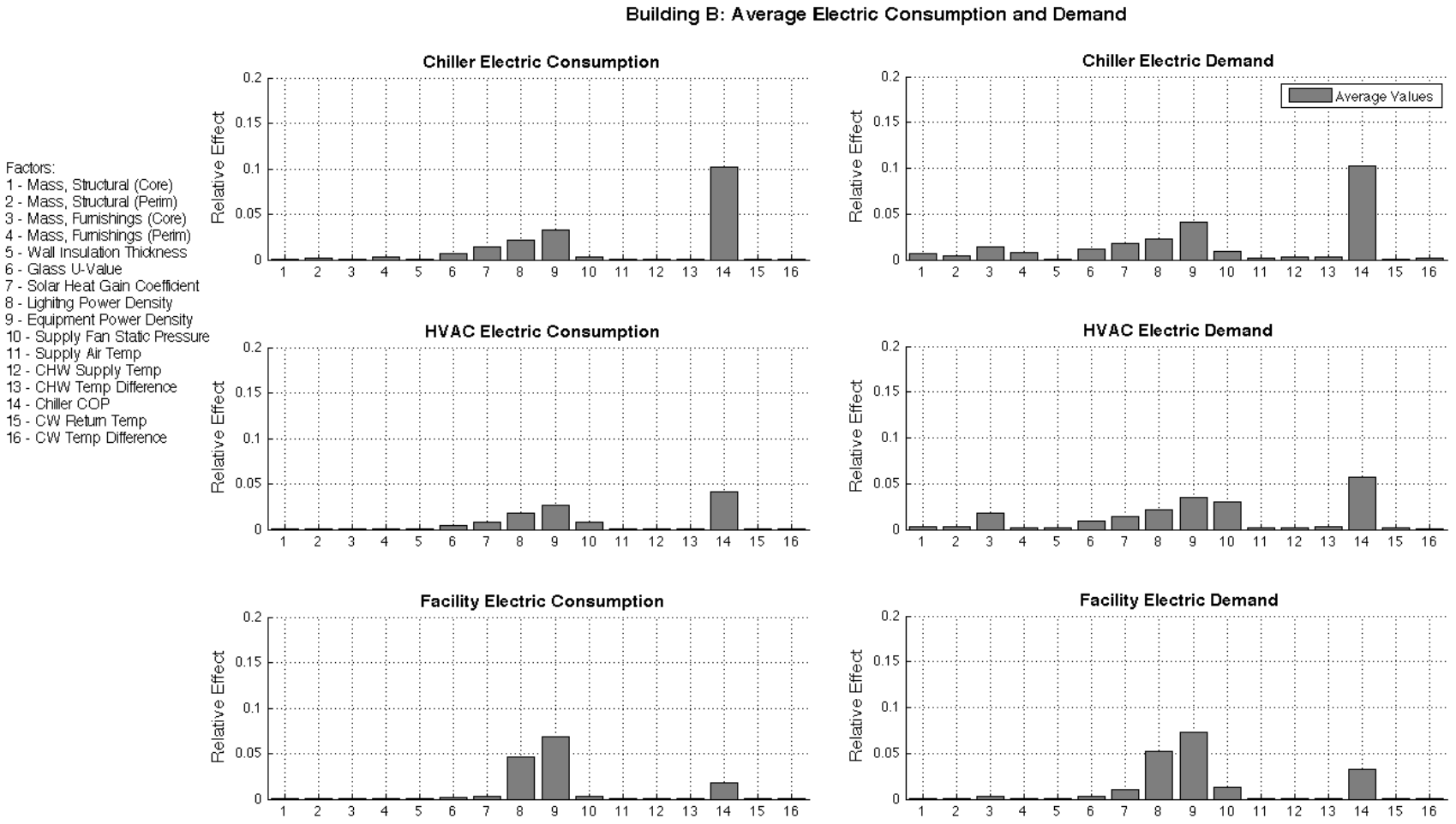

Figure C.4: Average relative impact over four climate zones on chiller, HVAC system, and facility electric consumption and demand for Building B

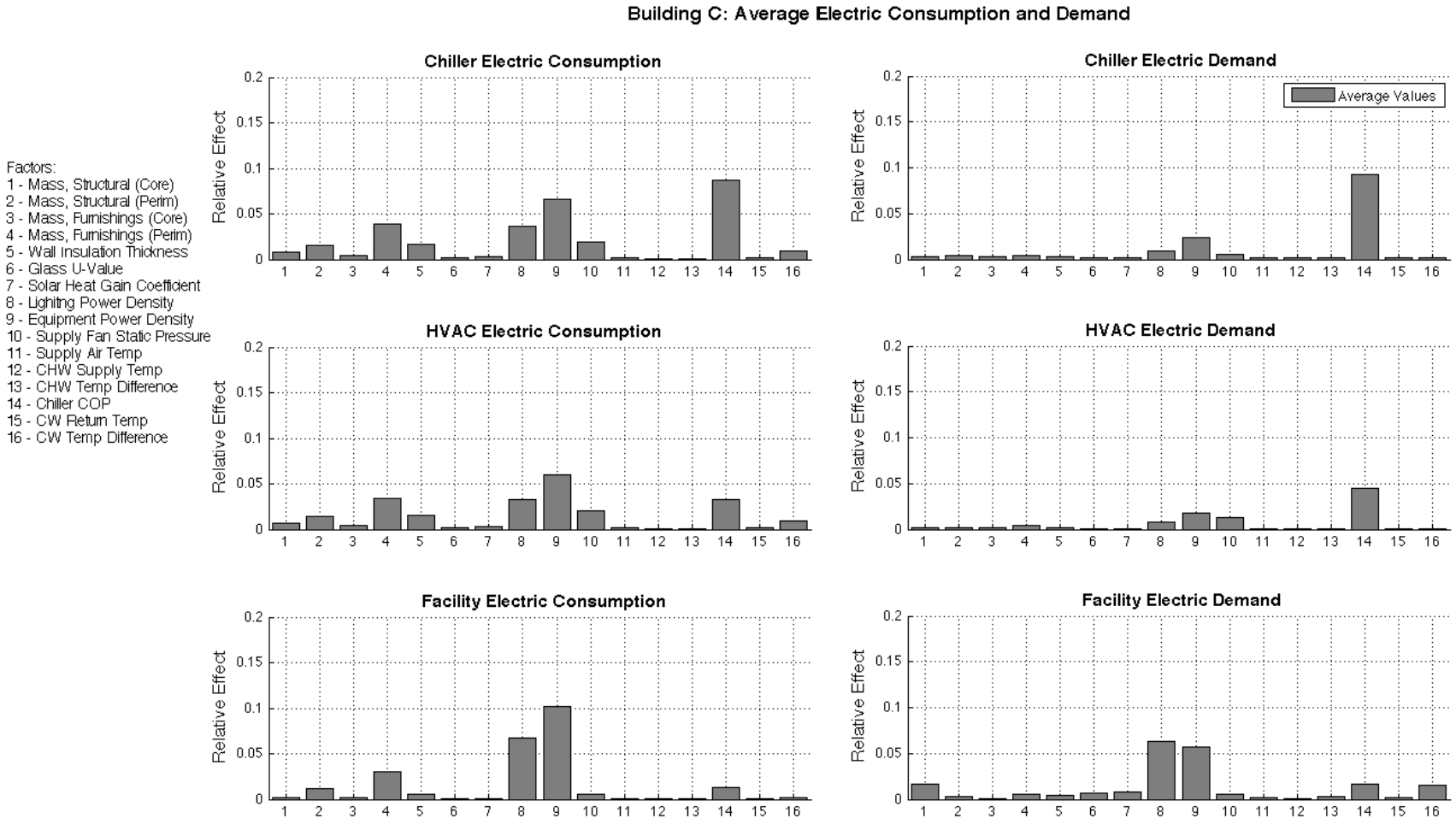

Figure C.5: Average relative impact over four climate zones on chiller, HVAC system, and facility electric consumption and demand for C

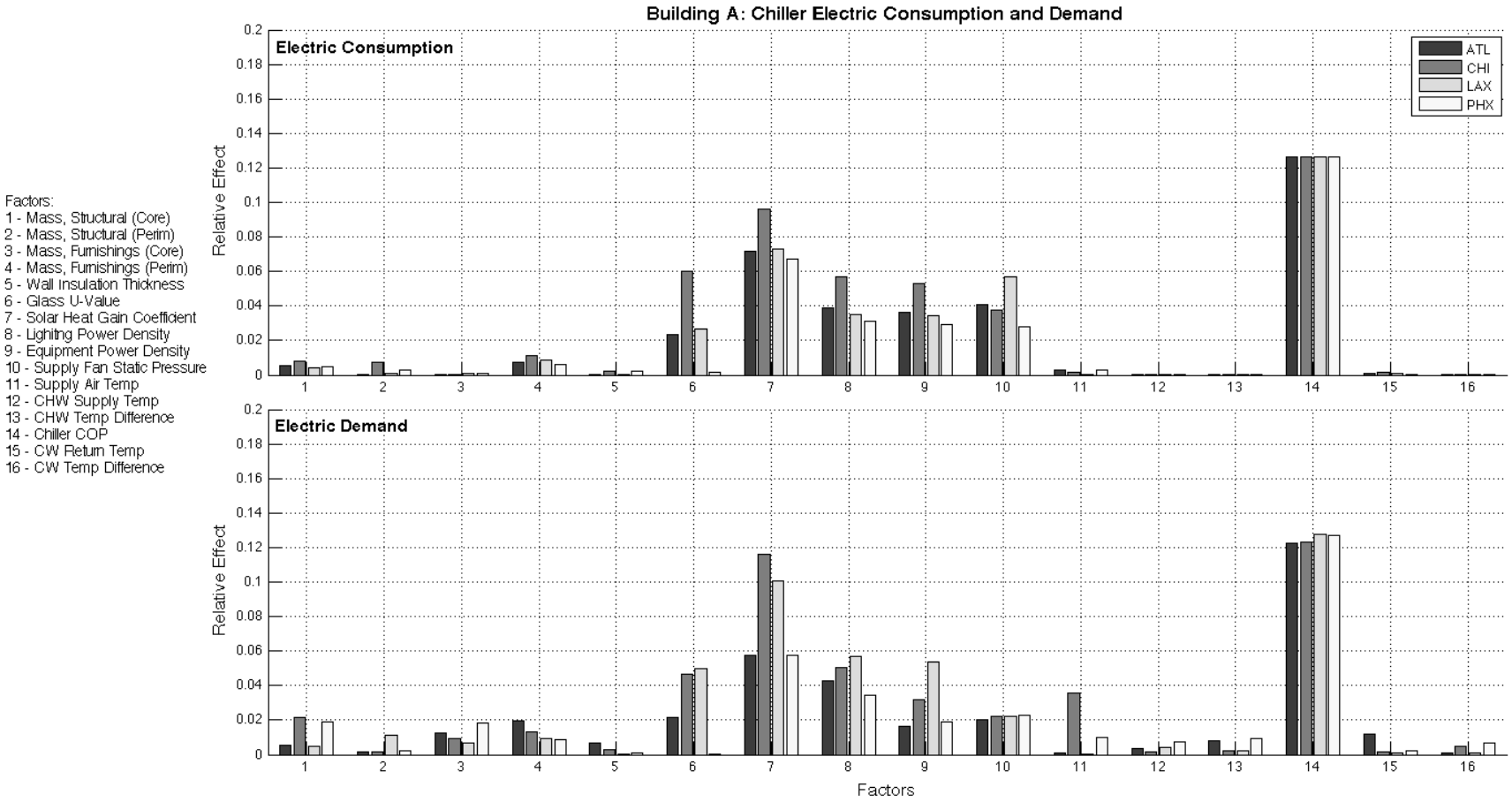

Figure C.6: Relative impact on chiller electric consumption and demand for Building A

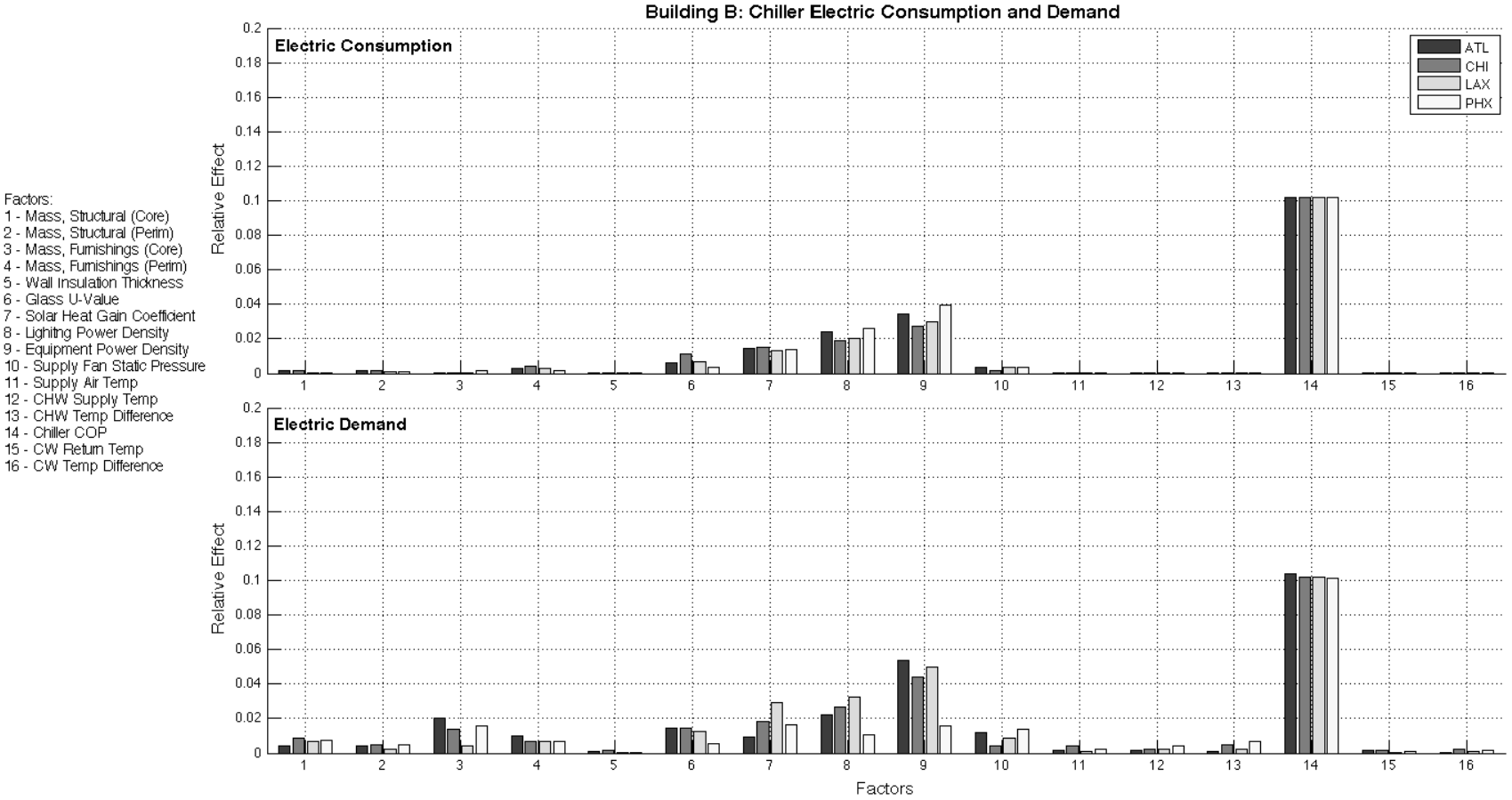

Figure C.7: Relative impact on chiller electric consumption and demand for Building B

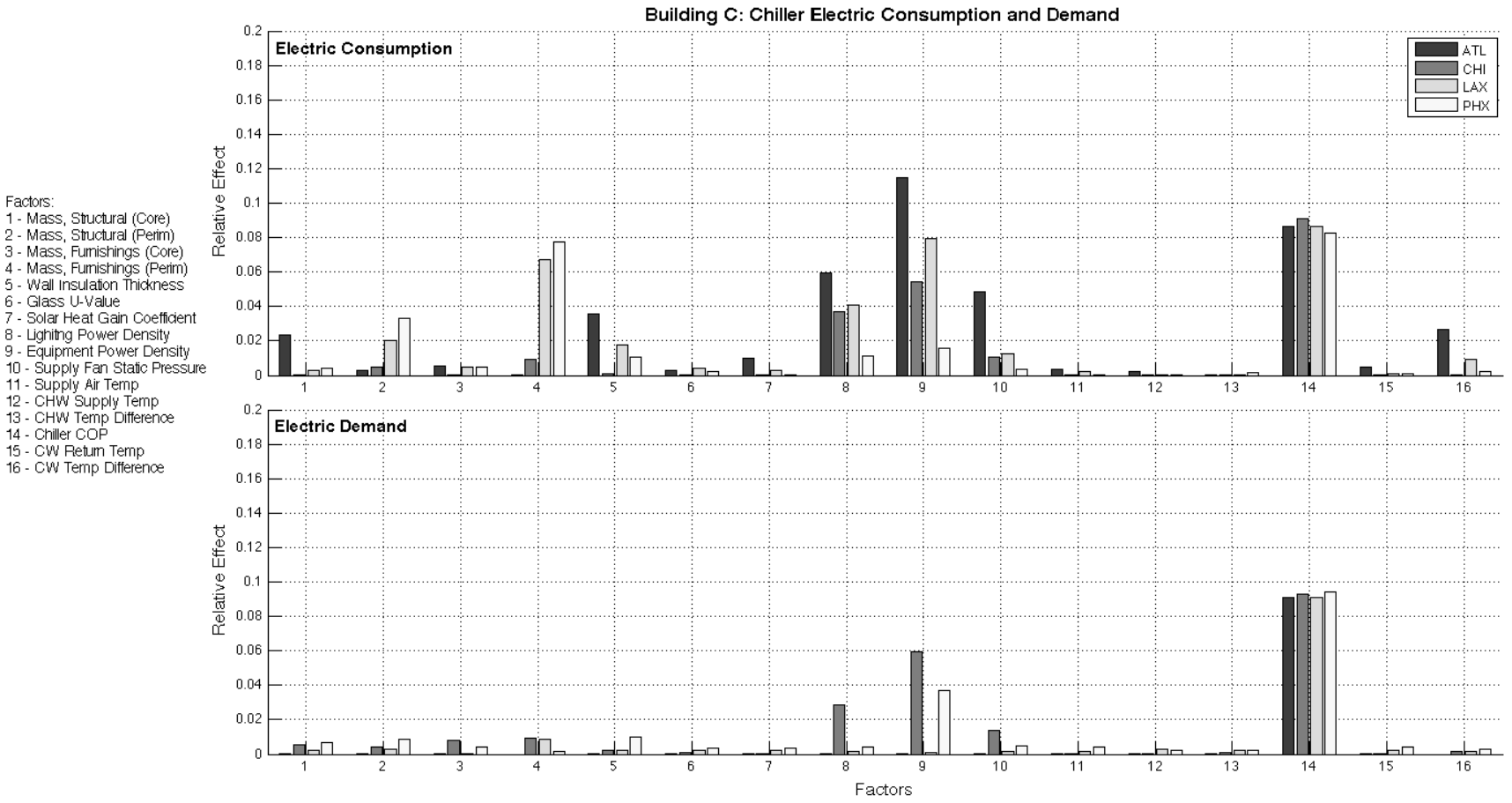

Figure C.8: Relative impact on chiller electric consumption and demand for Building C

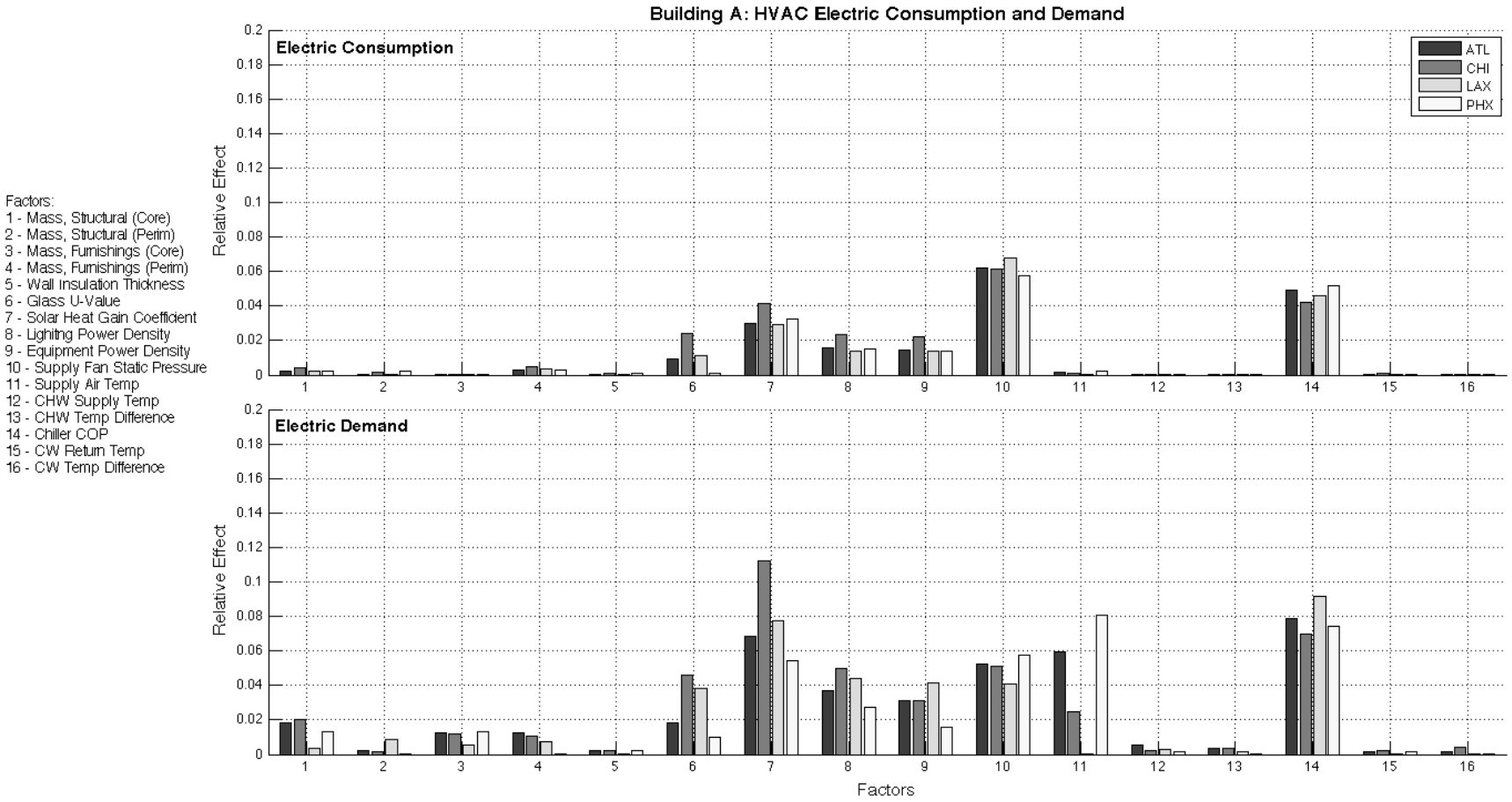

Figure C.9: Relative impact on HVAC system electric consumption and demand for Building A

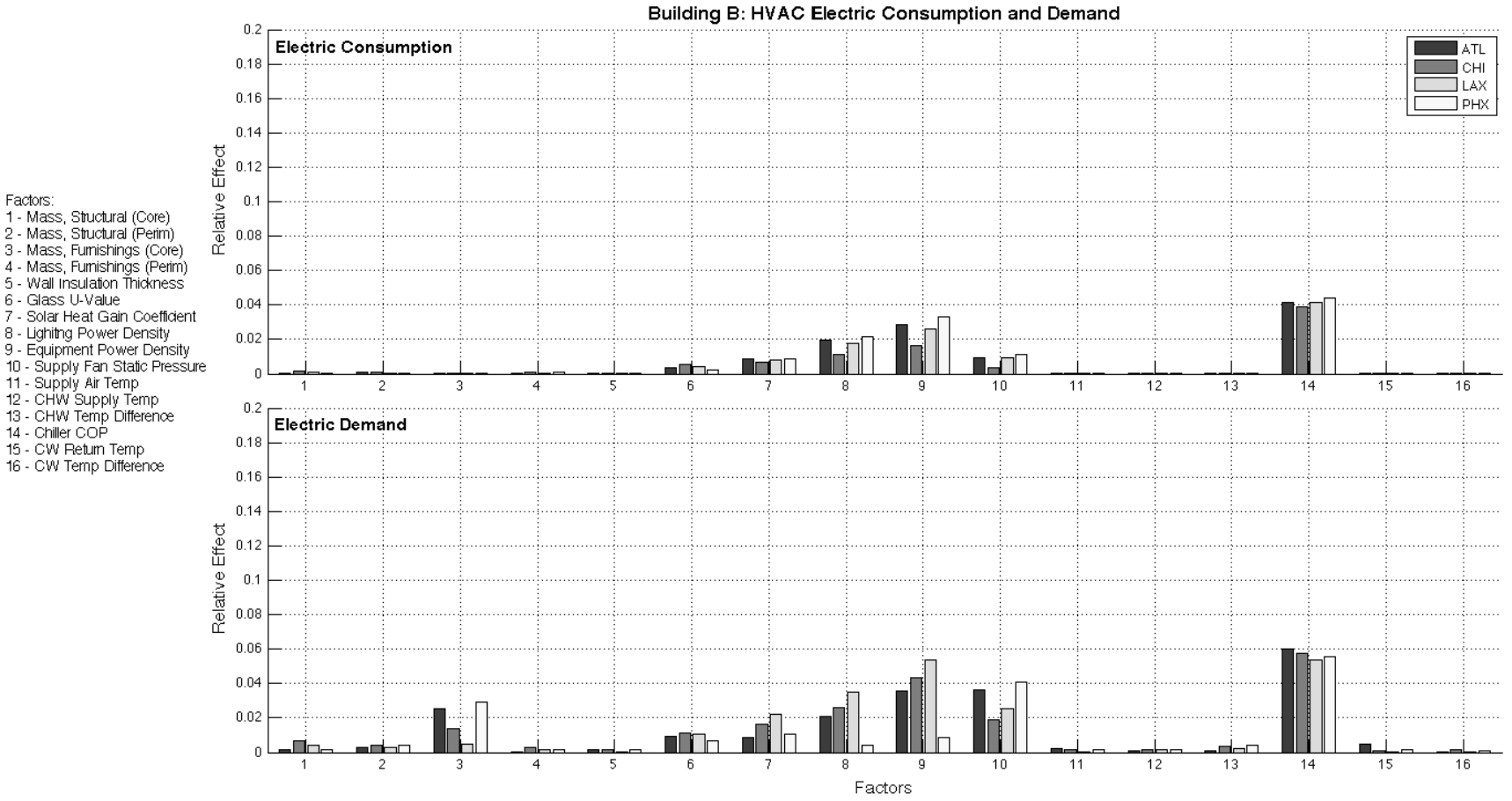

Figure C.10: Relative impact on HVAC system electric consumption and demand for Building B

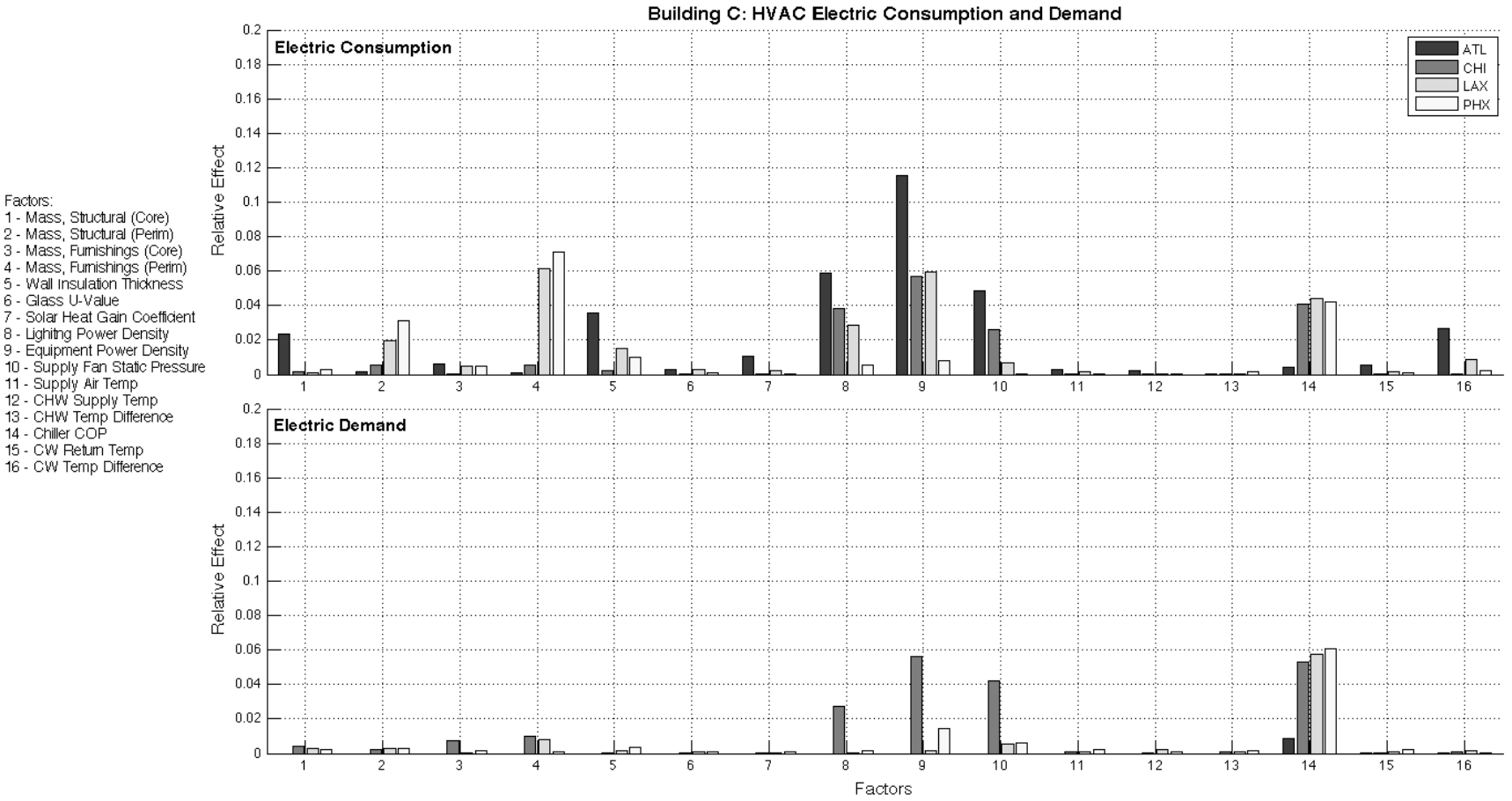

Figure C.11: Relative impact on HVAC system electric consumption and demand for Building C

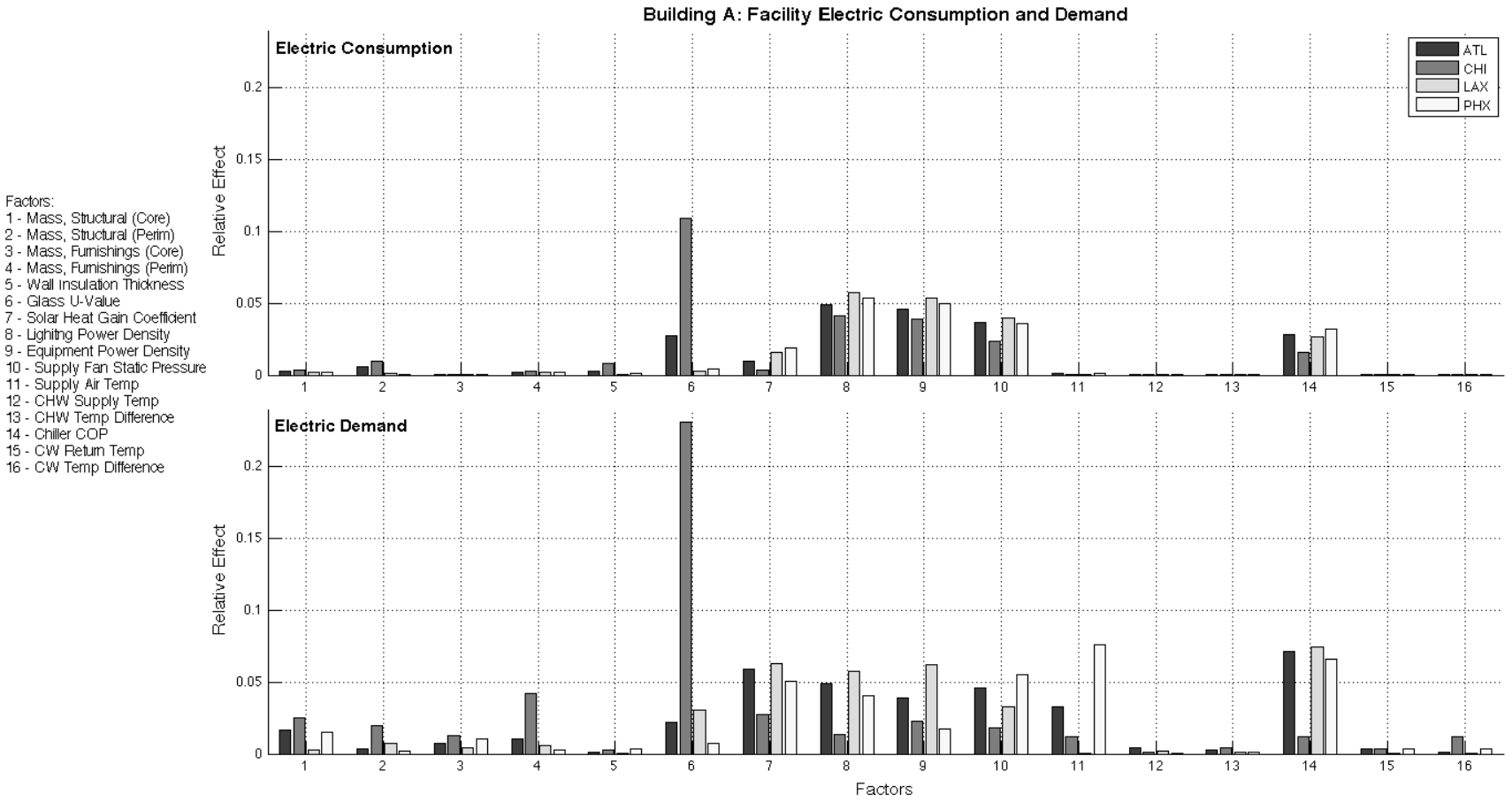

Figure C.12: Relative impact on facility electric consumption and demand for Building A

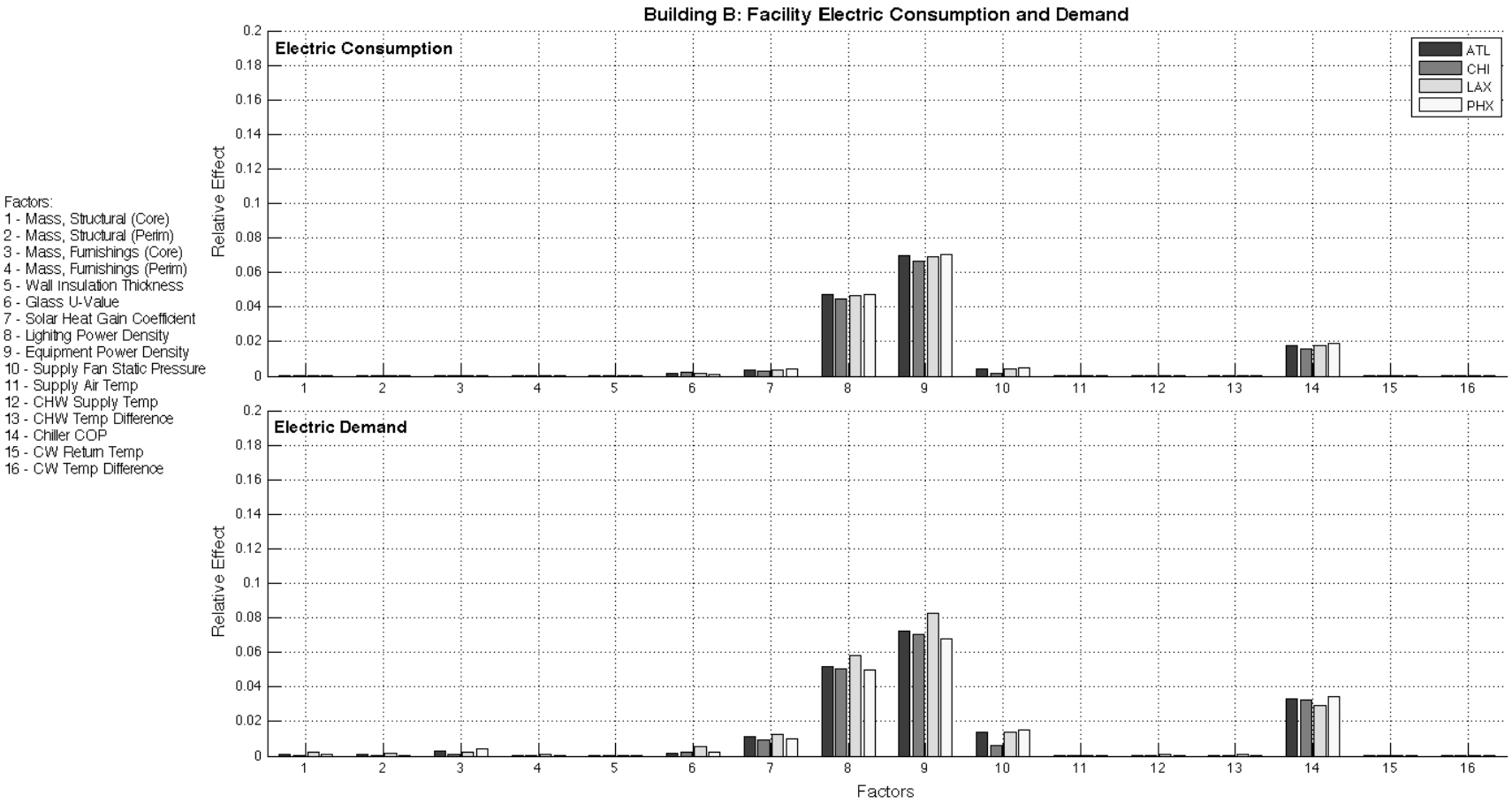

Figure C.13: Relative impact on facility electric consumption and demand for Building B

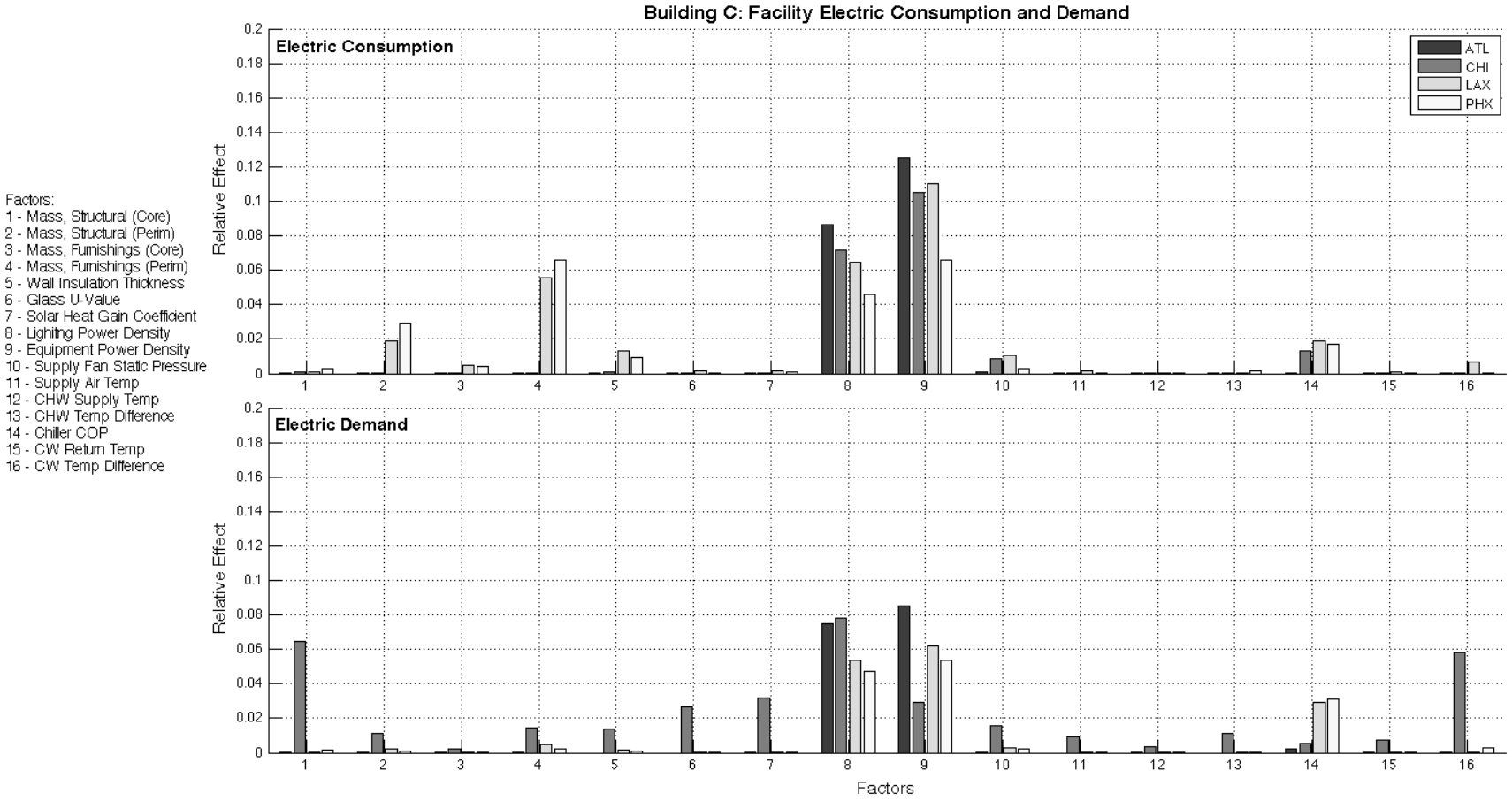

Figure C.14: Relative impact on facility electric consumption and demand for Building C

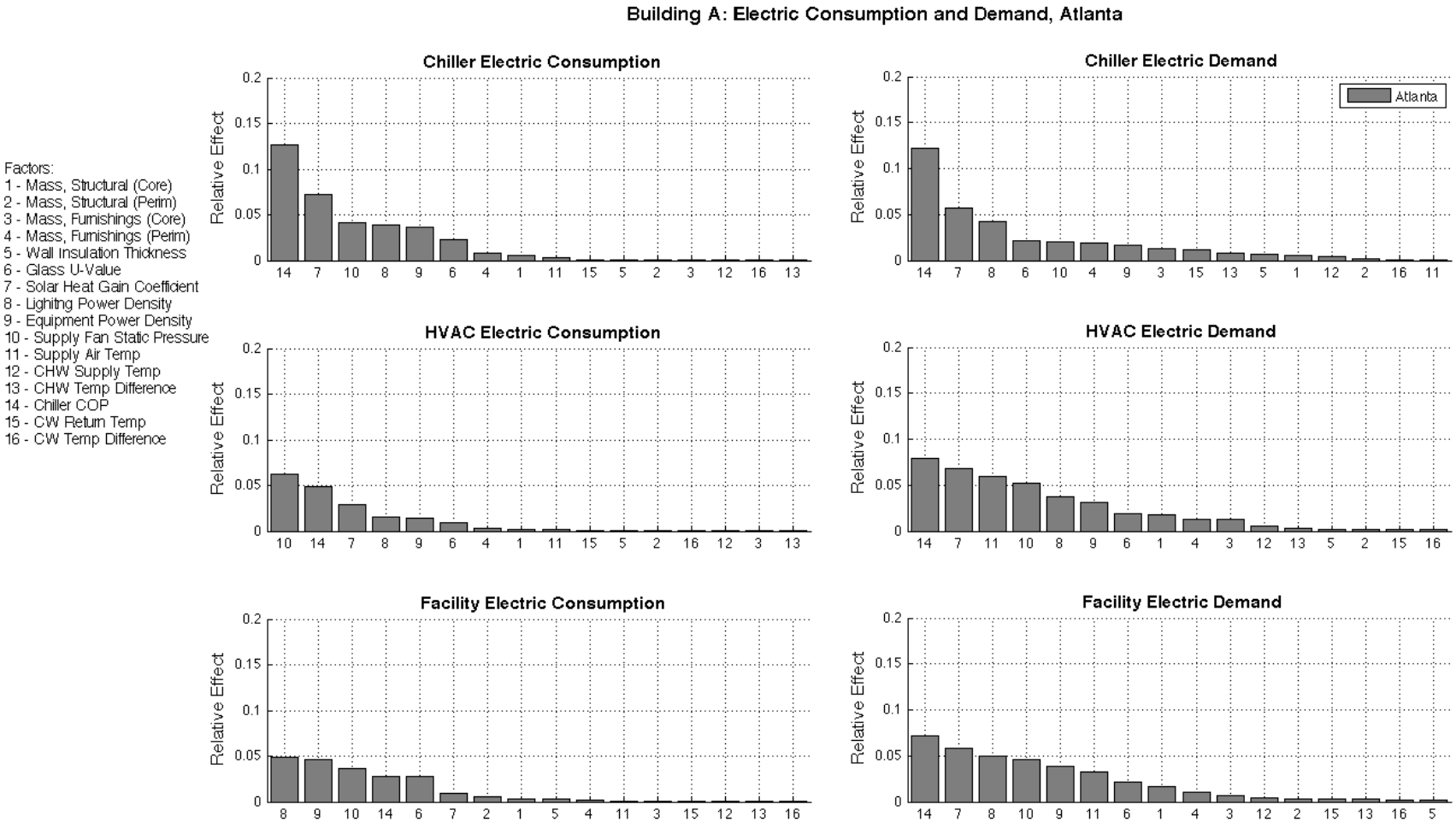

Figure C.15: Relative impact of each factor sorted by magnitude for Building A, Atlanta, GA

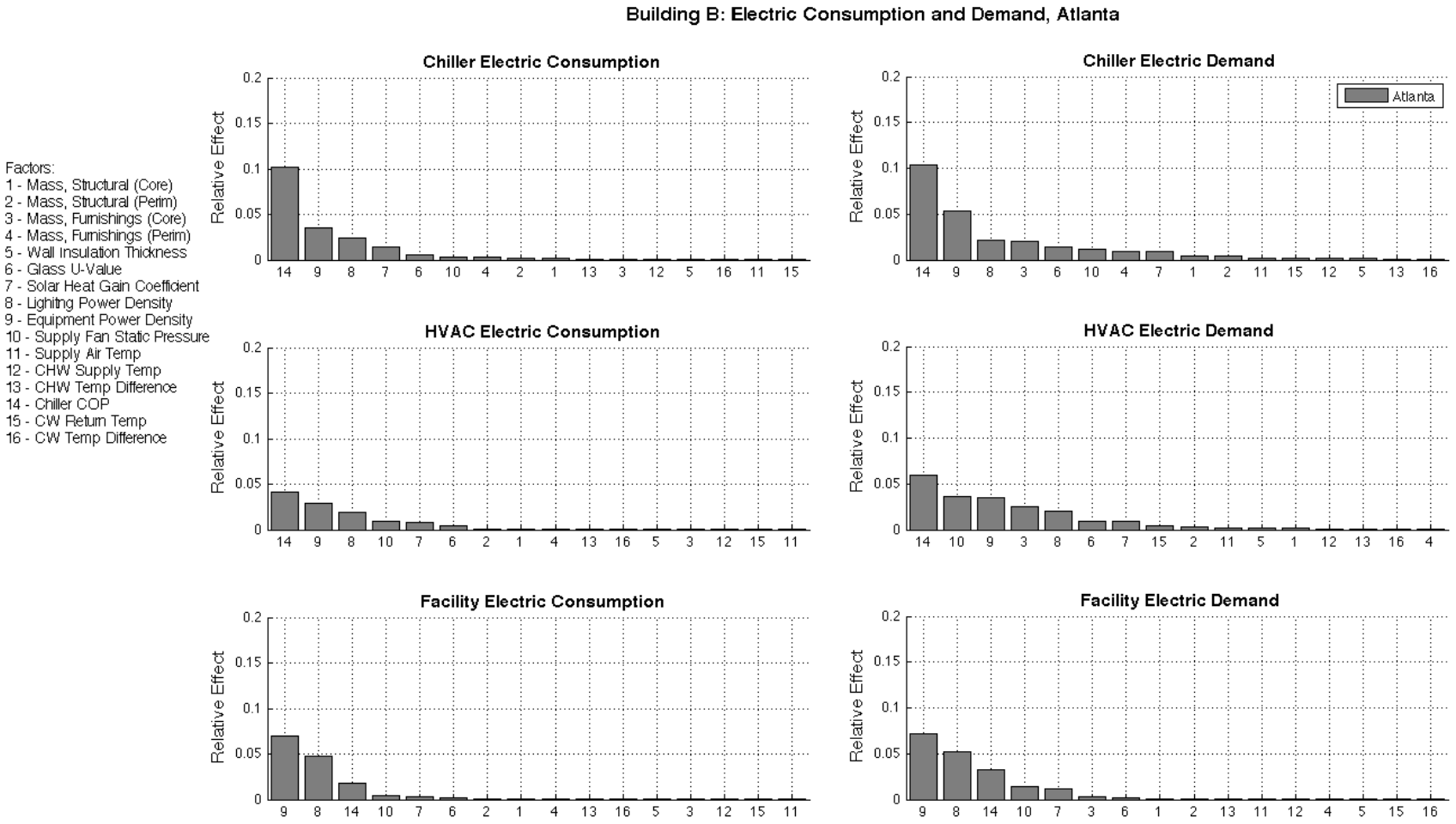

Figure C.16: Relative impact of each factor sorted by magnitude for Building B, Atlanta, GA

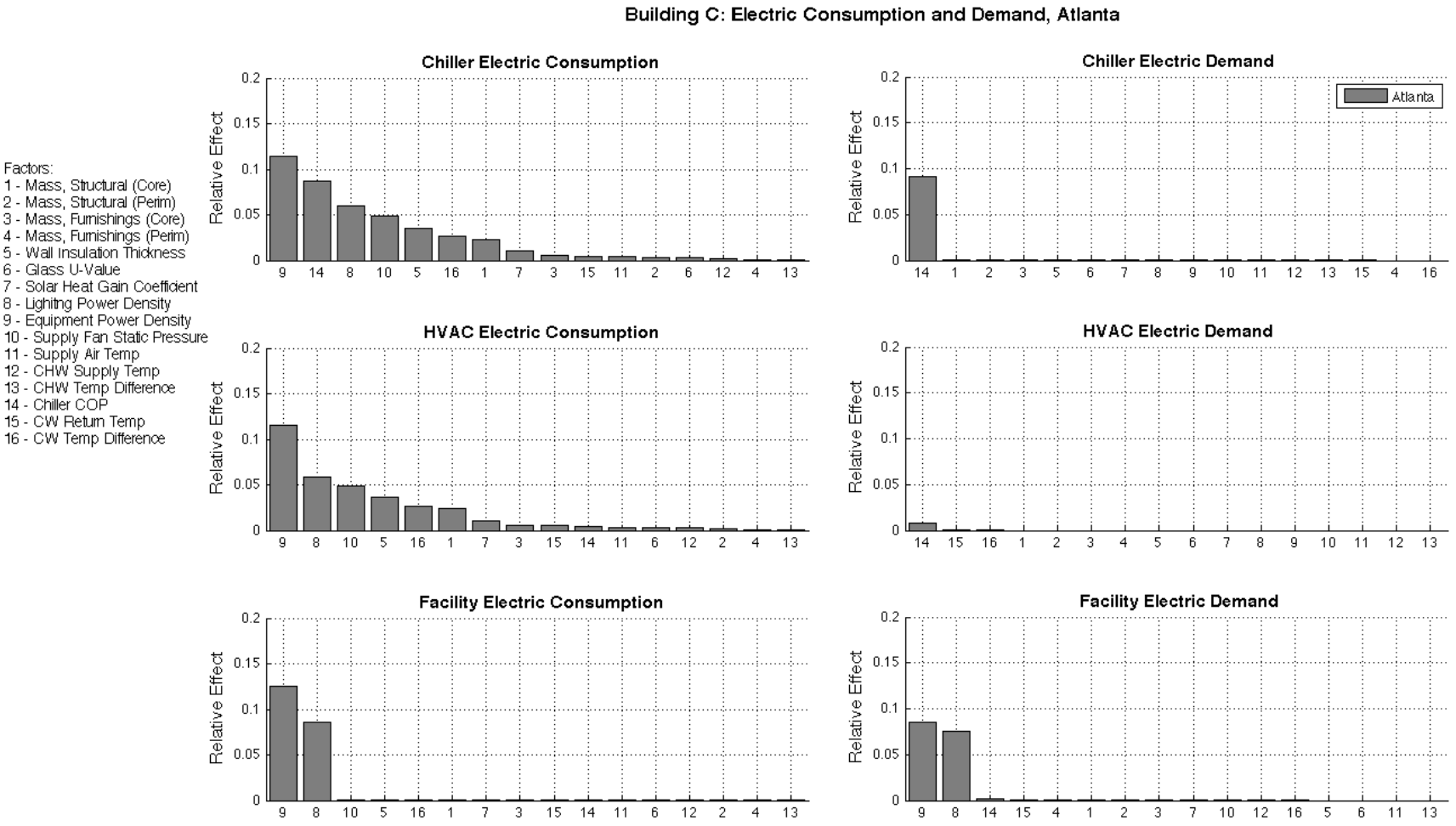

Figure C.17: Relative impact of each factor sorted by magnitude for Building C, Atlanta, GA

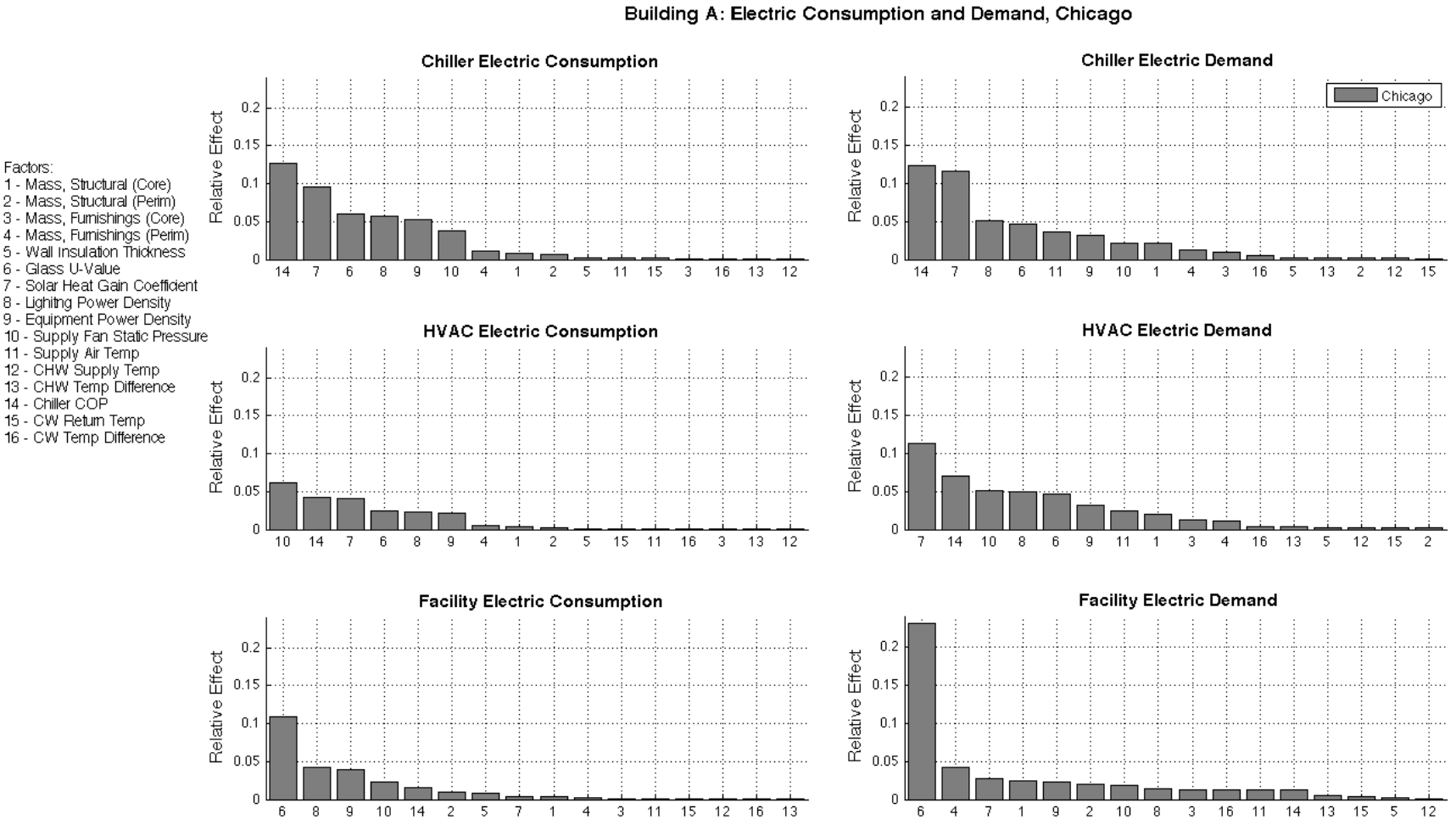

Figure C.18: Relative impact of each factor sorted by magnitude for Building A, Chicago, IL

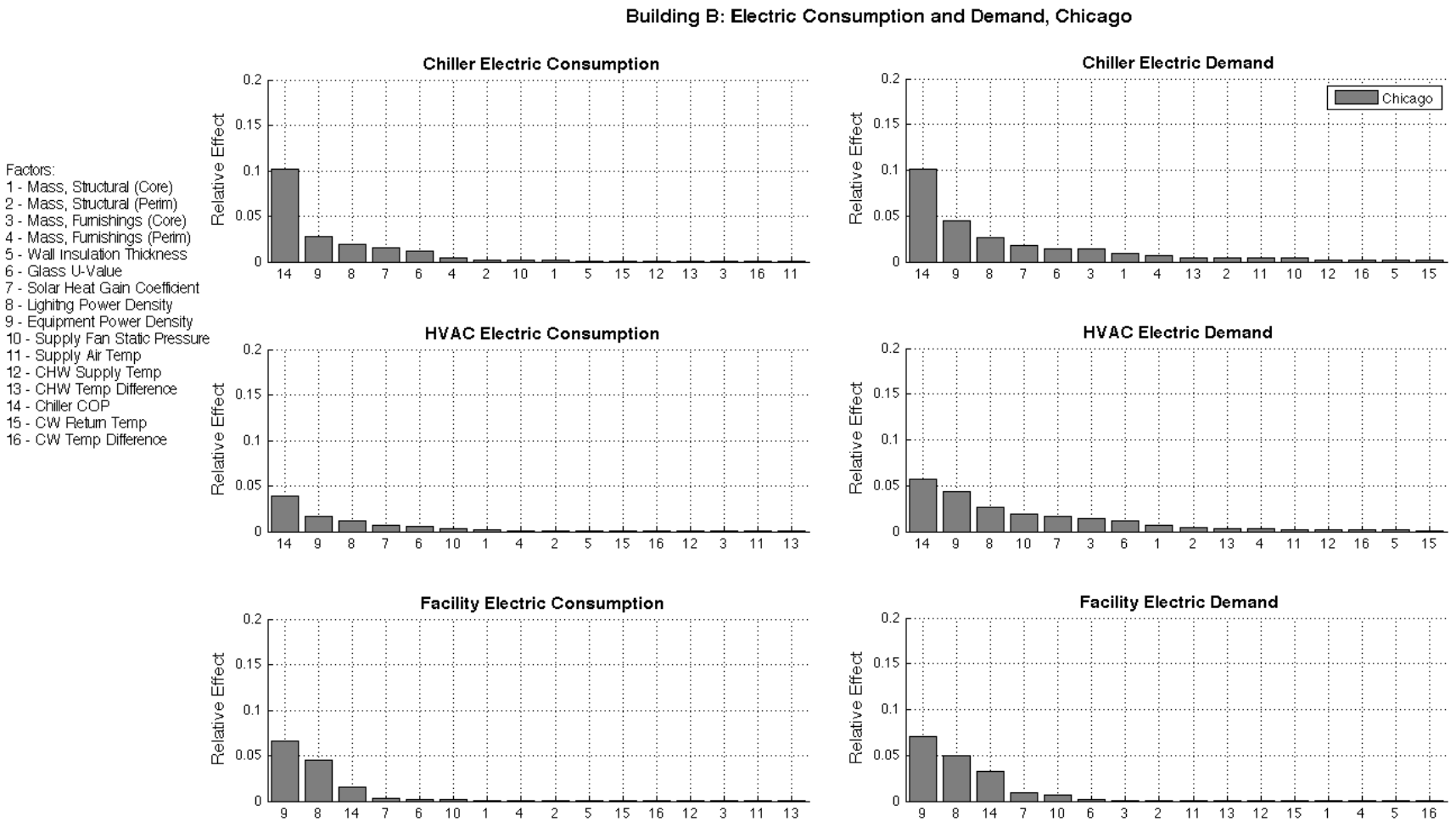

Figure C.19: Relative impact of each factor sorted by magnitude for Building B, Chicago, IL

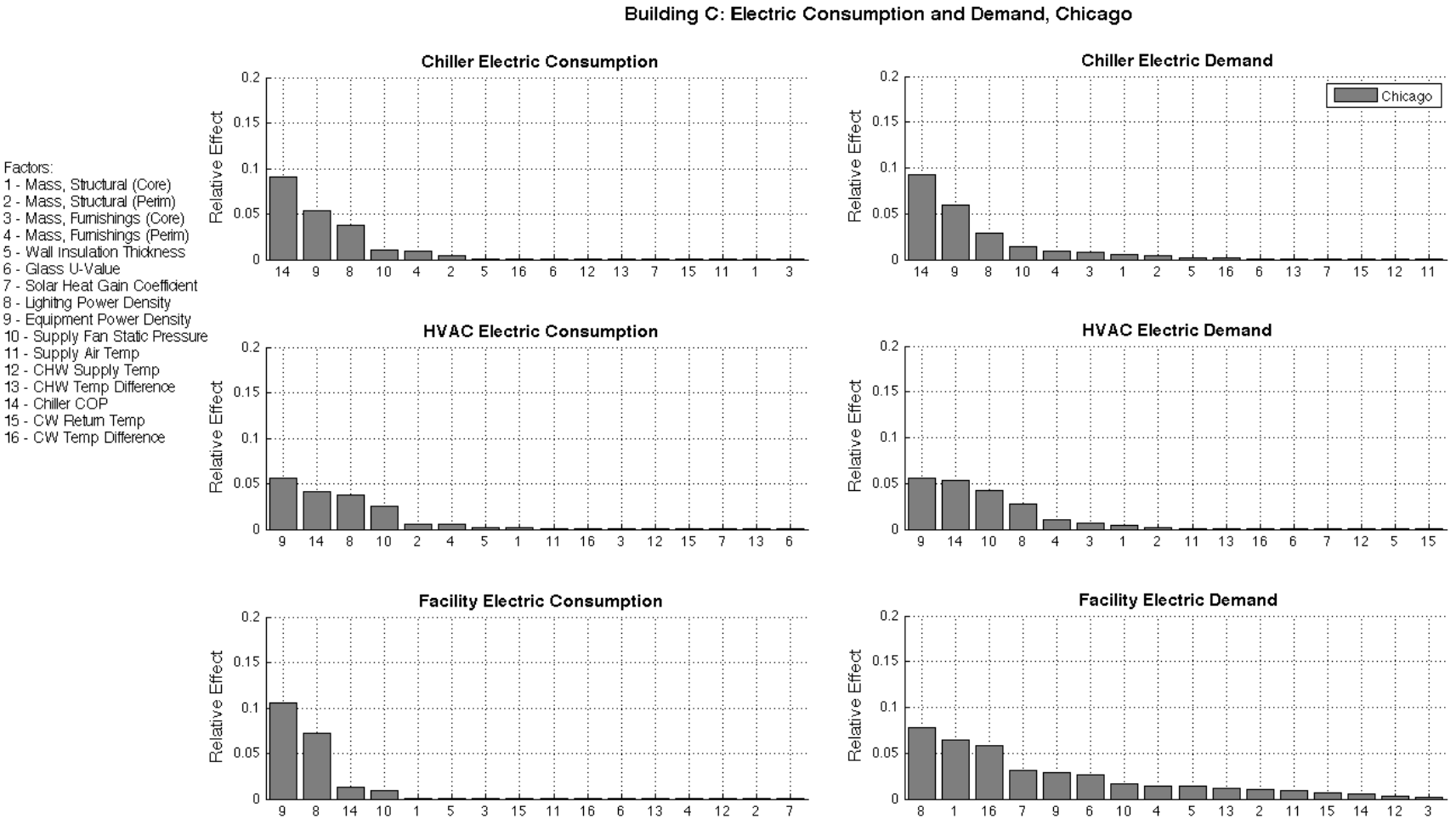

Figure C.20: Relative impact of each factor sorted by magnitude for Building C, Chicago, IL

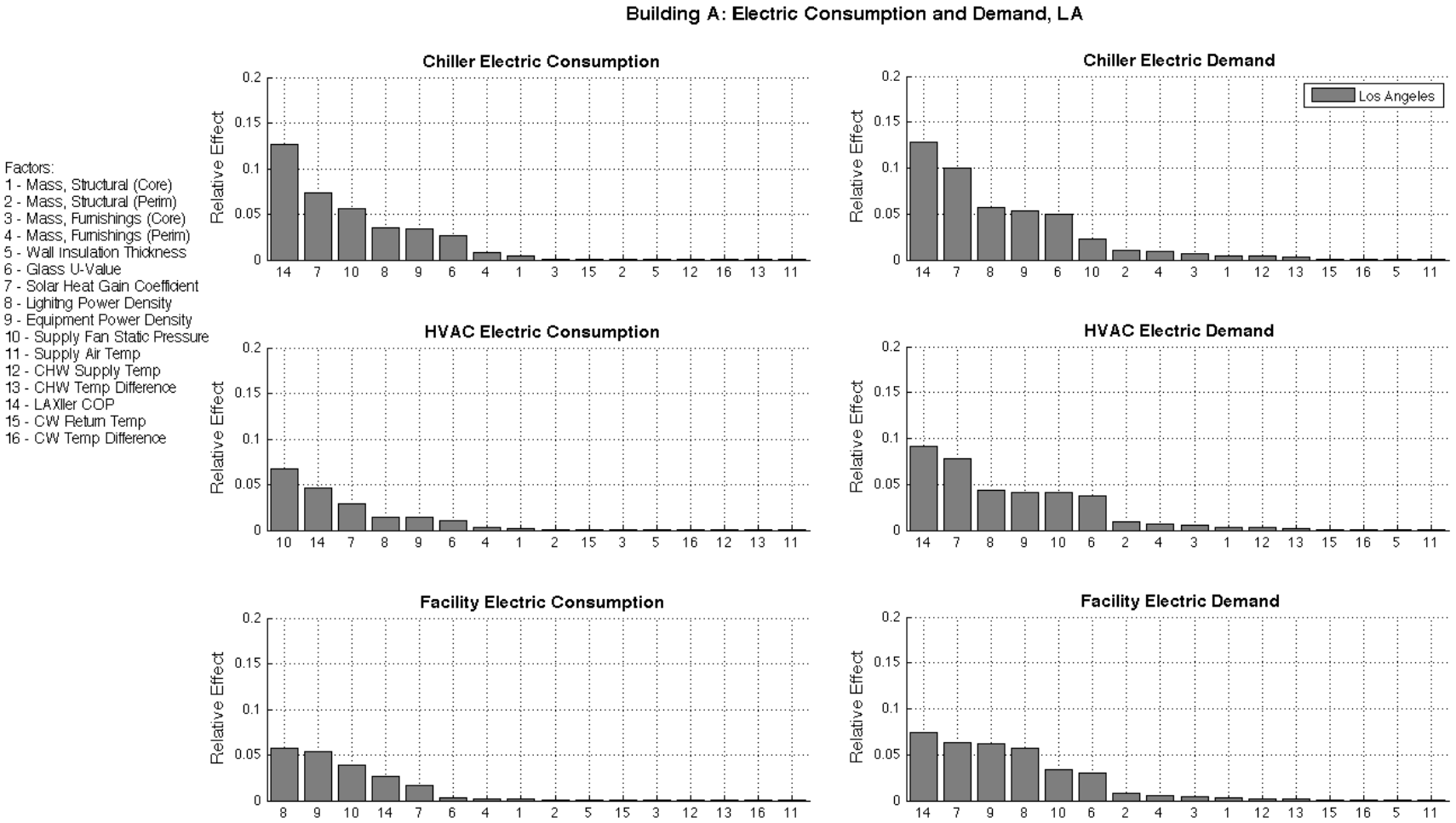

Figure C.21: Relative impact of each factor sorted by magnitude for Building A, Los Angeles, CA

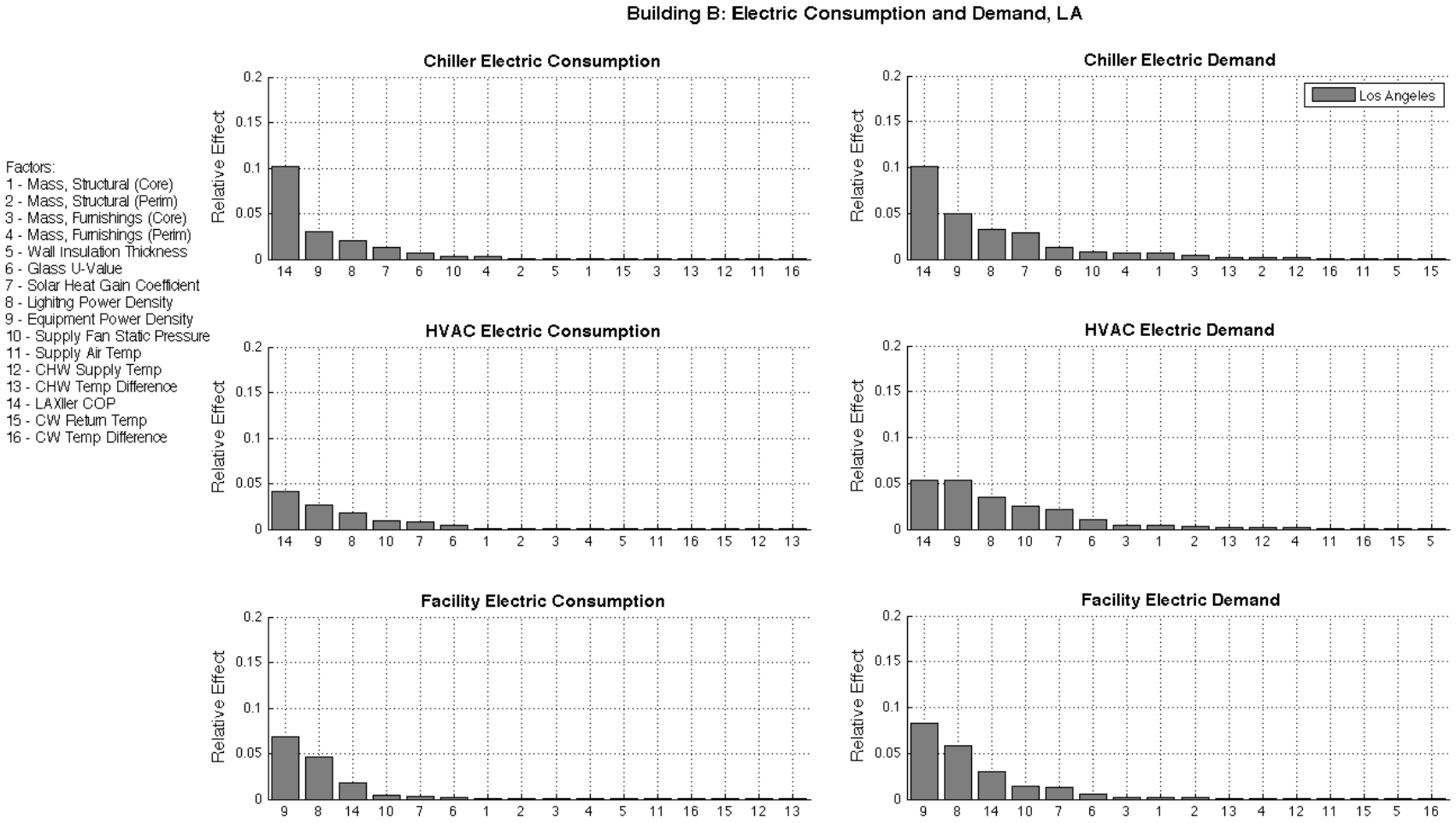

Figure C.22: Relative impact of each factor sorted by magnitude for Building B, Los Angeles, CA

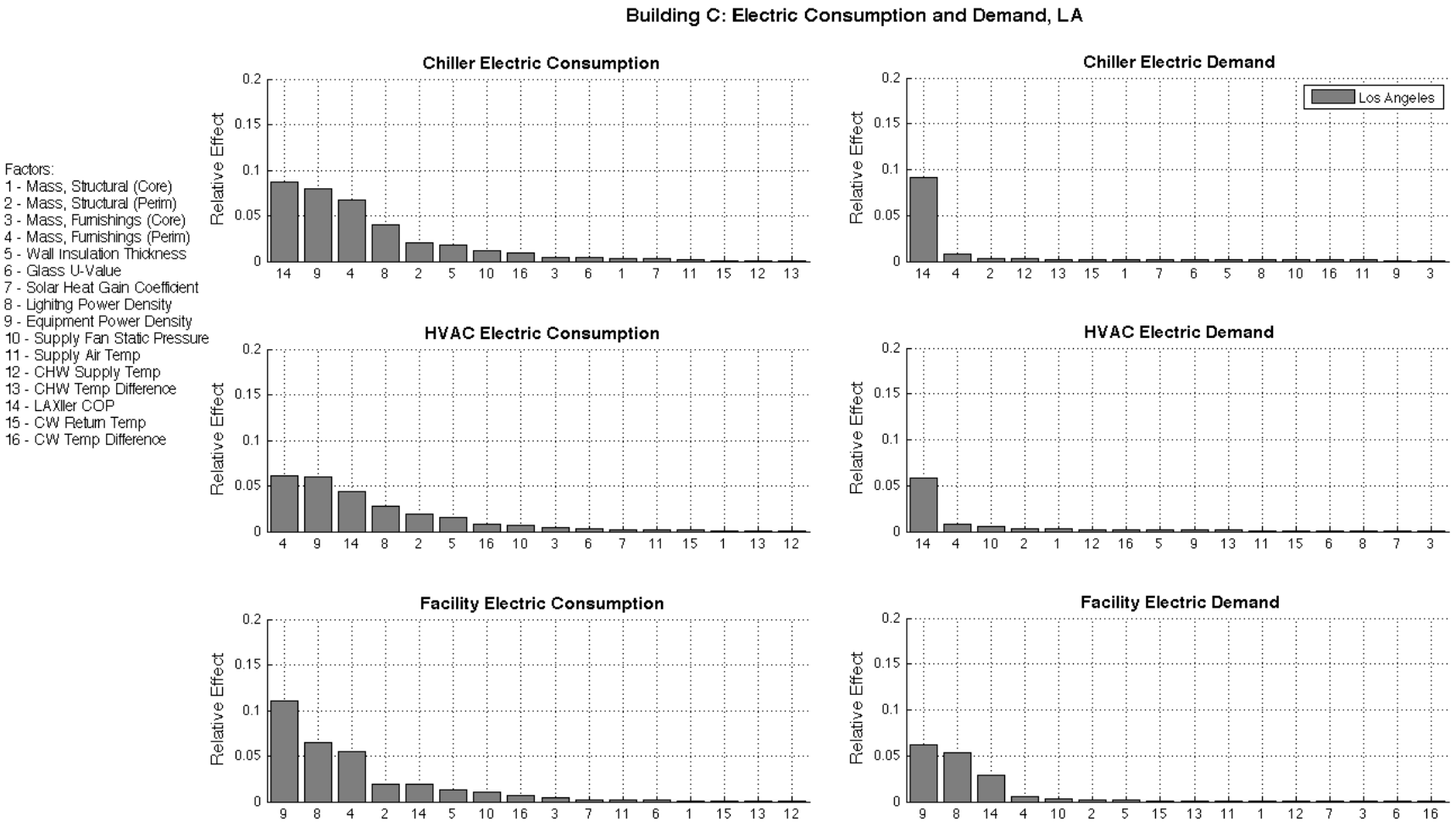

Figure C.23: Relative impact of each factor sorted by magnitude for Building C, Los Angeles, CA

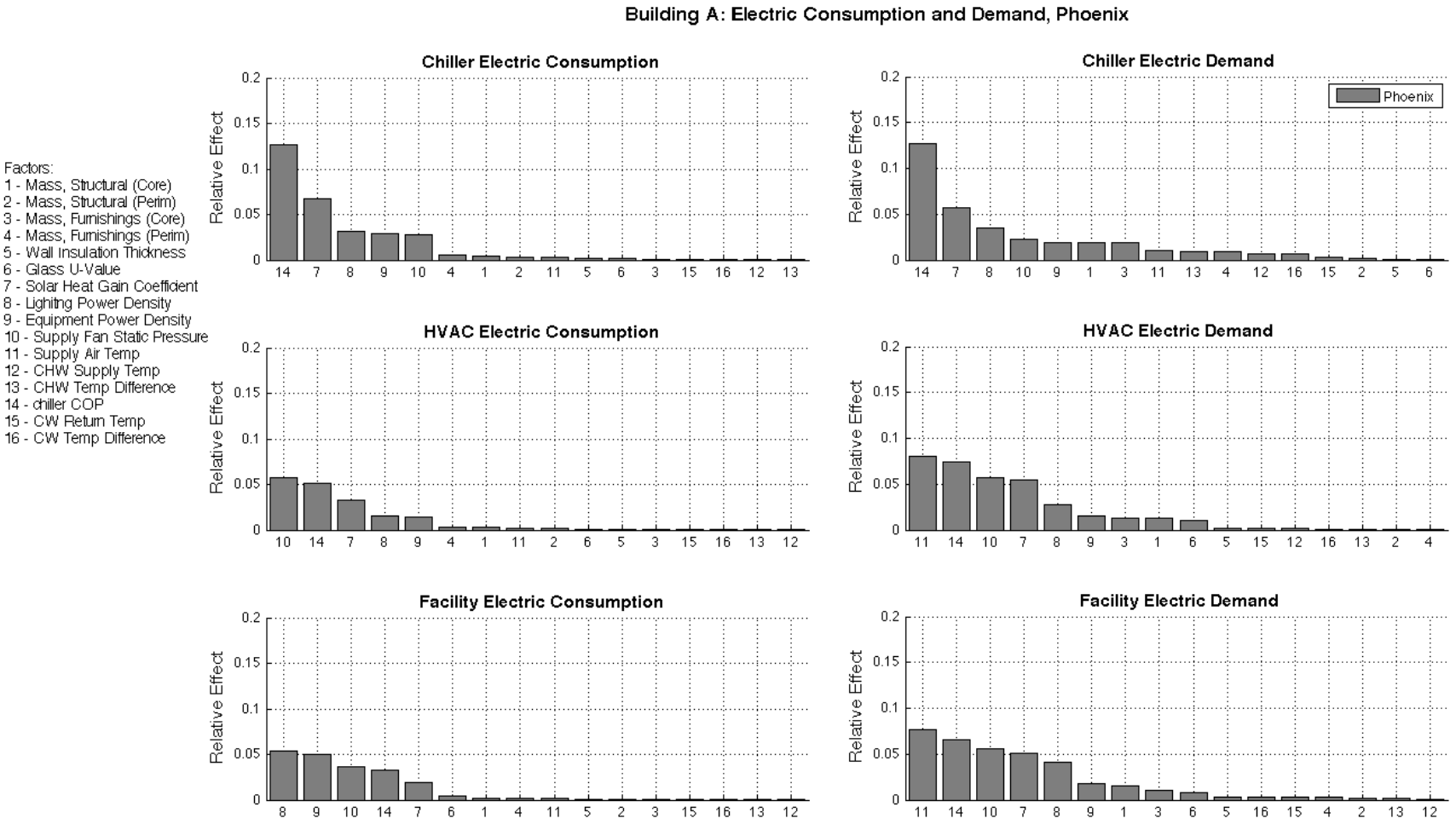

Figure C.24: Relative impact of each factor sorted by magnitude for Building A, Phoenix, AZ

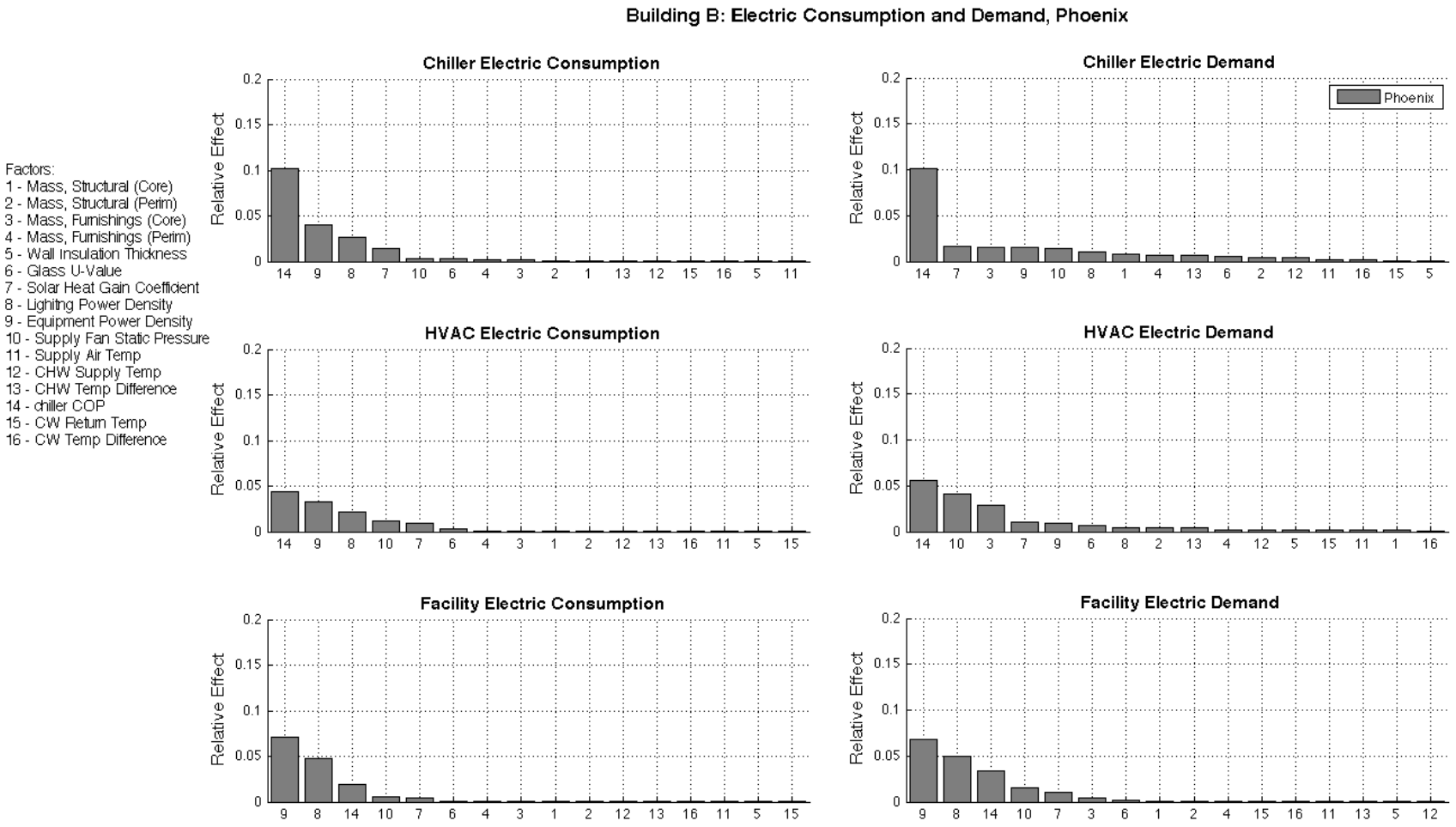

Figure C.25: Relative impact of each factor sorted by magnitude for Building B, Phoenix, AZ

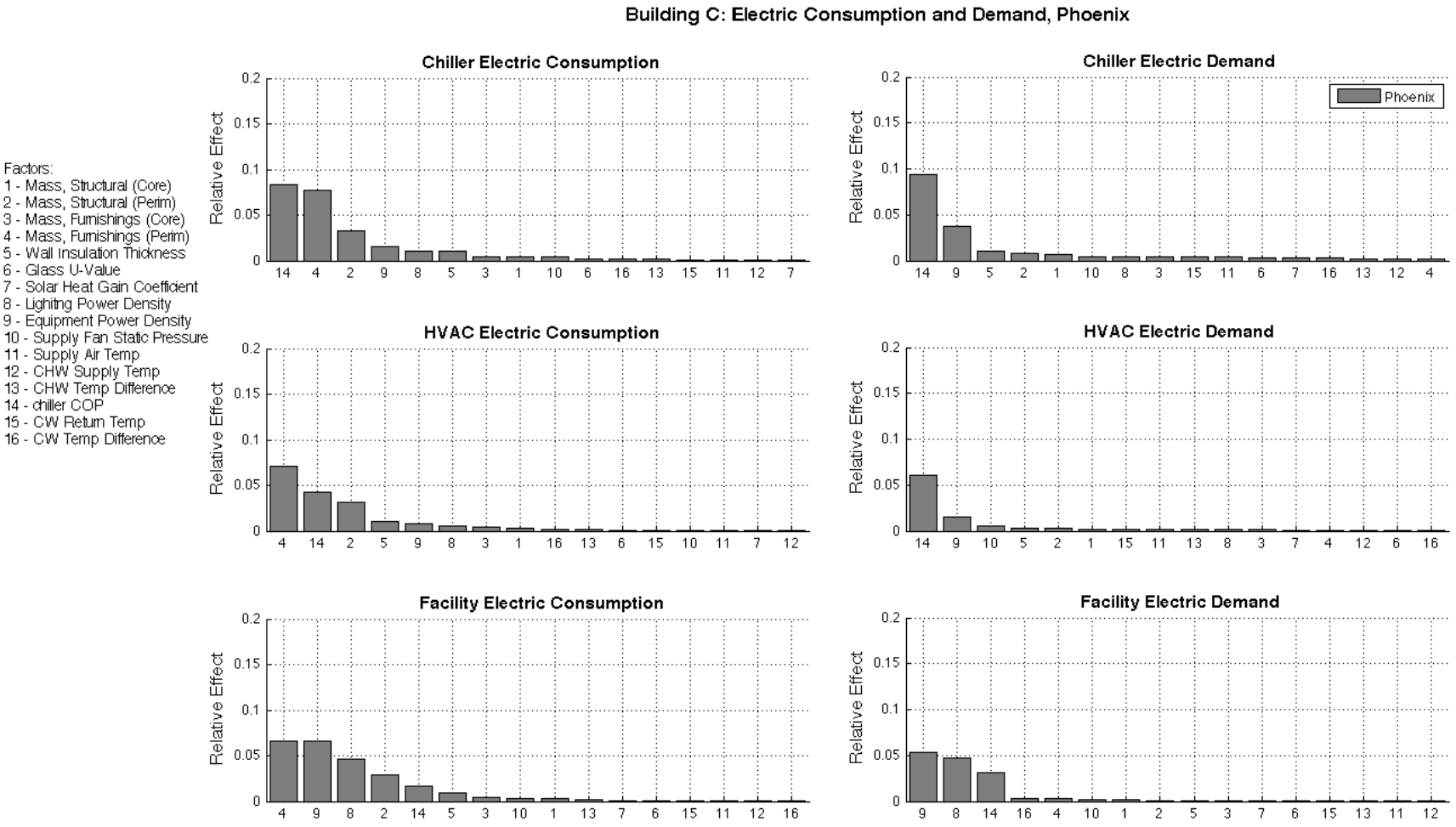

Figure C.26: Relative impact of each factor sorted by magnitude for Building C, Phoenix, AZ

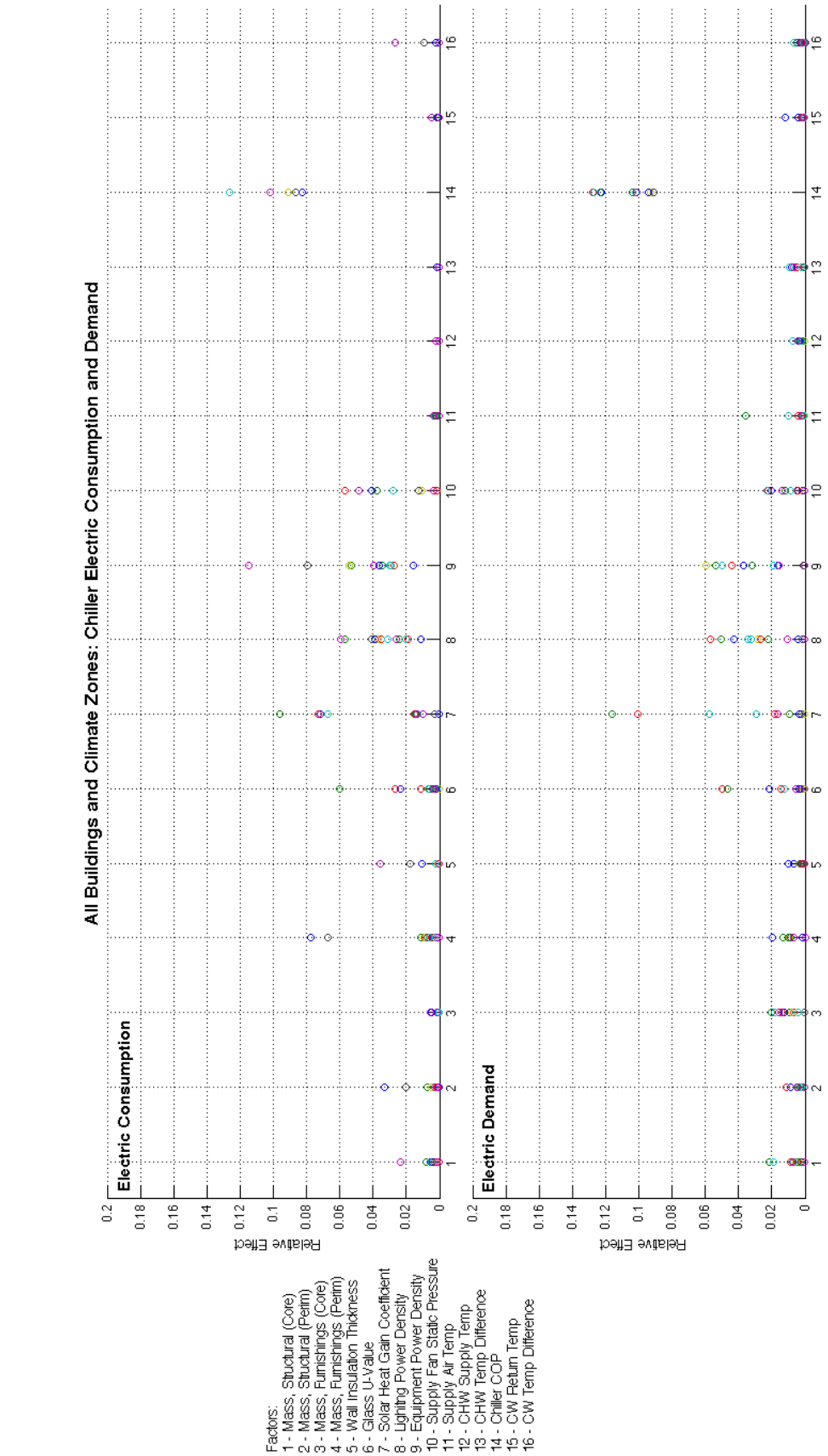

Figure C.27: Scatter plot of relative impact on chiller energy, including results from all buildings and climate zones

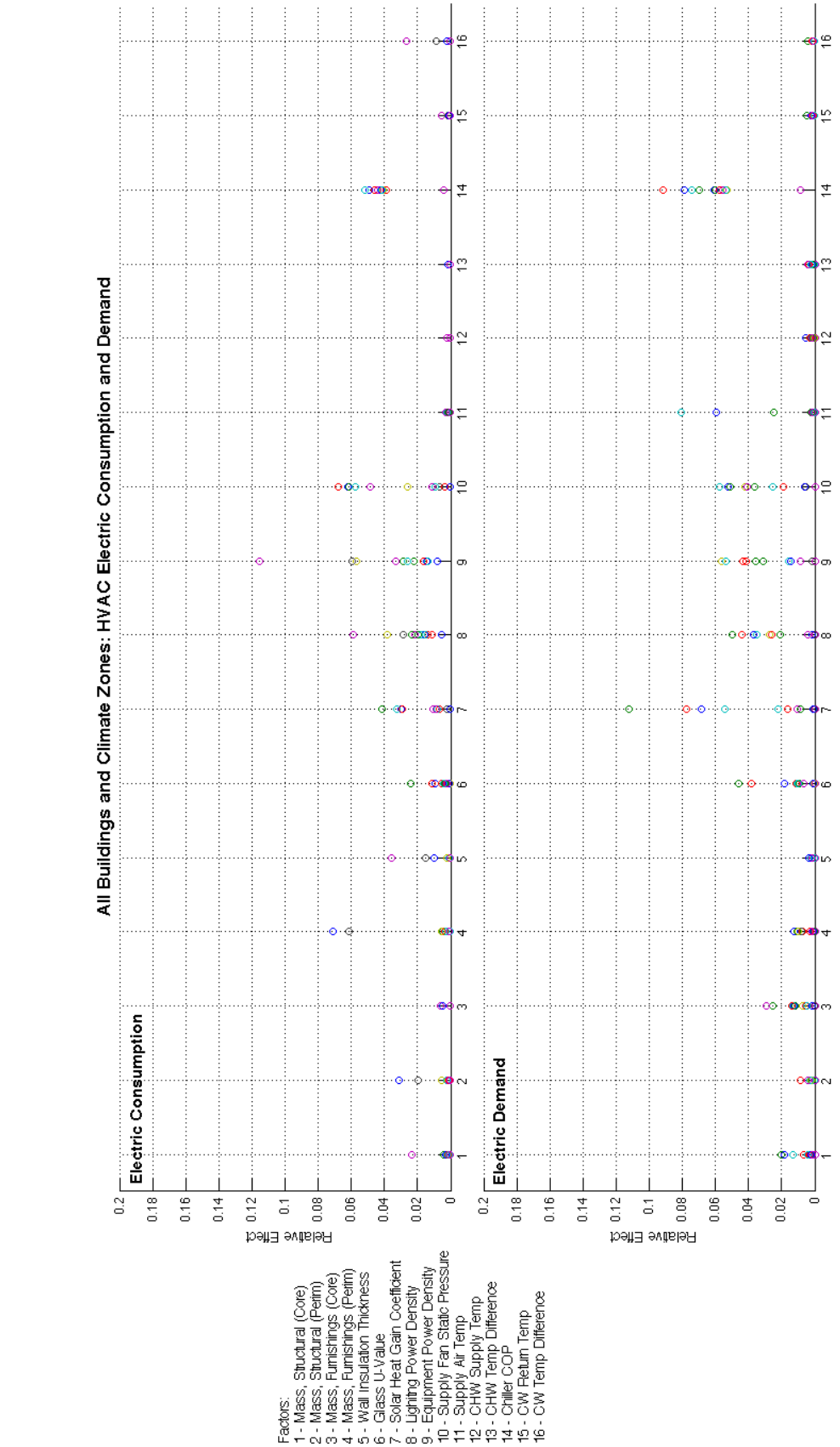

Figure C.28: Scatter plot of relative impact on HVAC energy, including results from all buildings and climate zones

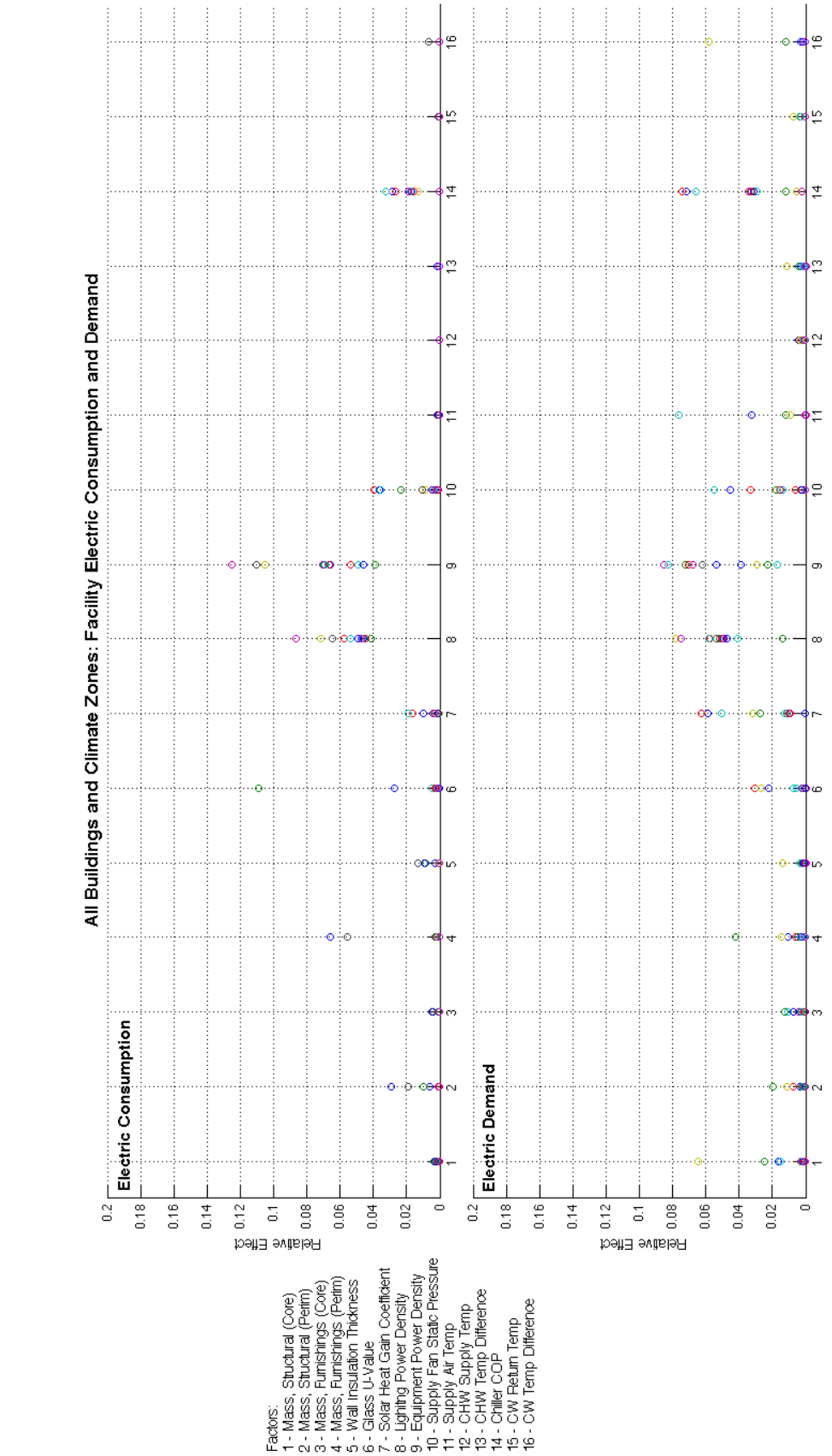

Figure C.29: Scatter plot of relative impact on facility energy, including results from all buildings and climate zones

Appendix D

Two-Factor Interactions

The following appendix of charts reports fractional factorial analysis results for the two-factor interaction study. The results are organized in a similar manner to Appendix C, where they exhibit relative impacts of each two-factor interaction on energy consumption and demand associated with the chiller, HVAC system, and facility for each building and climate zone. Since the two-factor interaction study involved over 100 cases, only the top ten results were chosen to report. The ten results are sorted by magnitude of the two-factor interaction effects in a descending order. Also note that the average of results over climate zones was not possible to calculate, since the top ten two-factor interactions change for each study.

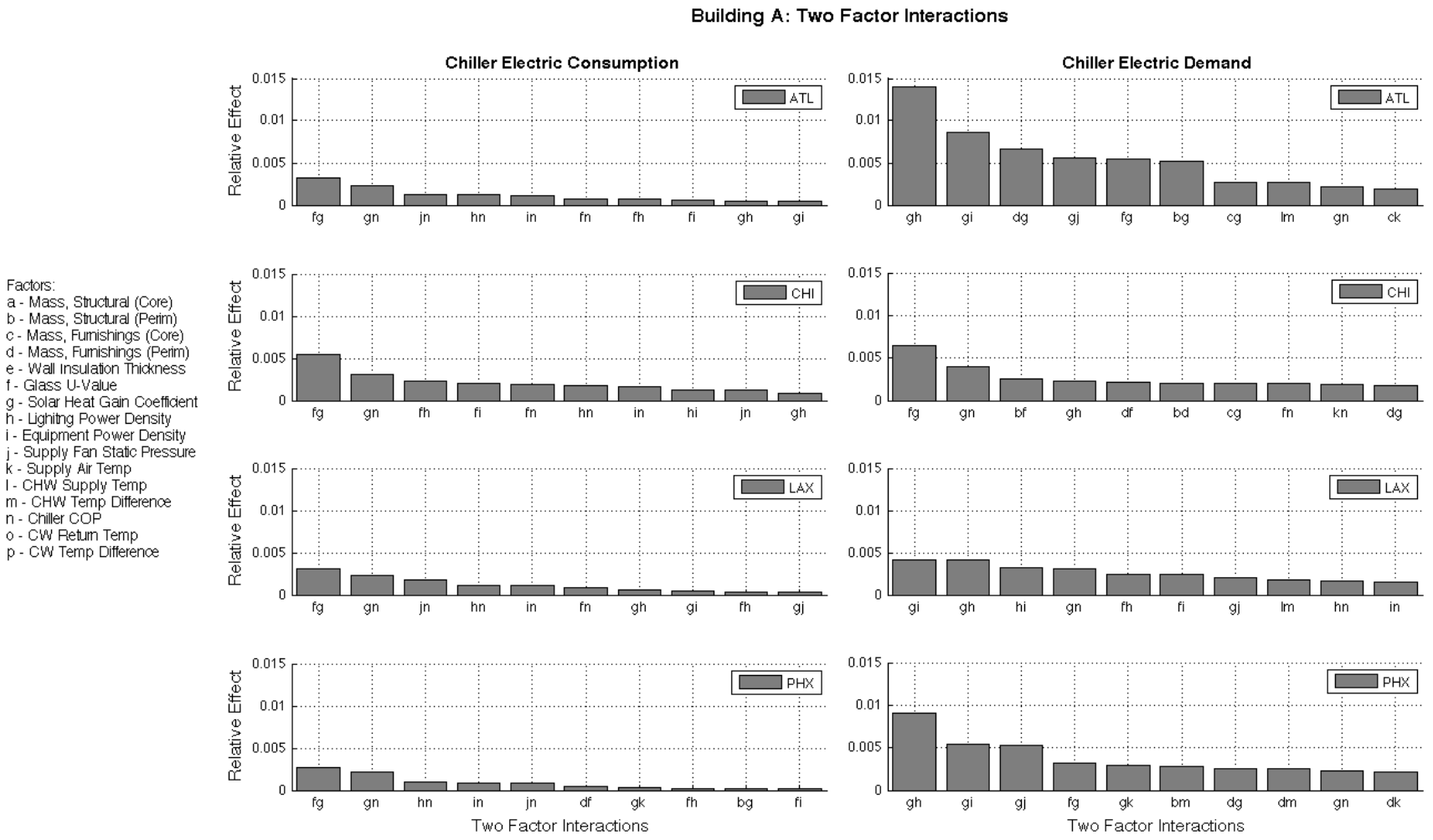

Figure D.1: Relative impact of two-factor interactions on chiller energy, Building A

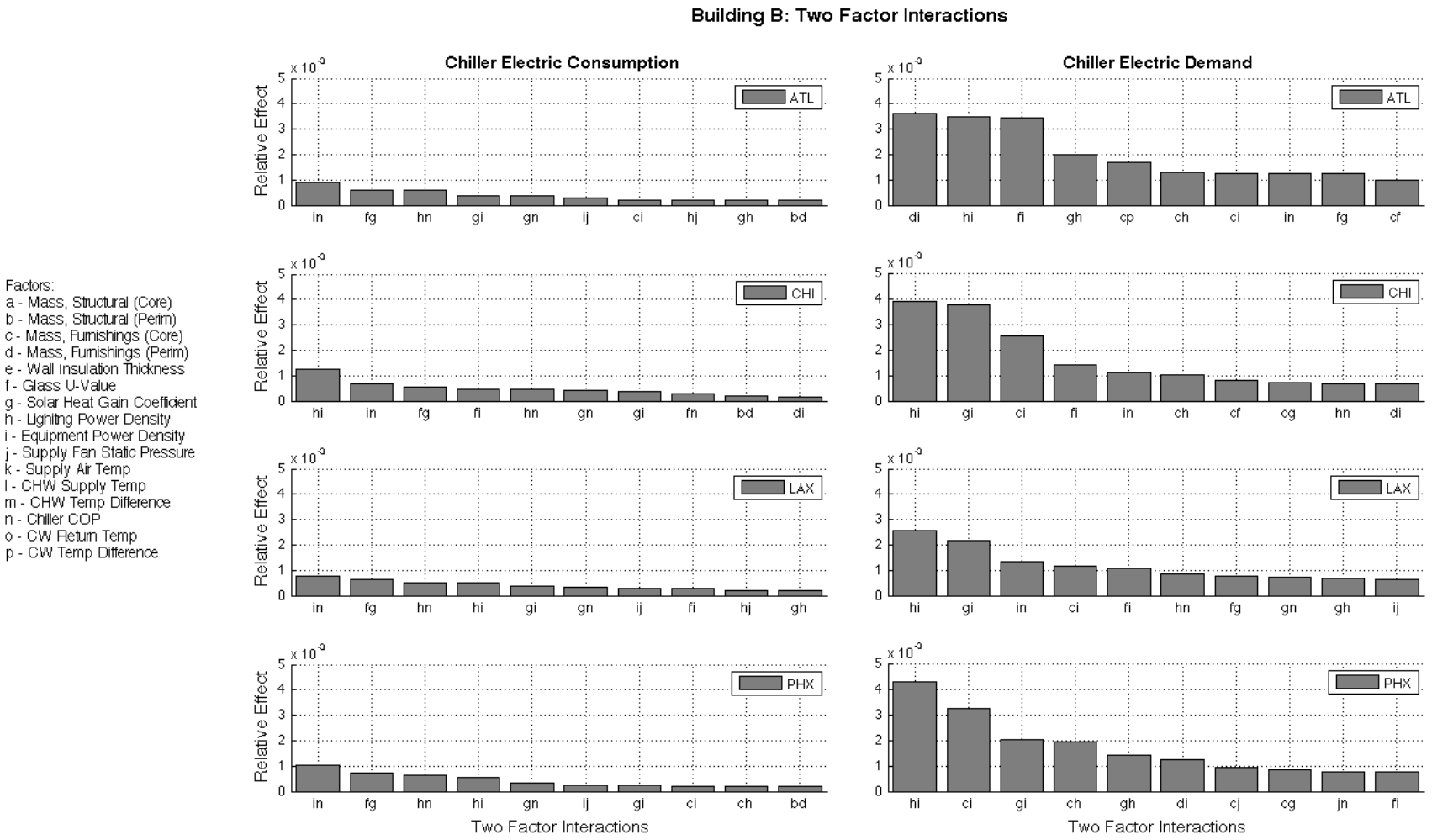

Figure D.2: Relative impact of two-factor interactions on chiller energy, Building B

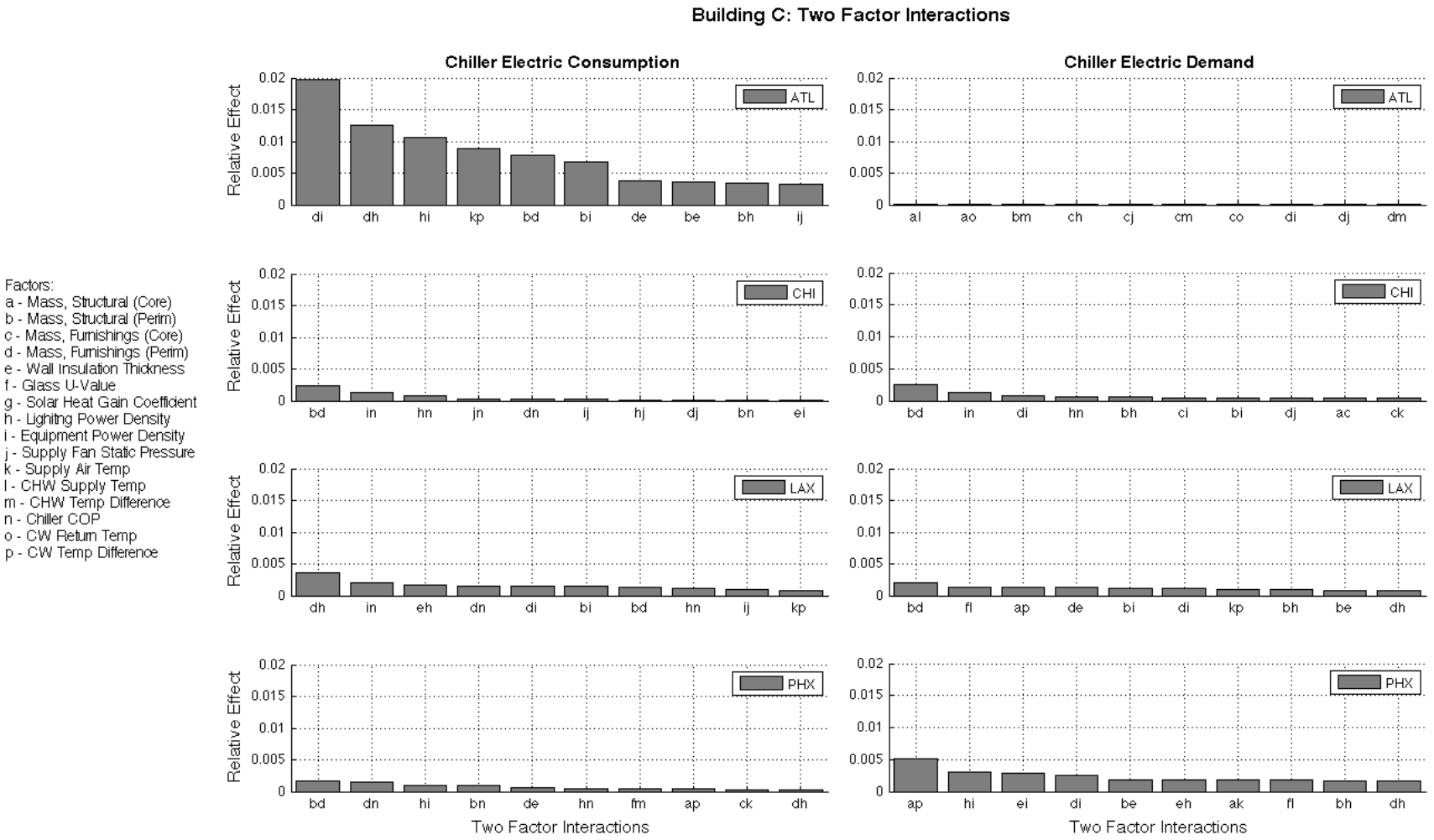

Figure D.3: Relative impact of two-factor interactions on chiller energy, Building C

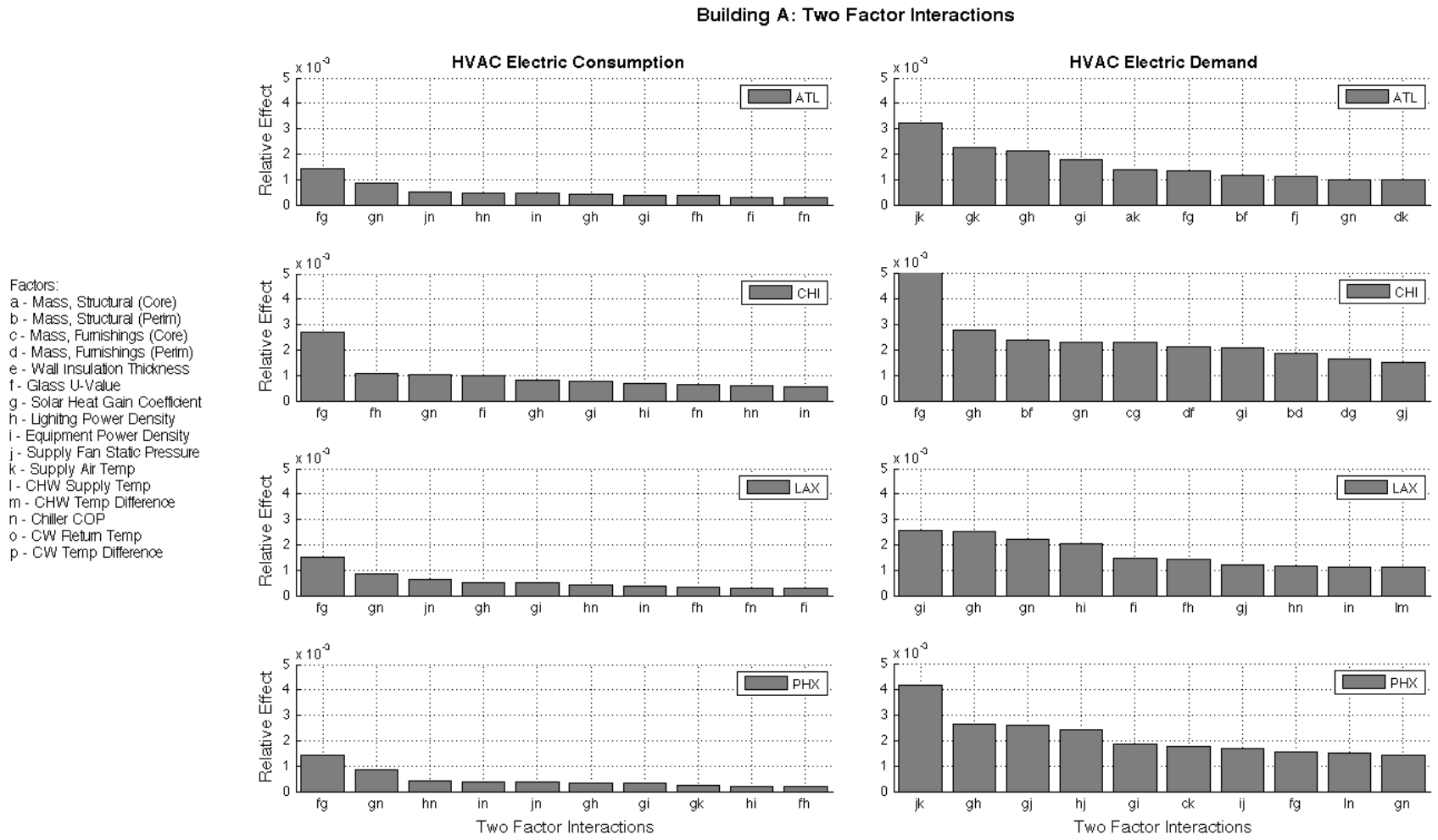

Figure D.4: Relative impact of two-factor interactions on HVAC system energy, Building A

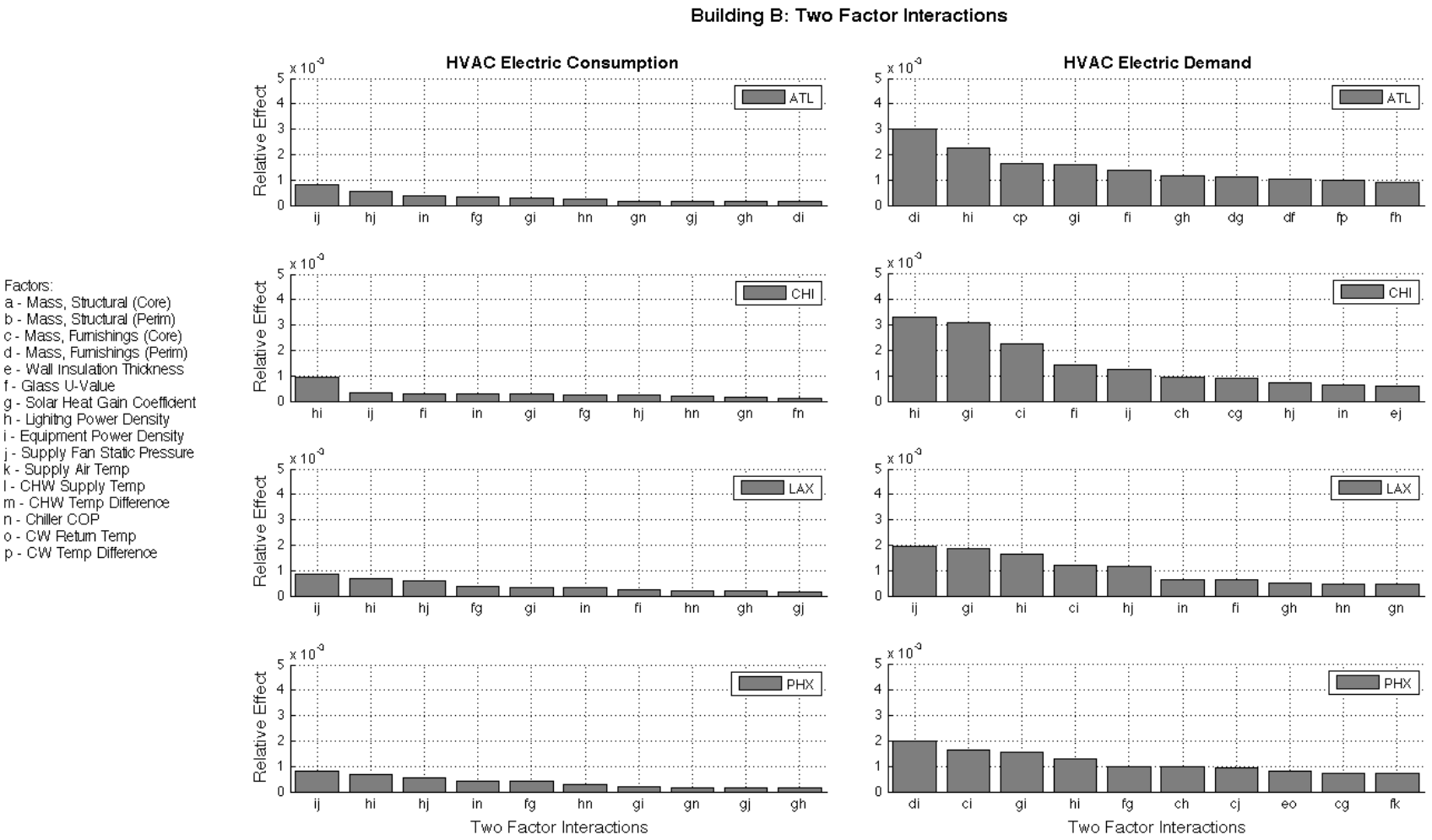

Figure D.5: Relative impact of two-factor interactions on HVAC system energy, Building B

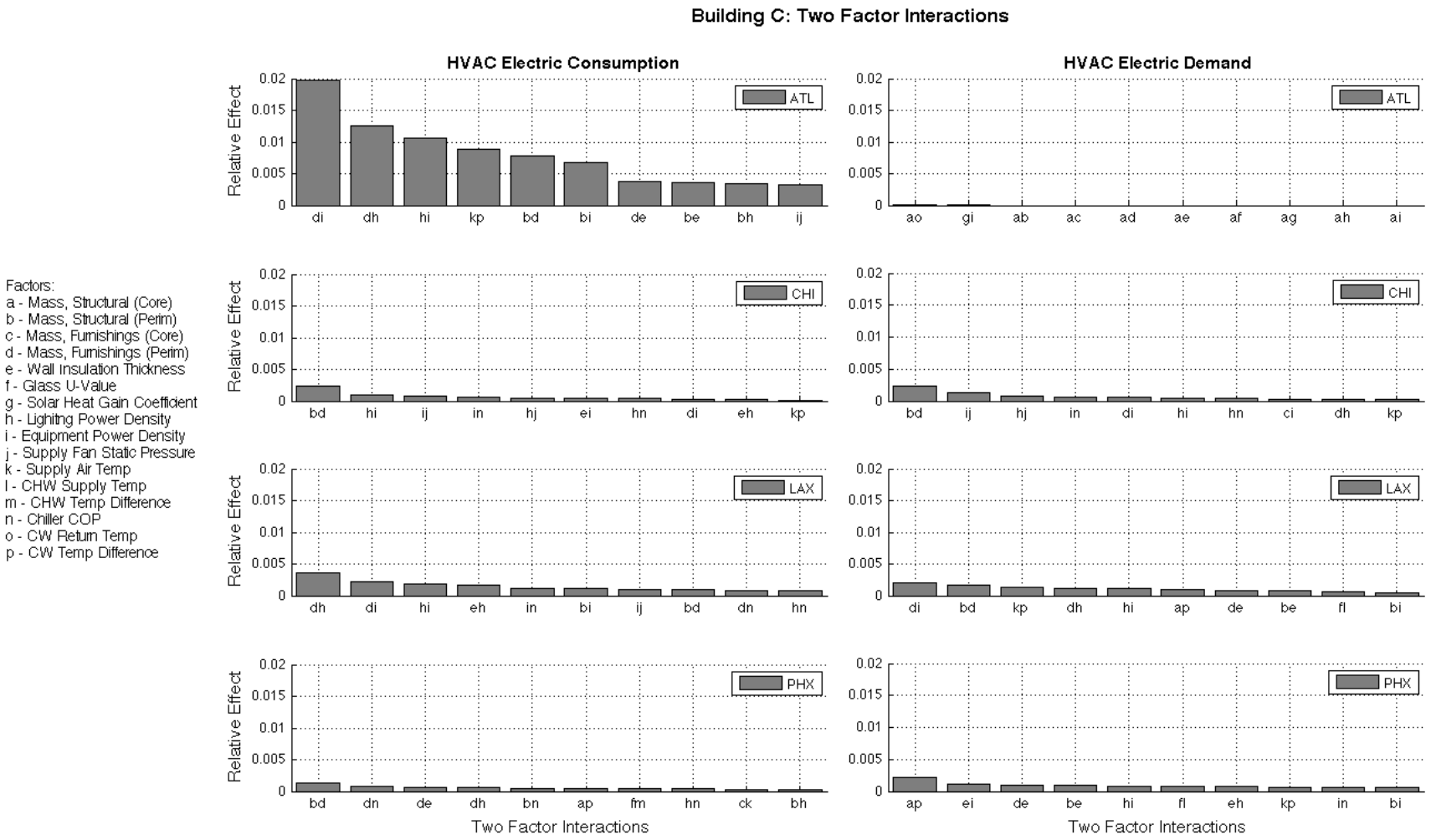

Figure D.6: Relative impact of two-factor interactions on HVAC system energy, Building C

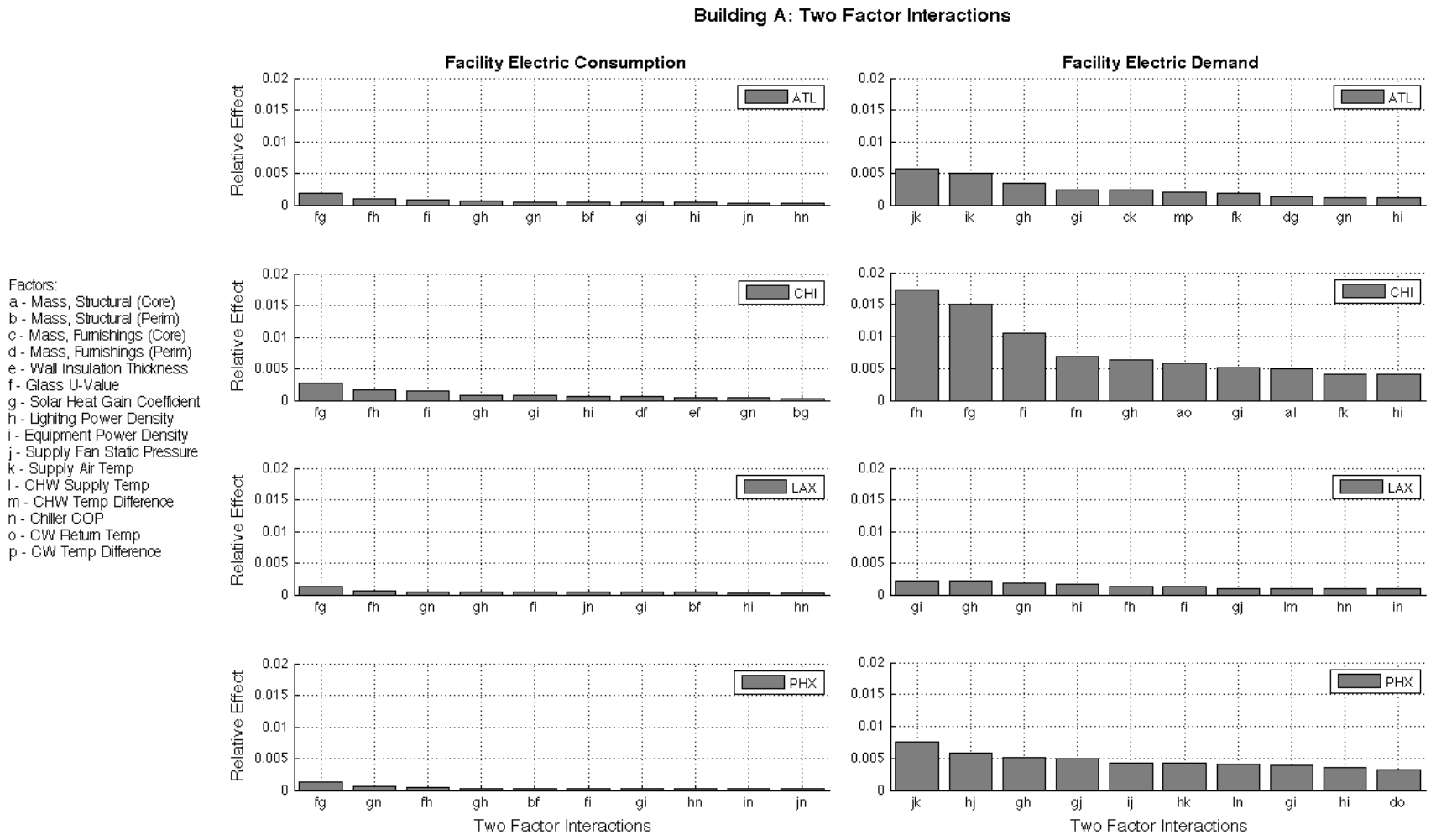

Figure D.7: Relative impact of two-factor interactions on facility energy, Building A

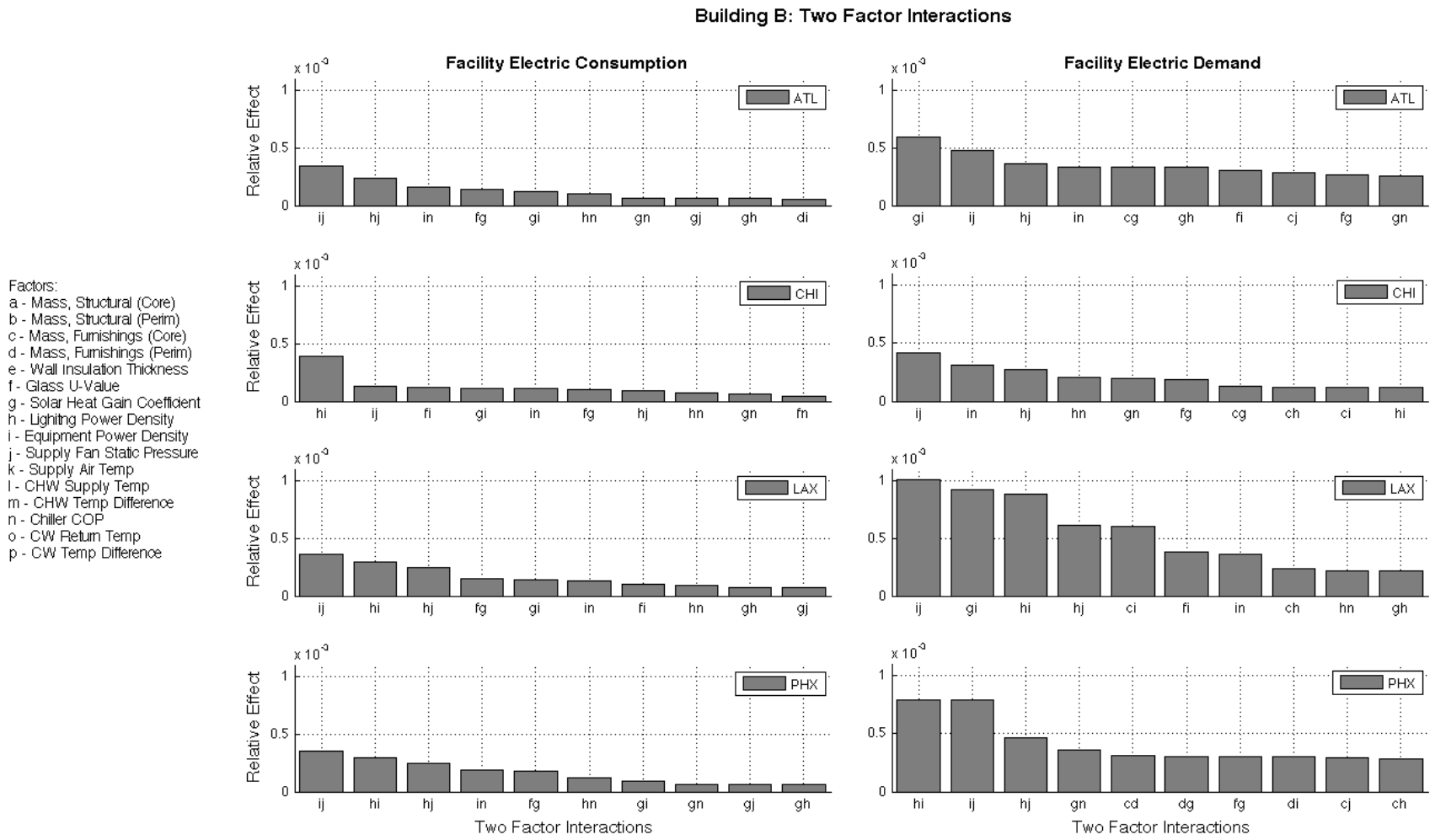

Figure D.8: Relative impact of two-factor interactions on facility energy, Building B

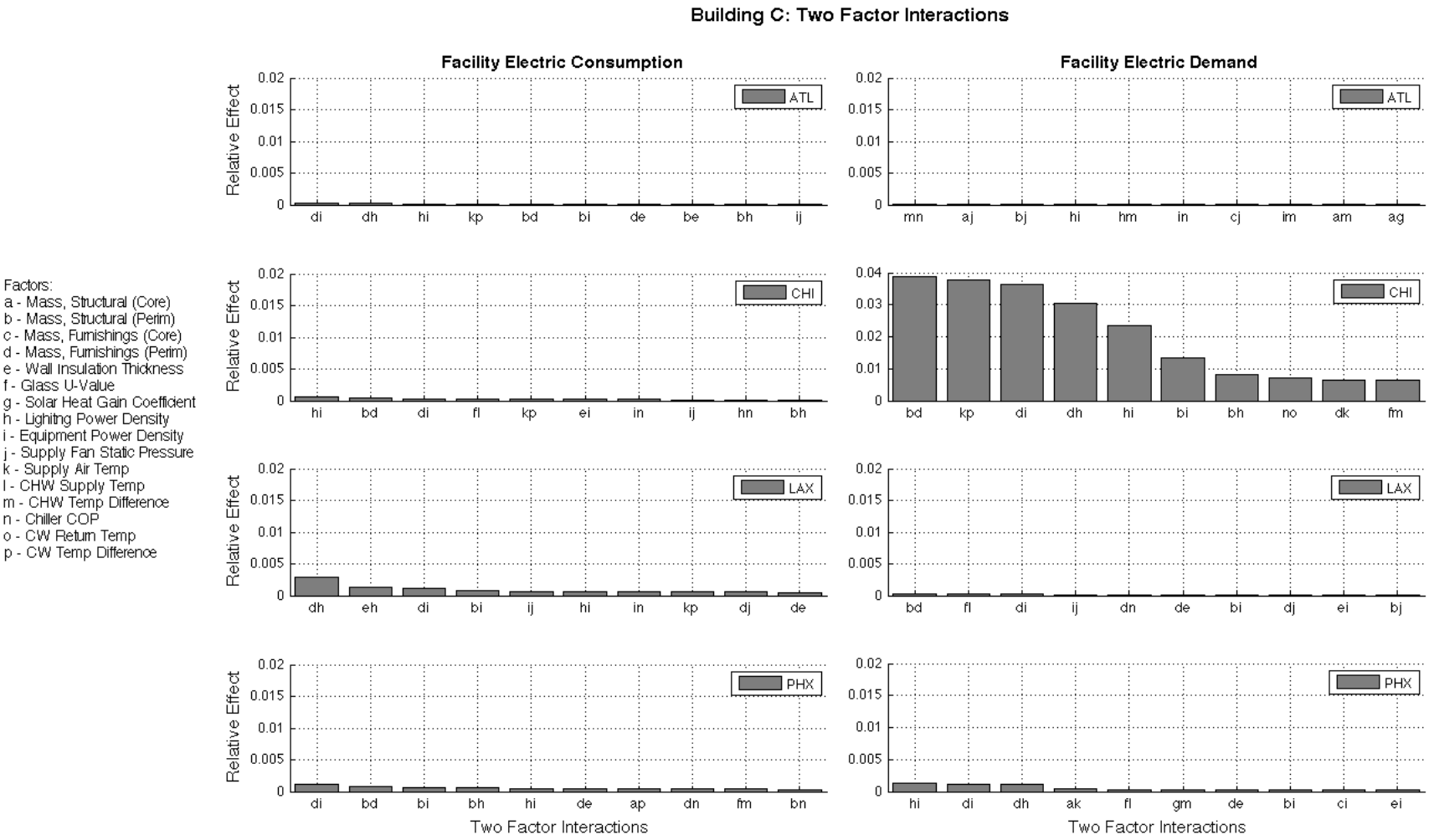

Figure D.9: Relative impact of two-factor interactions on facility energy, Building C

Appendix E

Audit and Modeling Procedure Flow Chart

The following charts in this appendix were developed to provide a graphical description of processes regarding the building audit, model development, and model calibration. Please note that the charts were developed specifically to aid in the 2009 CUE summer demonstration, and some of the tools may not apply to every building energy modeling case. However, the overall process and goals should be beneficial to any building energy modeling project.

In each chart, the light gray boxes describe the overall goal of each major step in the process. The yellow ovals describe the steps within each major goal. The dark gray ovals describe steps needed to take to meet each goal, and the orange ovals highlight specific tools that have proven beneficial for fulfilling that particular step in the process.

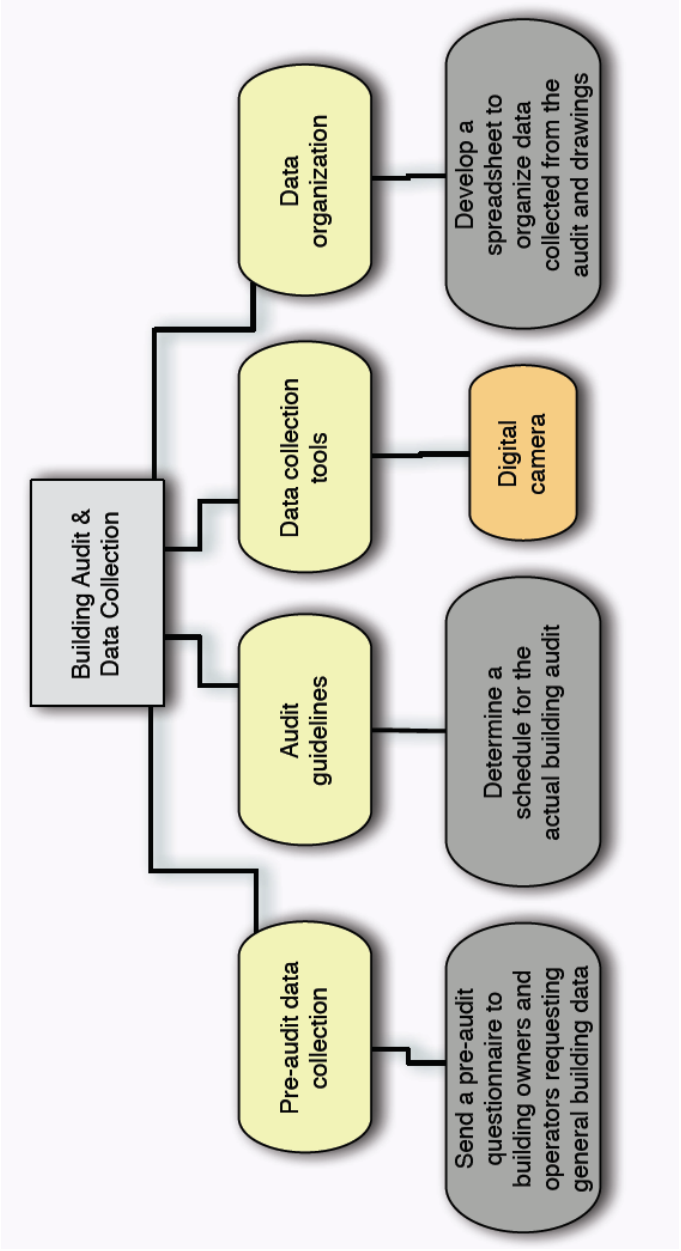

Figure E.1: Flow chart of the building audit and data collection process

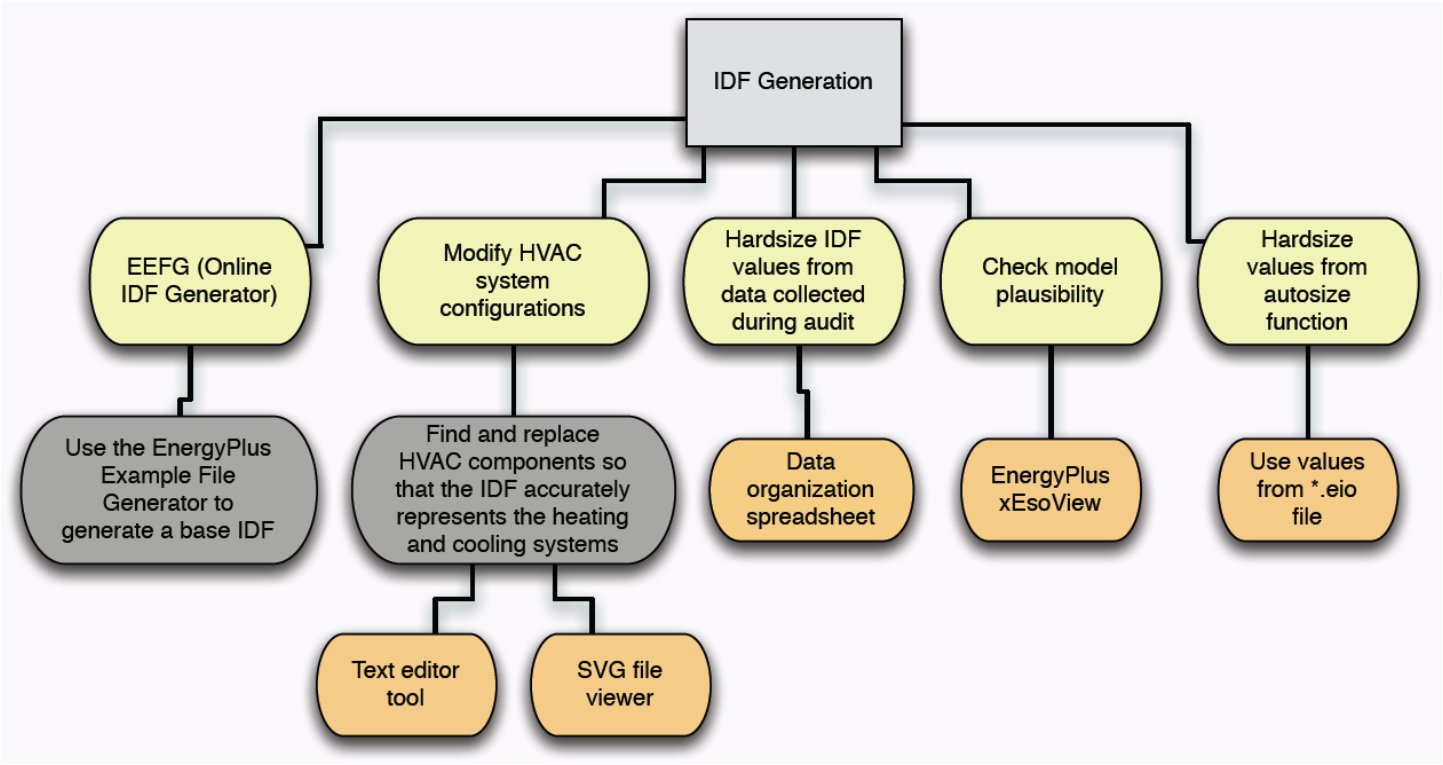

Figure E.2: Flow chart illustrating processes for building energy model development

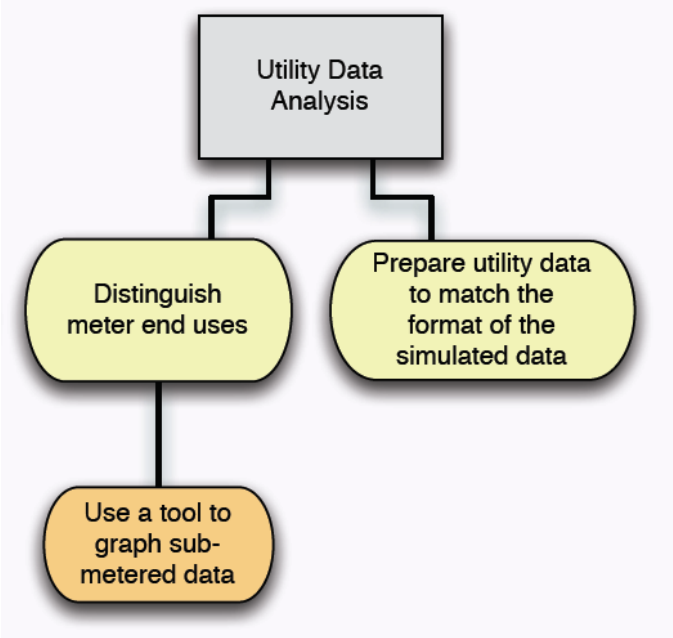

Figure E.3: Flow chart illustrating processes for analyzing utility data

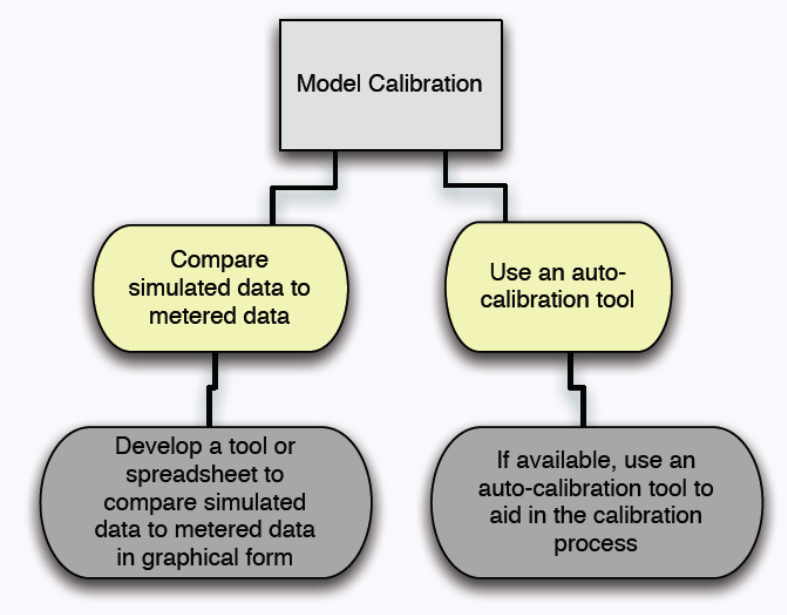

Figure E.4: Flow chart illustrating processes for calibrating building energy models